BIOGENESIS AND STRUCTURE OF GOLGI-DERIVED CELLULOSIC SCALES IN *PLEUROCHRYSIS.* I. ROLE OF THE ENDOMEMBRANE SYSTEM IN SCALE ASSEMBLY AND EXOCYTOSIS*

R. MALCOLM BROWN, JR. and DWIGHT K. ROMANOVICZ

Department of Botany,
University of North Carolina at Chapel Hill,
Chapel Hill, North Carolina 27514

SYNOPSIS

The Golgi apparatus of a marine haptophycean alga, *Pleurochrysis scherfellii,* has been studied with respect to its role in the assembly and transport of cell wall scales. In the vegetative cell the scale consists of three morphologically recognizable subunits: a quadriradial network of microfibrils rich in galactose and acidic sulphated polysaccharides, a spiral network of cellulosic microfibrils associated with a peptide rich in hydroxyproline, and amorphous coating substances rich in acidic polysaccharides. Scale structure, size, and composition is dependent upon specific phases of the life history. Unlike vegetative scales, those from the zoospore phase lack the amorphous coating substances and are about half the dimensions. The ratio of radial-to-spiral subcomponents remains unchanged. In the nutritionally induced coccolith phase, the scale rim is modified to consist of two concentric microfibrils. The ratio of radial-to-spiral subcomponents is dramatically altered.

Scale subcomponents are synthesized and assembled in association with the membranes of the endoplasmic reticulum and Golgi apparatus. Incipient Golgi membranes originate from budding regions of the endoplasmic reticulum. Precursor pools for radial subcomponents are differentiated from the spiral subcomponents by dense reaction products of silver methenamine when preceded by periodate oxidation. These pools which are about to be incorporated into the forming face of the Golgi membranes first appear within specific topographic regions of the endoplasmic reticulum. Radial microfibrils are synthesized in a folded configuration. Cytochemical enzyme localization reveals aryl sulfatase and alkaline phosphatase activity in the region of synthesis of the radial microfibrils. The radial microfibrils undergo an elaborate unfolding as observed by the presence of distinct "Z-stages". Following unfolding of the radial microfibrils, the spiral cellulosic microfibrils are presumably crystalized within a central feeding tubule on the distal face of the cisterna. Alkaline phosphatase activity is pronounced in the zone of centripetal amorphous polysaccharide addition. In vegetative cells, this sequence immediately follows the synthesis and deposition of cellulosic microfibrils.

Scale transport to the surface and ultimate exocytosis involve a subsurface cisterna which has the capacity to guide and direct Golgi cisternal membranes to the plasma membrane and to transfer "spent"

* Research presented in this paper was part of a Ph.D. dissertation (DKR) submitted to the Department of Botany at the University of North Carolina at Chapel Hill. This work was supported by an NDEA Title IV Fellowship to DKR and the National Science Foundation (GB 40937) to RMB. Part of this work has been submitted for publication in the Proceedings of the International Symposium on Plant Cell Differentiation held in Lisbon, Portugal, August, 1974.

Applied Polymer Symposium No. 28, 537–585 (1976)
© 1976 by John Wiley & Sons, Inc.

Golgi membranes to an autophagic vacuolar system. Acid phosphatase activity was prominent in the subsurface cisterna as well as the distal region of the Golgi apparatus. Colchicine prevents scale exocytosis and promotes autophagic consumption of accumulating scales and their cisternal membranes. Control of scale exocytosis seems to be under specific control of plasma membrane "acceptor" regions and Golgi cisternal coated vesicle "donor" regions. Protoplast rotation and exocytosis is discussed in terms of the "receptor-donor" hypothesis.

INTRODUCTION

In the study of plant cell walls, major emphasis has been placed upon the structure and biosynthesis of cellulose. One reason for this emphasis is that cellulose, as the predominant structural polysaccharide of green plants [14], is the most abundant macromolecule on earth, with 10^{11} tons produced and destroyed annually [95]. A second, and more immediate reason, is that the physical properties of cellulose made it one of the few biological materials amenable to electron microscopy in the early years when adequate fixation and ultrathin sectioning were yet to be developed. For example, in one of the first studies with the electron microscope, Ruska [110, 111] demonstrated the fibrillar nature of the wall of cotton.

With the development of replication techniques, excellent images of the microfibrillar organization of cell walls were obtained, both in the alga *Valonia* [98] and in higher plants [25]. In the last decade, replication has undergone a qualitative advance with the introduction of freeze-cleaving. Morphological observations based on this technique [73, 107] have supported Preston's model [94, 75] of a biosynthetic mechanism located within "granule bands" associated with the plasma membrane. Thus, the plasma membrane is widely accepted as the site of cellulose synthesis [95].

Biophysical investigation of the crystalline structure of cellulose [63, 116, 67] resulted in the adoption of a monoclinic unit cell belonging to the space group P_{2_1}. This structure, called the Meyer-Misch unit cell, remains the most satisfactory explanation of experimental evidence to date [114, 14, 78], despite recent proposals of a super-lattice structure in the highly crystalline cellulose of certain marine algae [43, 21, 20, 77]. After further investigation had indicated that the 101 and 101 planes of the unit cell are parallel to the surfaces of the microfibril [96, 76], the biophysical and morphological data were combined to yield the earliest models of the cellulose microfibril, namely Frey-Wyssling's [24] elementary fibril proposal, and Preston and Cronshaw's [97] solid-core model.

Concurrent with the later morphological studies has been the increasing importance of biochemical techniques as a means of understanding both the structure of the cell wall and the mechanism of its biogenesis. While earlier cell wall models were based almost entirely on the structure of the crystalline polysaccharide constituents [26, 27, 28], analysis of the composition of cell wall fractions [47, 48, 124, 10] has revealed that the structural polysaccharide is accompanied by a protein moiety. In recent cell wall models [1, 49] this protein moiety has been incorporated as a single polypeptide chain linked to cellulose microfibrils by short oligosaccharides, and Lamport [48] has discussed the possible role of the protein in wall metabolism and growth.

Concerning the mechanism of cellulose biosynthesis, Glaser [33] first demonstrated the incorporation of glucose from uridine diphosphoglucose (UDPG) into

cellulose by cell-free extracts. Further investigation confirmed the role of sugar nucleotides as glycosyl donors in polysaccharide synthesis [41, 84, 127, 40] and suggested the possibility that a lipid intermediate might be involved as a carrier of the activated sugar molecules (13, 46, 54]. There is no agreement, however, upon the organelle responsible for cellulose synthesis. Villemez et al. [128] have implicated the plasma membrane, based on physical properties of the active fraction, while Ray and co-workers [103] have concluded that other enzymatic activity present in the cellulose-synthesizing fraction identifies it as the Golgi apparatus. More recently, Van Der Woude et al. [125] have demonstrated the presence of β-1, 4-glucan synthetase in both Golgi and plasma membrane fractions, but the plasma membrane had a greater synthesizing capacity at higher UDPG concentrations.

By combining morphological and biochemical techniques, cytochemical research has contributed valuable insight into the composition and biogenesis of plant cell walls. With regard to composition, the presence of protein in cell walls was confirmed by Sadava and Chrispeels [112, 113] using labelled proline and autoradiographic localization. Northcote and Pickett-Heaps [82] utilized autoradiographic localization of labelled glucose to hypothesize that there are two separate biosynthetic pathways for polysaccharides: one via the Golgi apparatus which results in the synthesis of pectic substances, and the other, a pool of soluble hexoses, which contributes to the synthesis of cellulose and starch. Attempts to confirm or refute this hypothesis have been hampered by the lack of a specific cytochemical stain for cellulose. Staining techniques which localize 1,2 glycols have supported the Golgi pathway [93, 22, 126], but these techniques are specific only for polysaccharides in general, and in some cases do not even stain cellulose [10]. Enzyme localization has been used to demonstrate the presence of alkaline phosphatase in the Golgi apparatus concomitant with the production of secretory vesicles [18]; but the absence of a specific cytochemical reaction to localize glycosyl transferase activity leaves open the question of the site of cellulose synthesis.

In many of the studies cited above, the unique characteristics of a particular experimental organism were responsible for the conclusions drawn. The marine alga, *Valonia ventricosa,* has a wall of large area that can easily be isolated without mechanical deformation. These properties permitted electron microscopic observation of the organization of the wall [98] and the demonstration that the 101 and $10\bar{1}$ planes of the Meyer-Misch lattice lie parallel to the surface of the cellulose microfibril [96, 99]. In addition, the high crystallinity of *Valonia* cellulose has made possible increased structural information by yielding a larger number of reflections in x-ray [77] and electron diffraction studies [43] and a greater resolution in infrared absorption spectra [114, 66]. Colvin [14] postulated the extracellular tip growth mechanism of microfibril formation, based on observations of the extracellular cellulose synthesis in the bacterium *Acetobacter xylinum* [15, 68].

In the past fifteen years, principally through the work of Irene Manton and her students, a number of organisms have been described which synthesize a cell wall composed of discrete subunits called scales. Initially observed in the haptophycean alga *Chrysochromulina* [88, 89, 90, 91] scales have since been found in other haptophycean species [60, 51], in the Chrysophyceae [58, 115, 105], in the Prasinophyceae [57, 52], in the Chlorophyceae [70], and in several other protists [29, 17]. The unique morphology of the scales has permitted the observation that scales are synthesized intracellularly via the Golgi apparatus [59, 61, 55, 56, 5, 92,

85]. In addition, the discrete nature of the scales has facilitated the preparation of cell-free scale fractions for chemical and physical analysis [35].

In the non-motile vegetative cells of the haptophycean alga *Pleurochrysis*, the scales adhere to form a compact cell wall [5]. With further investigation, Brown and co-workers [9, 42] described the Golgi-mediated synthesis of the complex microfibrillar scale and presented a compositional analysis of isolated scale material. Despite the accumulation of chemical and physical data supporting the presence of cellulose [10], there continues to be considerable resistance to the idea that cellulose biosynthesis can occur in the Golgi apparatus, as illustrated by the recent statement of Preston [95]: . . ."The case for synthesis [of cellulose] in the Golgi vesicles of *Pleurochrysis* must be considered unproven . . ." While we are ready to admit that the occurrence of Golgi-derived cellulose is not universal or even predominant in plant cells, it is important to establish unequivocally the presence of Golgi-derived cellulose in *Pleurochrysis*.

In the first paper of this series, the architecture and biosynthetic pathway of the scale will be described. In the second paper, the composition of the scale subcomponents and the supramolecular structure of the cellulosic microfibril will be presented. Finally, we shall attempt to relate the dynamic processes of cell wall biogenesis in the specialized cell of *Pleurochrysis* to those of more complex cells of higher plants.

EXPERIMENTAL

Culture Conditions and Scale Isolation

Axenic cultures of *Pleurochrysis scherffelii* Pringsheim were maintained on an artificial seawater medium (Rila Products, N.J.), enriched by the addition of 2X von Stosch medium [118] and three amino acids. The final concentrations in one liter of medium were as follows:

Rila salts—40 gm
disodium EDTA (2 H_2O)—7.4 mg
ferrous sulfate (7 H_2O)—0.56 mg
sodium nitrate—85 mg
manganous chloride (4 H_2O)—0.04 mg
sodium phosphate, dibasic—8.2 mg
biotin—120 μg
B_{12}—14 μg
thiamine—172 μg
L-serine—0.2 gm
L-alanine—0.2 gm
L-asparagine—0.2 gm.

For growth of non-motile vegetative cells, 0.85% Ionagar (Wilson Diagnostics, Inc.) was added and the medium was solidified in 100-mm Petri dishes. Cultures were grown at 3000 lux on a 16 hour light-8 hour dark cycle, in a room maintained at 68°C.

For induction of the *Cricosphaera* phase, zoospores were innoculated onto the

agarized media containing serine as the sole organic nitrogen source. Subsequent flooding of these plates with serine-containing liquid media produced the exclusively motile *Cricosphaera* phase.

Fixation

For electron microscopy and cytochemistry, four- to six-day-old vegetative cells or active zoospores were fixed (a) with a solution of 2 or 3% glutaraldehyde in 0.1M cacodylate buffer pH 7.2, to which sucrose had been added to a final concentration of 0.25M, or (b) with the same fixative to which 0.5% tannic acid was added [30]. Fixation was conducted for 90 minutes, after which the cells were washed in three changes of the buffer, reducing the sucrose concentration to zero by equivalent increments. The cells were then post-fixed for 2–18 hours in 2% osmium tetroxide buffered to pH 7.2 with 0.1M cacodylate. For additional contrast, some samples were post-fixed in a saturated solution of Ruthenium red in buffered 2% osmium tetroxide [53]. This solution was filtered immediately prior to use. Up to this point, the cells were handled as a suspension and pelleted with a clinical centrifuge for solution changes. Following post-fixation, the cells were washed with distilled water, embedded in 1% Ionagar, and dehydrated with an ethanol series. All steps through dehydration were carried out at 4°C. After dehydration, the small agar blocks containing cells were transferred to absolute acetone, then infiltrated and embedded in Epon 812, and polymerized. Silver grey to pale yellow sections were cut with a DuPont diamond knife on a Reichart Om U2 ultramicrotome and mounted on Formvar-carbon coated grids. Routine post-staining was done with lead citrate for 5–10 minutes [106].

To test for the presence of endocytotic activity in *Pleurochrysis*, the cells were incubated for 60 minutes with cationized ferritin [16] (1.2 mg/ml) prior to standard fixation as described above.

Freeze-etching of unfixed vegetative cells of *Pleurochrysis* was performed according to the procedures of Brown et al. [9]. No cryoprotectant was used.

Cytochemistry

Polysaccharide localization was achieved with the periodic acid-silver methenamine staining reaction [93, 101, 102, 45], for which the basic staining solution was made as follows (24 hour shelf life):

3% methenamine—15 ml
0.05M borate buffer—25 ml
1% silver nitrate—5 ml
distilled water to 50 ml.

The borate buffer was adjusted to the desired pH before mixing (pH must be measured with pH papers as pH electrodes introduce chloride ions which precipitate

* Staining rings were prepared from Tygon tubing; 3-mm segments were cut and the grids were placed in radial slits.

silver); staining increases with increasing pH in the range of 7.8 to 9.2. Pale yellow sections on stainless steel grids in staining rings* were immersed in the staining solution, pH 8.2, for 45–60 minutes at 60°C, after which the grids were washed with distilled water and treated for 60 minutes with 5% sodium thiosulfate to remove unreduced silver ions. Specificity of silver reduction depends upon specimen pretreatment [62, 93, 123] and the following oxidizing or blocking agents were employed:

1% periodic acid—10 to 30 minutes, room temperature
10% hydrogen peroxide—30 to 60 minutes, room temperature
2% sodium bisulfite—60 to 90 minutes, 60°C
0.1M iodoacetate, pH 8.0 (with ammonium hydroxide) 60 to 90 minutes, 60°C.

Incubation for cytochemical enzyme localization was carried out between glutaraldehyde fixation and osmication. (Substitution of paraformaldehyde for glutaraldehyde did not substantially alter localization but did result in poor ultrastructural preservation.) Cells were maintained at 0–4°C after glutaraldehyde fixation and washed in several changes of 0.25M sucrose in 0.1M cacodylate buffer, pH 7.2. For the procedures involving cupric ferricyanide, it was necessary to wash the material for 48 hours, while 2–3 hours washing was adequate for all other localizations. Control reactions were run in incubation medium without substrate or with complete medium and heat-treated cells (10 minutes, 100°C). After incubation, all material was osmicated, embedded, and sectioned following routine procedures.

Aryl sulfatase activity was localized as the hydrolysis of p-nitocathechol sulfate (p-NCS), using either barium [44] or copper [38] as capture reagents. For barium capture, the following incubation medium was used:

p-NCS—80 mg
distilled water—2 ml
0.1M acetate buffer pH 5.5—6ml
5% $BaCl_2$—2ml.

The pH was adjusted to 5.5 with a 0.2M acetic acid and the medium was filtered into the reaction tube containing glutaraldehyde-fixed cells. After 60-minute reaction at 37°C, the cells were washed briefly with the acetate buffer and then post-fixed and embedded as described above. Alternately, copper capture was accomplished with the following incubation medium (using w/v aqueous stock solutions):

p-NCS—20 mg
0.8% sodium acetate—7.9 ml
0.6% acetic acid—0.25 ml
2.9% sodium nitrate—0.60 ml
0.75% copper sulfate, dropwise—1.25 ml
0.17% potassium ferricyanide, dropwise—1.25 ml.

The solutions were added in order, with stirring, after which the pH was adjusted to 5.2 with acetic acid and the medium was filtered. Cells were incubated 30 minutes at room temperature, washed with distilled water, and immersed in a freshly prepared solution of 5 mg diaminobenzidine tetrahydrochloride (DAB) in 10 ml 0.05M acetate buffer, pH 5.6, for 20 minutes at 0–4°C. The material was then washed with distilled water and routine processing continued.

Alkaline phosphatase activity was localized as the hydrolysis of the nucleotide diphosphates, thiamine pyrophosphate (TPP) and guanine diphosphate (GDP), visualized by lead capture [18]. The following incubation medium was used:

0.02M TPP or GDP—1.0 ml
distilled water—0.4 ml
0.2M Tris-maleate buffer pH 7.2—2.0 ml
1% lead nitrate—0.6 ml
0.025M manganous chloride—1.0 ml.

The complete medium was adjusted to pH 7.2 (if necessary) and filtered into a test tube containing the glutaraldehyde-fixed cells. Following a 60-minute incubation at 37°C, the cells were washed in 0.1M Tris-maleate buffer and then processed routinely.

Acid phosphatase activity was localized either as hydrolysis of β-glycerophosphate (β-GP) or guanine diphosphate (GDP) with lead as the capture reagent [18], or as hydrolysis of the synthetic substrate, di(dicyclohexylammonium)-2-naphthylthiolphosphate (DDNTP), with the cupric ferricyanide capture reagent [39]. The lead capture incubation medium was made as follows:

0.25% lead nitrate—5 ml
0.1M acetate buffer pH 5.0—5 ml
0.1M sodium β-glycerophosphate (or GDP)—0.5 ml.

The medium was adjusted to pH 5.0 (if necessary), allowed to stand over-night at 37°C, and filtered immediately prior to use. After 60-minute incubation at 37°C, cells were washed briefly in the acetate buffer and then routine processing was resumed. For localization of DDNTP hydrolysis, the cupric ferricyanide medium was identical to that described for aryl sulfatase, except that 5 mg DDNTP suspended in 0.1 ml dimethyl formamide was added as the substrate and the pH was adjusted to 5.6 (if necessary). Subsequent DAB incubation and washings were as described above, after which routine processing was continued.

RESULTS

Life History and Cell Cycle

Pleurochrysis, a member of the Haptophyceae [12], is characterized by two major criteria: the presence of Golgi-derived scales on the cell surface and an attachment organelle known as the haptonema [56]. When Pringsheim [100] first described *Pleurochrysis* he placed it in the Chrysophyta because no haptonema was detected. Although the taxonmic position of *Pleurochrysis* is now better known, there are many phases of the life history which remain enigmatic [50].

The predominant cell of *Pleurochrysis* is the vegetative or nonmotile cell which exists in multiple-cluster pseudofilaments. The non-motile vegetative stage predominates when the cultures are maintained on an agarized marine medium; however, when vegetative cells are flooded with liquid marine medium, they divide to form zoospores [7]. Each vegetative cell divides once to produce two daughter zoospores, which escape into the medium by dissolving the cementing substances

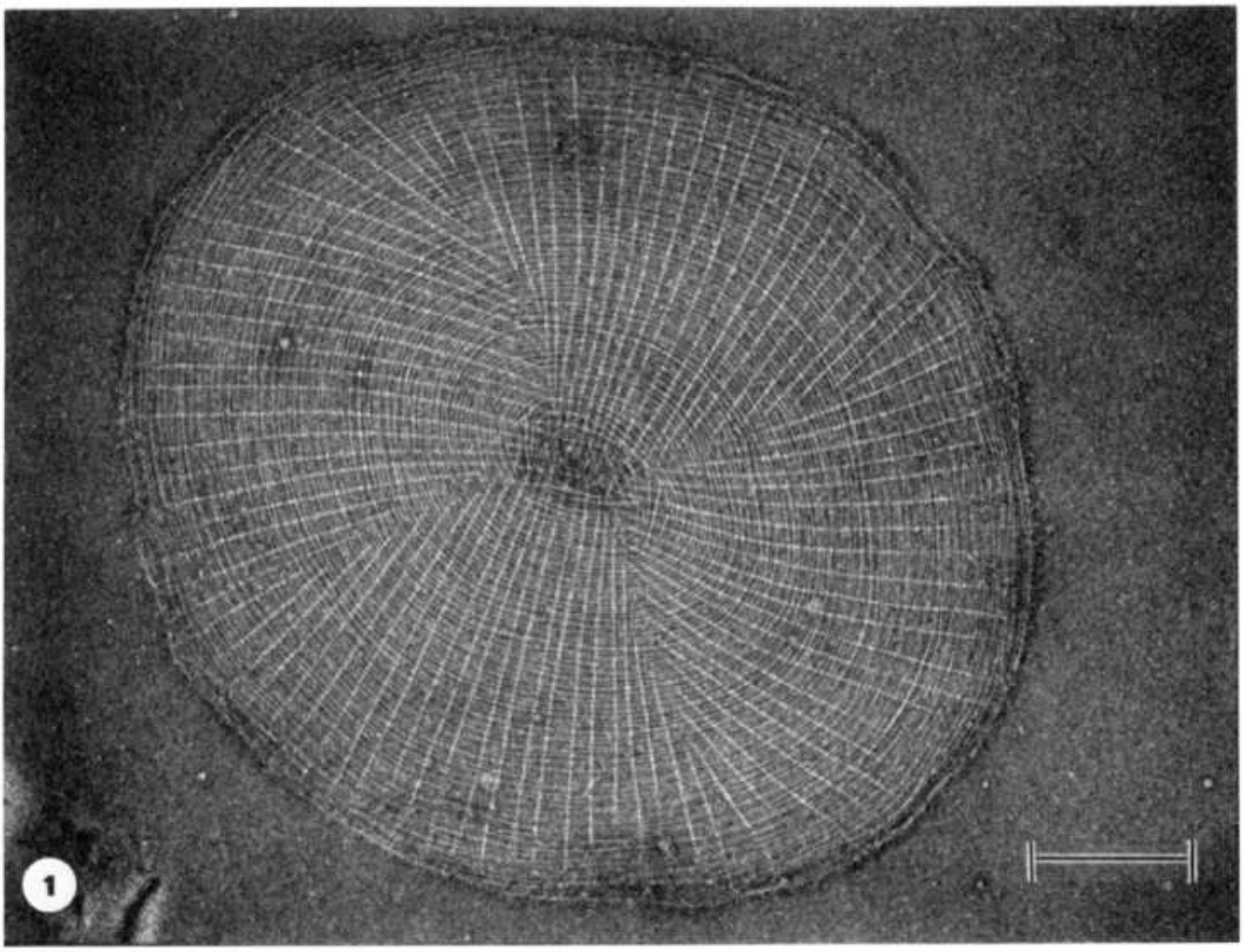

FIG. 1. Wall scale from the zoospore stage, prepared by the uranyl acetate, Bacitracin negative stain. Note the distinct quadriradial network and the compact spiral microfibrillar network. Magnification bar = 0.1 μm.

which maintain the integrity of the parent cell wall. The zoospore is the ephemeral stage in *Pleurochrysis*. Within two days after induction, zoospores settle down and differentiate into typical vegetative cells. Subsequent division every 2–3 days results in colonies or aggregates of diads, tetrads, or pseudofilamentous groups of vegetative cells.

The basic wall unit of *Pleurochrysis* is the scale, the morphology of which is illustrated in Figures 1–3. In the vegetative cells, the scales are cemented into place to form a coherent and compact cell wall. In the zoospores, scales are loosely distributed over the cell surface and frequently become dispersed into the medium. In both cases, the basic scale architecture is identical; however, it can be experimentally modified upon induction of the coccolith-producing phase as follows: If vegetative cells of *Pleurochrysis* are grown on an artificial marine medium with serine as the sole organic nitrogen source and flooded with liquid marine medium, the resultant zoospore phase will produce coccolith-bearing motile cells (Fig. 4). A coccolith is a modified scale with a calcified rim (Fig. 5).

These two different phases in the *Pleurochrysis-Cricosphaera* complex suggest the possibility of an alteration of generations. Rayns [104] and Leadbeater [50] have postulated that the *Pleurochrysis* phase is haploid while the *Cricosphaera* phase is diploid. Such an explanation would imply a sexual fusion in the zoospore phase. This has never been directly confirmed, although Von Stosch [117] has indicated the possibility of sexual fusion. An alternate explanation is the achievement of the diploid state through apogamy (self-fusion) of the motile cell.

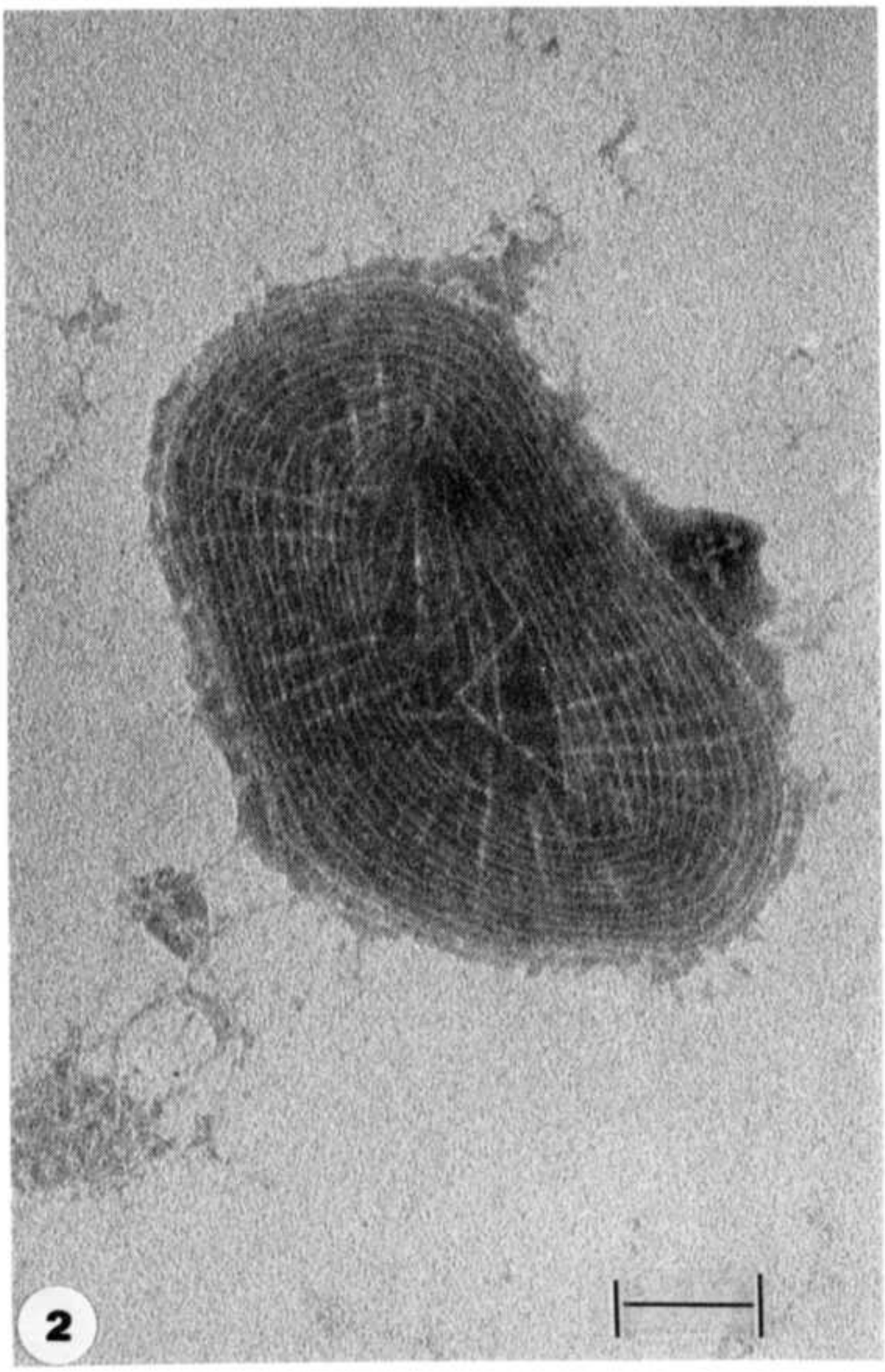

FIG. 2. "Ultraminor" scale from the zoospore stage. This miniature scale consists only of a single turn of the spiral band of cellulose microfibrils. A rudimentary quadriradial network is visible. Negative stain preparation (phosphotungstic acid). Magnification bar = 0.1 μm.

One of the most interesting unsolved problems in the life history studies concerns the role played by organic nitrogen sources in determining which phase will develop and predominate. For instance, we have been able to maintain the *Pleurochrysis* phase indefinitely on an agarized medium containing serine, alanine, and asparagine. The *Cricosphaera* phase can be induced at will by deleting asparagine and alanine from the medium. A reversal back to *Pleurochrysis* phase can be achieved by transferring *Cricosphaera* cells onto agarized media containing serine, alanine, and asparagine. In spite of our success with the experimental conversion of these two different phases, we know essentially nothing about the molecular basis for this phenomenon.

Scale Structure and Diversity

We shall first examine the molecular architecture of scales from the *Pleurochrysis* phase. Vegetative cells synthesize scales with at least three recognizable subcomponents. The "backbone" of the scale consists of a non-cellulosic microfibrillar system organized into four quadrants, hence the term quadriradial (Fig. 1).

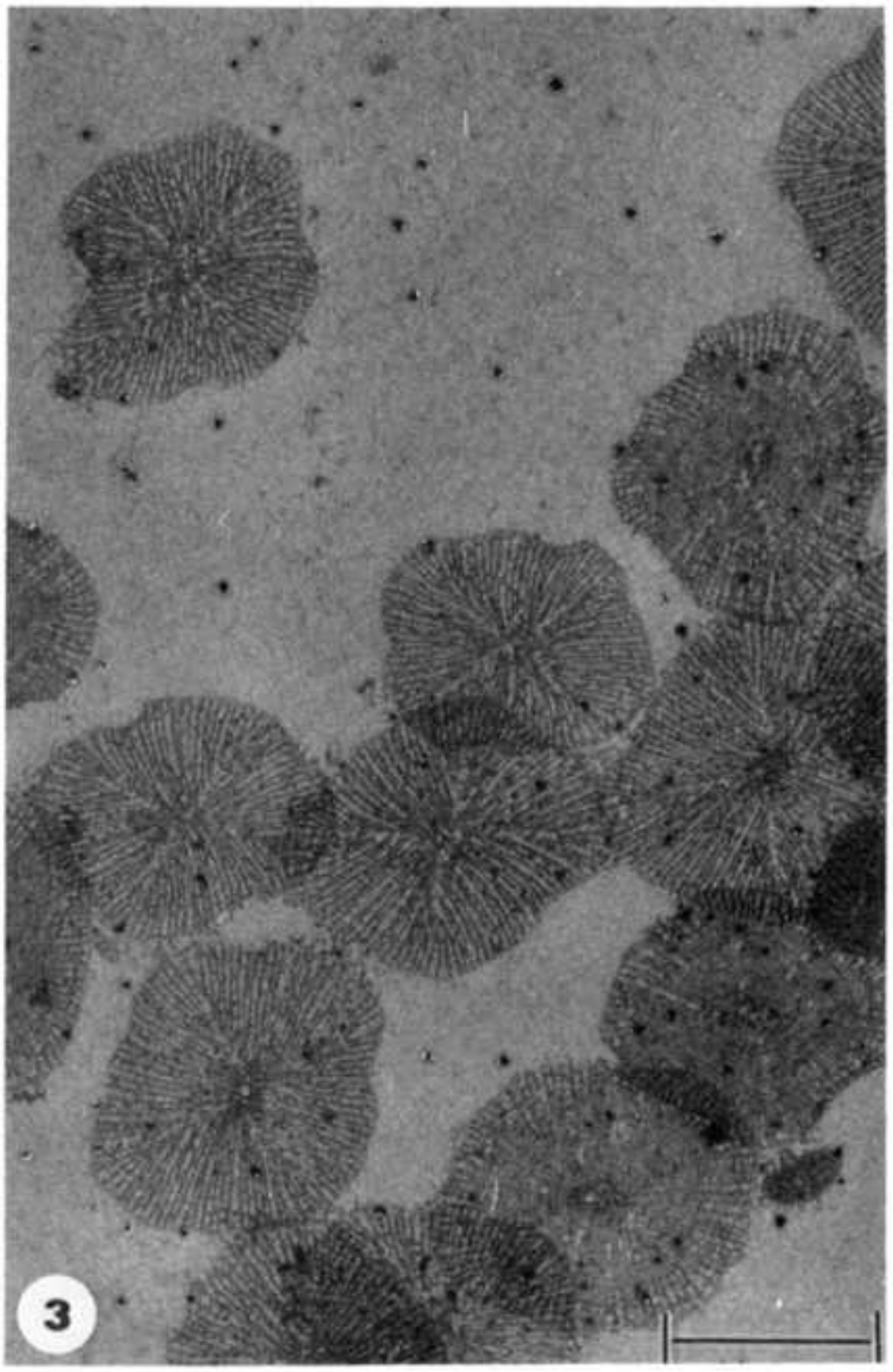

FIG. 3. Wall scales from the vegetative cell stage. Note the distinct patterns of amorphous material in between the quadriradial microfibrils. Magnification bar = 1.0 μm.

Regardless of variability in scale size or shape, the quadriradial pattern is consistent. The second scale subcomponent is a spiral band of 8–10 microfibrils of cellulose which is tightly wound onto the distal surface of the quadriradial microfibrillar network (Fig. 1). The length of the spiral microfibrillar band is proportional to the overall diameter of the scale. In vegetative scales, the band makes 4–5 turns, resulting in a scale 1.5–2.0μ in diameter and composed of spiral microfibrils 12–14μ in length. Zoospores scales generally are half the diameter of vegetative scales, but are more variable, ranging down to scales so small as to consist of only one turn of the spiraling band (diameter $\cong$ .25μ, Fig. 2).

The third subcomponent consists of an amorphous, galactose-rich polysaccharide deposited on both surfaces (Fig. 3). This subcomponent is responsible for scale coherence, leading to the formation of the compact wall of the vegetative phase, and is lacking in the zoospore phase.

The scale architecture in *Cricosphaera* differs considerably from that of *Pleurochrysis*. The major similarity is a quadriradial network identical to that of *Pleurochrysis* phase. A band of spiral microfibrils is present, but greatly reduced in quantity and order (Fig. 6). In addition, two concentric microfibrils occupy the circumference or rim of the *Cricosphaera* scale. Two types of scales are observed

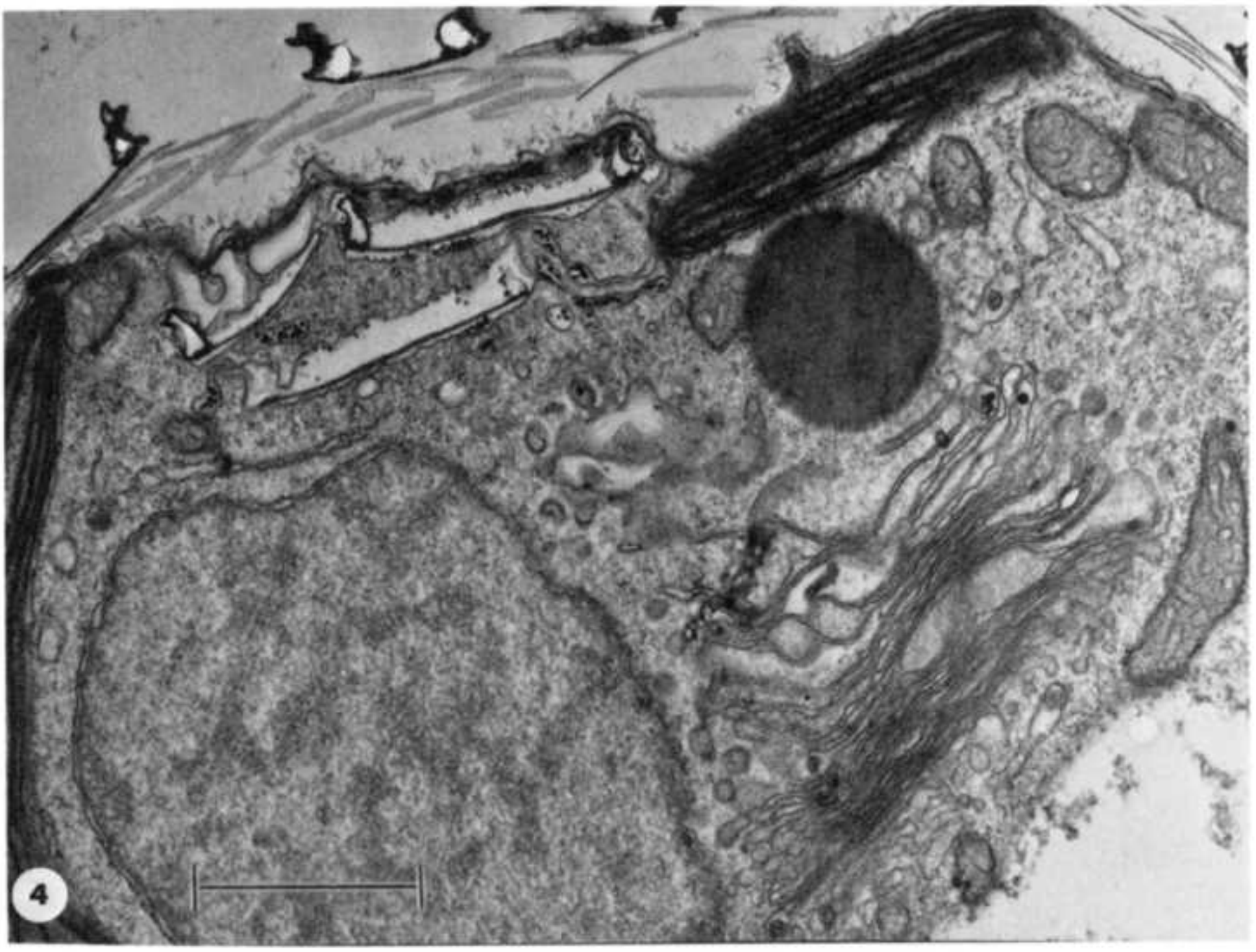

FIG. 4. Thin section of a coccolith-producing cell. Note the outermost layer of coccolith scales and the subtending circular scales. Several coccolith scales are shown near the cell surface (top left), and circular scales are demonstrated in the Golgi cisternae (middle right). Micrograph courtesy Kay Cooper. Magnification bar = 1.0 μm.

in *Cricosphaera:* circular non-coccolith scales with the morphology described above (Fig. 6), and elliptical coccolith scales which are conspicuously calcified at the rims (Fig. 5). An amorphous substance may be present on the distal surface of the coccolith.

In *Cricosphaera* and *Pleurochrysis*, a single Golgi apparatus is responsible for the assembly and transport of these diverse scale types. The biogenic pathway of the *Pleurochrysis* phase will be described below.

The Scale Biogenic Pathway

The distinctive microfibrillar morphology of the scale described above has facilitated the observation that the scales are synthesized and assembled within the Golgi apparatus. Brown and co-workers [5, 9] have described the Golgi-mediated scale biogenesis in terms of the concept of cell surface-oriented membrane flow [74, 81, 131]. Although the evidence is completely morphological, several key aspects of the pathway have been documented. Within the first third of the proximal, or forming face of the Golgi apparatus are located characteristic dilated regions [23]. Since these dilations frequently were observed to be filled with an electron-dense product, and since their appearance always preceded that of any recognizable microfibrils, the dilations were termed polymerization centers [9].

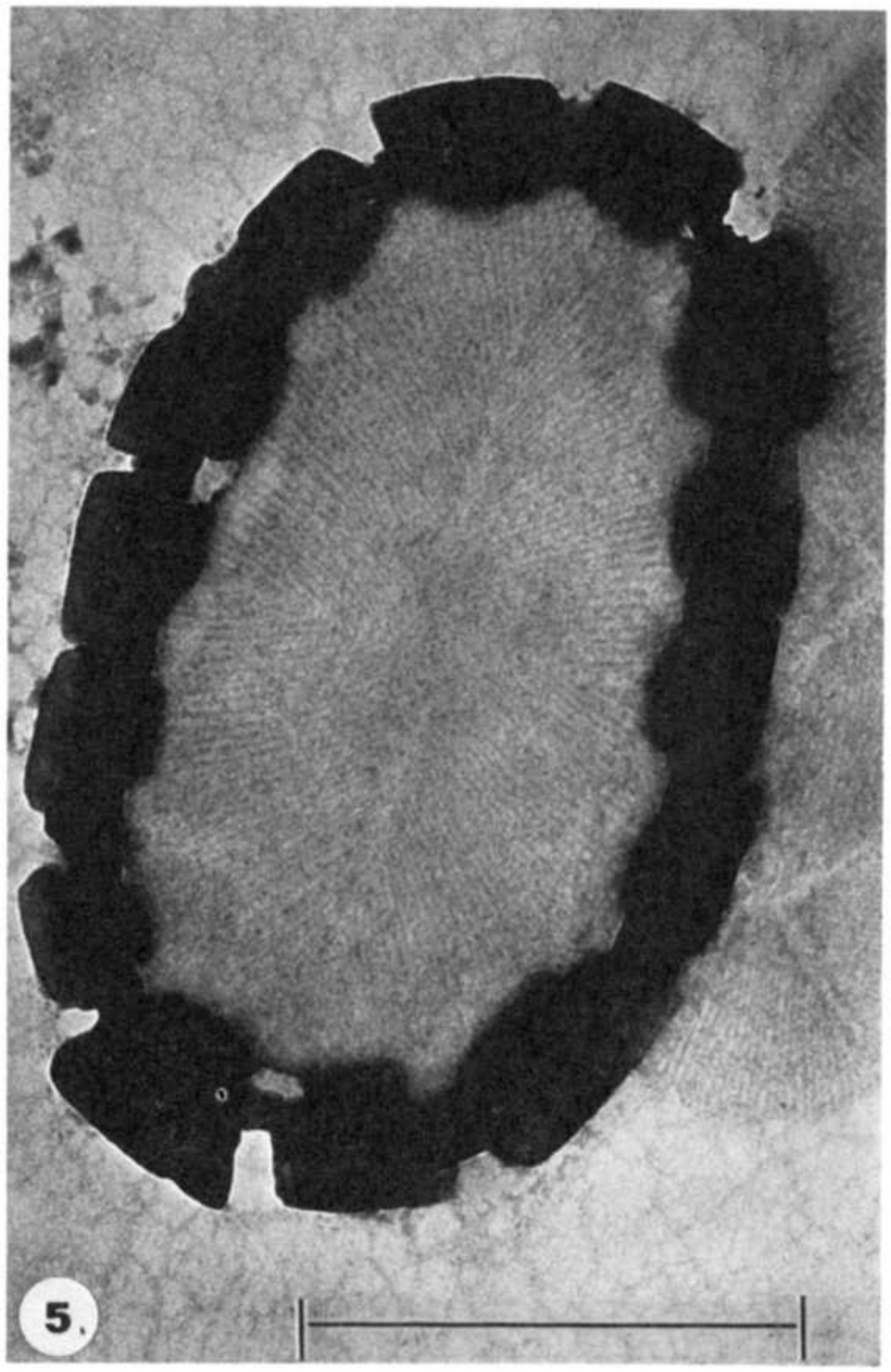

FIG. 5. Negative stain preparation (phosphotungstic acid) of a coccolith. Note the quadriradial network and the peripheral crystals of calcium carbonate. Magnification bar = 1.0 μm.

It was further observed that the earliest appearance of microfibrils occurred adjacent to each limiting cisternal membrane in the central region of the cisterna [9]. With the use of cytochemical staining techniques, the significance of these observations has been underscored, and a more complete biosynthetic pathway of the scale components has been elucidated.

Ontogeny of the Golgi Apparatus

The forming face of the Golgi apparatus lies opposite the rough endoplasmic reticulum (RER) which can be traced to have continuity with the nuclear envelope (Fig. 7). Specific topographical regions of this RER bud off into smooth vesicular configurations which can be interpreted as incipient regions of the Golgi cisternae. Notable is the radial microfibril precursor pool region (see below) which can be recognized by a product within the dilated cisternal membranes (Fig. 8). If the Golgi region destined to function in radial microfibril biosynthesis is identifiable while still continuous with the rough endoplasmic reticulum, it is conceivable that other regions of the incipient Golgi apparatus develop from specific topographical loci of the RER. For example, the small budding vesicles (Fig. 8) may reflect

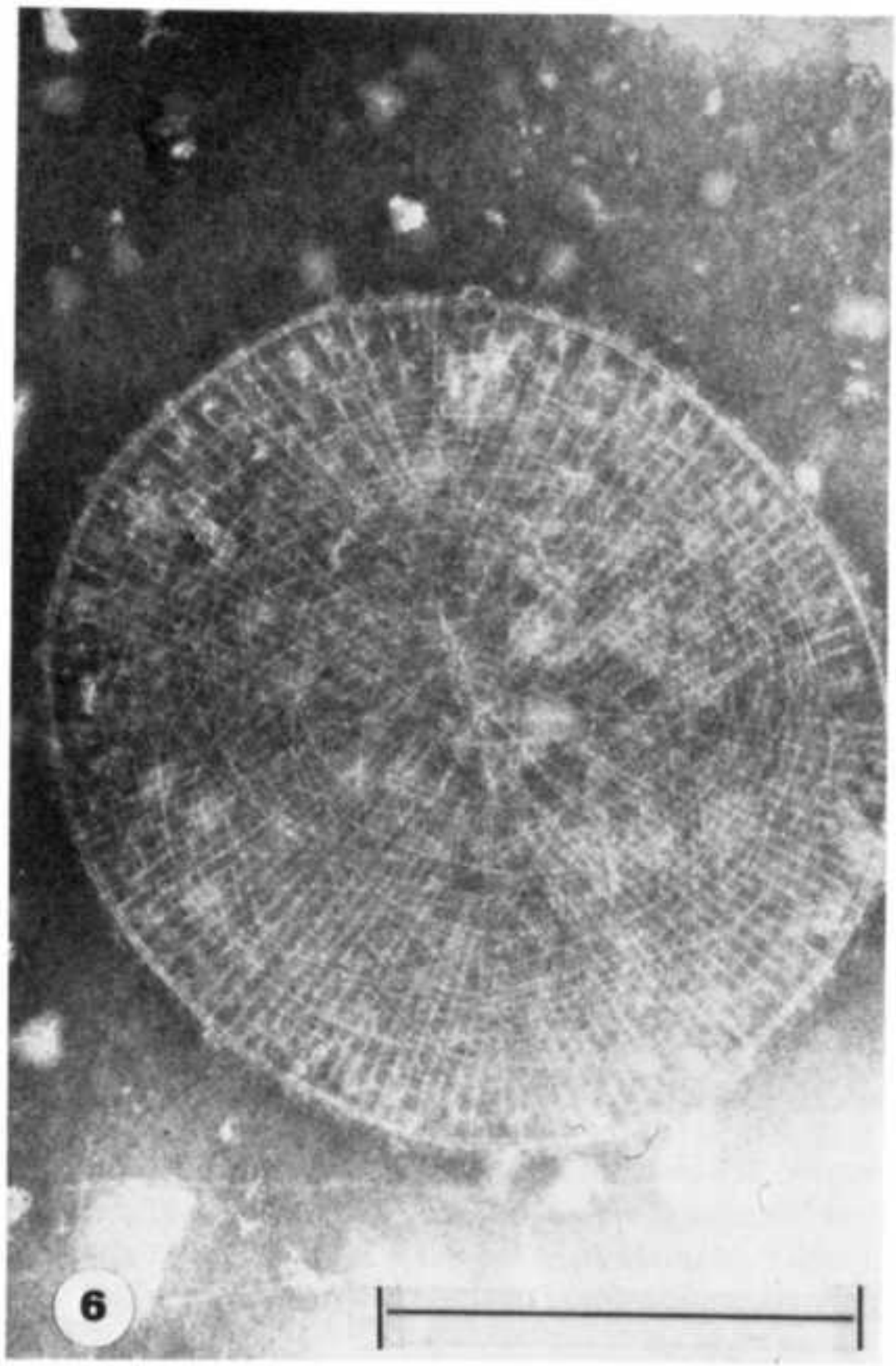

FIG. 6. Negative stain preparation (phosphotungstic acid) of the subtending circular scale. Note the typical quadriradial microfibrillar network, the sparce and poorly organized spiral microfibrillar network, and the rim of doublet microfibrils. Magnification bar = 0.25 μm. (*Cricosphaera*).

"filler membrane" of the incipient Golgi apparatus. Also, certain regions of the RER destined to carry out the synthesis of the cellulosic subcomponents could be pre-assembled at specific loci within the RER. If this is true, then the direct role of the endoplasmic reticulum in cellulose biosynthesis, as suggested by Westafer [129] for the secondary wall of the cotton fiber, may apply to *Pleurochrysis* when the ontogeny of the Golgi apparatus is considered.

Direct evidence on the scale biogenic pathway at the forming face of the Golgi apparatus has been rather difficult to obtain since enzymatic activities, if they exist in this region, may be latent, and polysaccharide precursors may not be retained by standard fixation methods. Thus, the biogenic pathway will be described in terms of specific morphological structures retained by the fixation and revealed by certain cytochemical methods.

Scale Assembly

Because a major part of the scale biogenic pathway in *Pleurochrysis* has been elucidated through the fortuitous localization of the subcomponents by the silver methenamine technique, attention first will be directed to the application of this

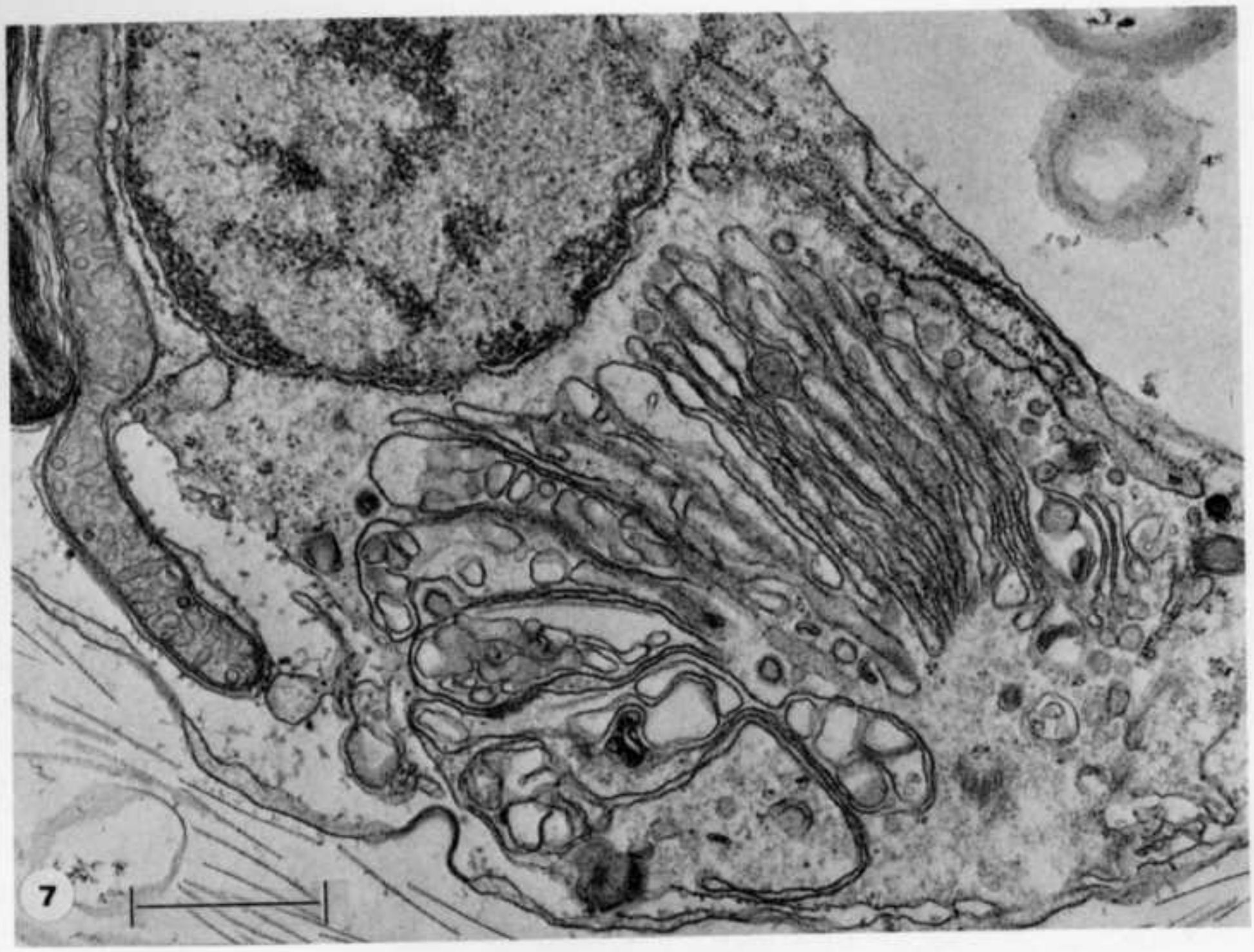

FIG. 7. Note the extension of the outer nuclear membrane (= amplexus). The amplexus extends across the forming face of the Golgi apparatus. The secretion face of the Golgi apparatus is toward the bottom. (*Plenrochrysis*) Magnification bar = 1.0 μm.

technique for polysaccharide localization in the Golgi apparatus.

Cytochemical localization of polysaccharides with the silver methenamine reagent is dependent upon prior oxidation with periodic acid (PA). This treatment oxidizes 1,2 glycol groups of the polysaccharide, yielding aldehydes which can then reduce silver ions, depositing metallic silver. When control sections of glutaraldehyde-osmium fixed tissue were directly incubated in the staining reagent, silver was deposited on extra- and intracellular scales as well as on all membranes. Thus, before polysaccharide localization could be undertaken, it was necessary to explain this control reaction through the use of specific blocking reagents. Since aldehyde blockage with bisulfite did not diminish the control staining, the reaction was not due to residual aldehyde groups within the tissue. However, oxidation with peroxide eliminated all control staining, removing bound osmium from the membranes [62] and presumably oxidizing the staining moiety present in the scales. Treatment with iodoacetate also blocked staining of the scales, a blockage which is generally attributed to the alkylation of sulfhydryl groups [93, 122] but which could also be due the alkylation of amino acids containing strong amines, such as histidine or lysine [37]. This explanation of iodoacetate blockage is consistent with the finding that a peptide constituent is present in the scale subcomponents.

With the control reaction thus understood, it was possible to stain for polysaccharides by pretreating sections with iodoacetate blockage followed by periodic

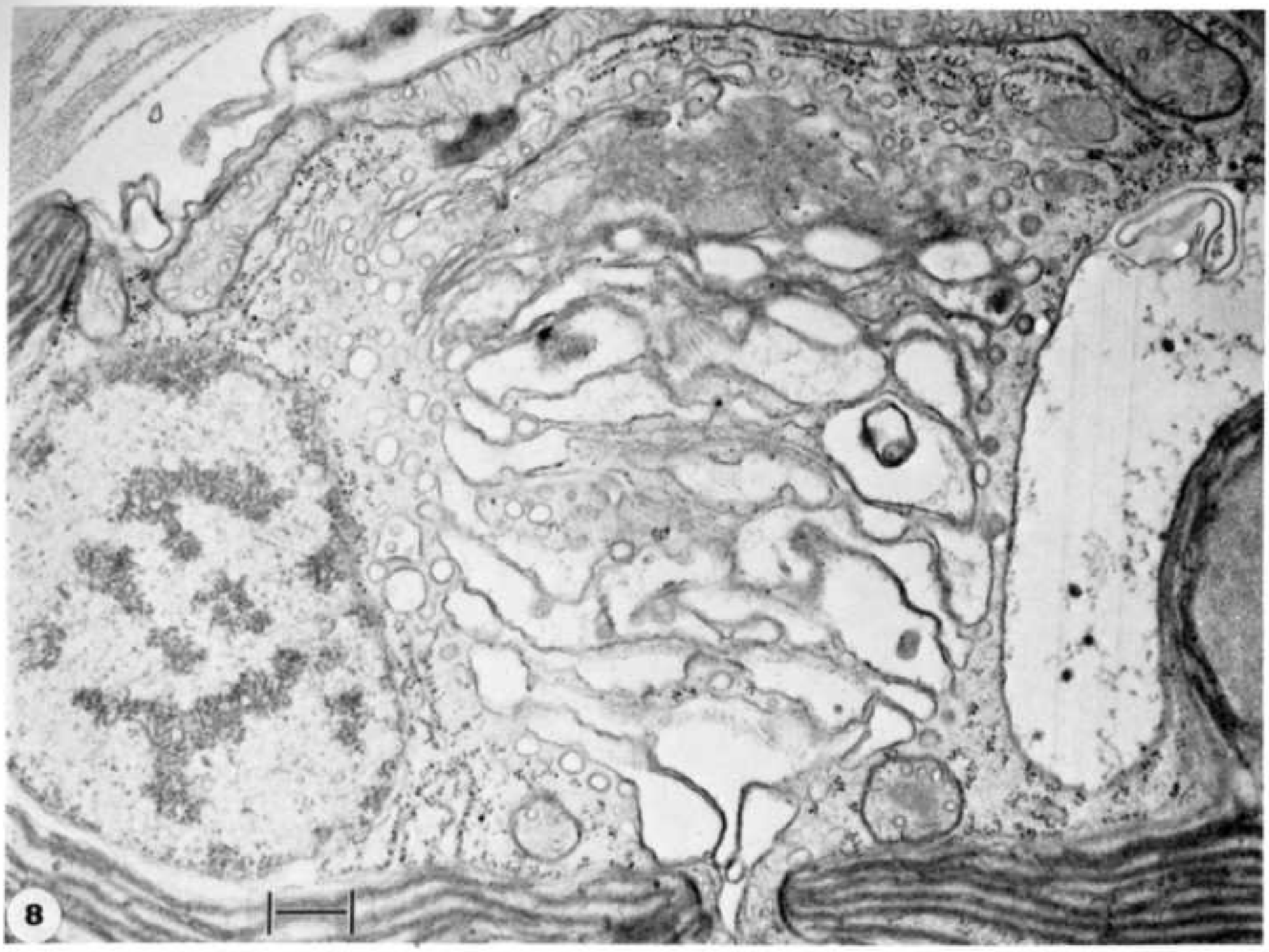

FIG. 8. This micrograph demonstrates the topographical differentiation of the amplexus into pre-Golgi stages before release into the forming face. Note the possible radial microfibrillar precursor pool still attached to the amplexus (arrow a) and the radial precursor pool integrated into the active Golgi apparatus (arrow b). The secreting face of the Golgi apparatus projects downward. (*Plenrochrysis*) Magnification bar = 1.0 μm.

acid oxidation. The result of such staining can be seen in Figure 9. The cell wall stains heavily as do the scales visible within the distal Golgi cisternae. Non-specific staining of membranes was also reduced by the PA treatment, which oxidizes bound osmium. The length of exposure to PA was quite critical in this reaction: a ten minute treatment was insufficient, while a fifteen minute treatment reduced staining by oxidizing the newly formed aldehyde groups to non-reactive carboxyl groups. That the staining observed was indeed due to oxidized polysaccharides was supported by the demonstration that if PA oxidation was followed with bisulfite, the aldehyde blockage would completely remove all reactivity. These results are summarized in Table I.

The most useful aspect of the PA-silver methenamine staining reaction was that it stained the radial microfibrils but not the spiral microfibrils (see Fig. 10), thus making it possible to distinguish between the two fibrillar components even before they were assembled into the distinctive morphological arrangement of the scale. In Figure 11 it is seen that the polymerization center and the double row of microfibrils observed by Brown et al. [9] stains with silver. This established the polymerization center as a pool of precursor products for the synthesis of the radial microfibrils, and the double-row configuration as an early step in the process of assembling these microfibrils into the quadriradial arrangement of the completed scale. Further observation of this region of the Golgi apparatus yielded more

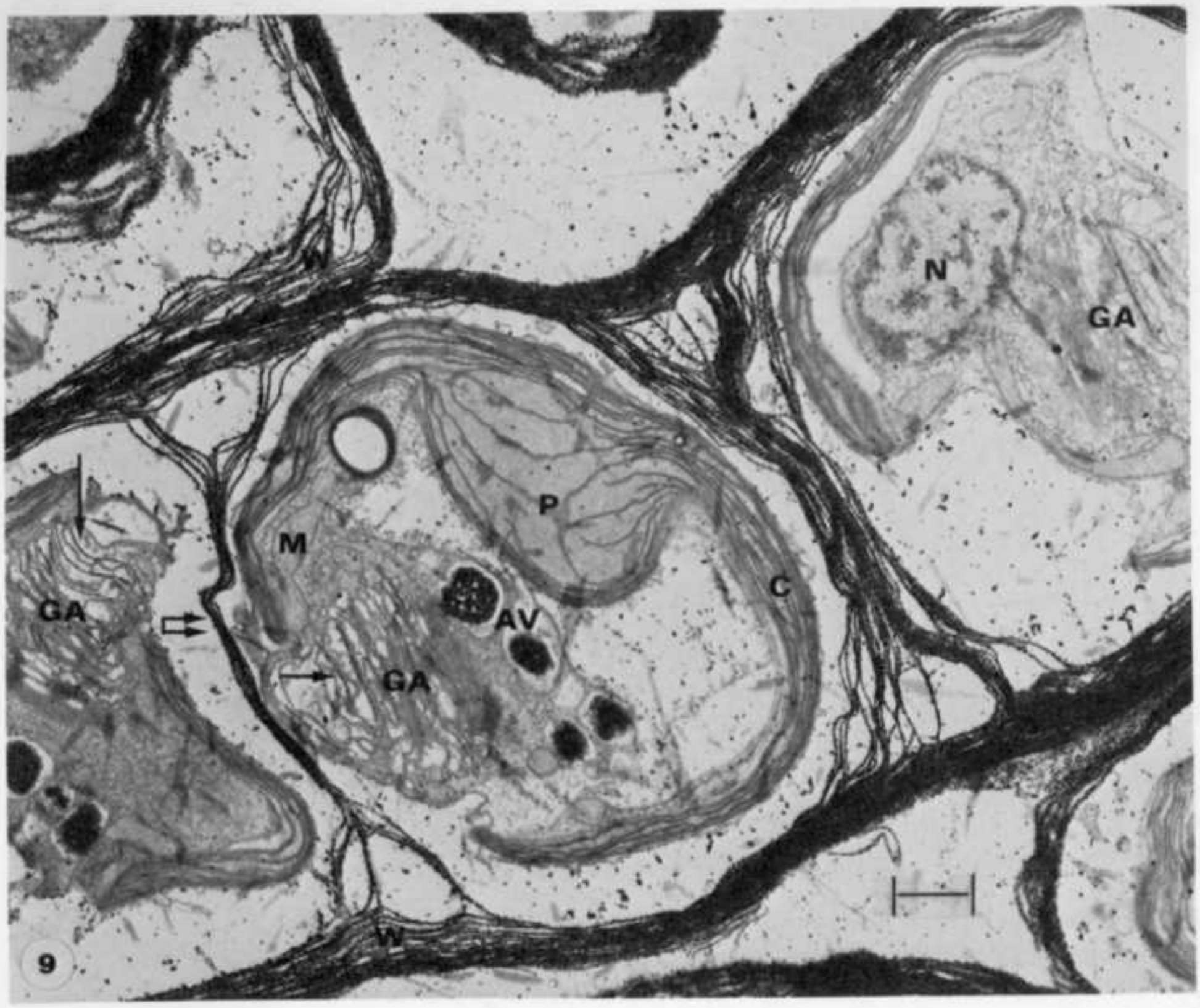

FIG. 9. Section of glutaraldehyde-osmium fixed vegetative cells of *Pleurochrysis*, stained for polysaccharide localization with periodic acid-silver methenamine an post stained with lead citrate. Magnification bar = 1.0 μ. Actively growing cells in the filamentous stage. Parietal chloroplast (C) with bulging pyrenoid (P), dense autophagic vacuoles (AV), nucleus (N), mitochondria (M), and Golgi apparatus (GA) are visible within the section. Dense silver deposition is evident on the wall (W) and intracisternal scales (arrows). Note the newly synthesized transverse wall (double arrow).

TABLE I

Silver Methenamine Staining[a]

Pretreatment	Spiral Microfibrils	Radial Microfibrils	Amorphous Polysaccharide	Membranes
None	–	+	+	+
Bisulfite[b]	–	+	+	+
Peroxide[c]	–	–	–	–
Peroxide-PA[d]	–	+	+	–
Peroxide-PA-bisulfite	–	–	–	–
Iodoacetate[e]	–	–	–	+
Iodo-PA	–	+	+	–
Iodo-PA-bisulfite	–	–	–	–

[a] + indicates staining, – indicates lack of staining.
[b] 2% sodium bisulfite, 60 minutes, 60° C.
[c] 10% hydrogen peroxide, 30 minutes, room temp.
[d] 1% periodic acid, 12 minutes, room temp.
[e] 0.1M iodoacetate, 60 minutes, 60° C.

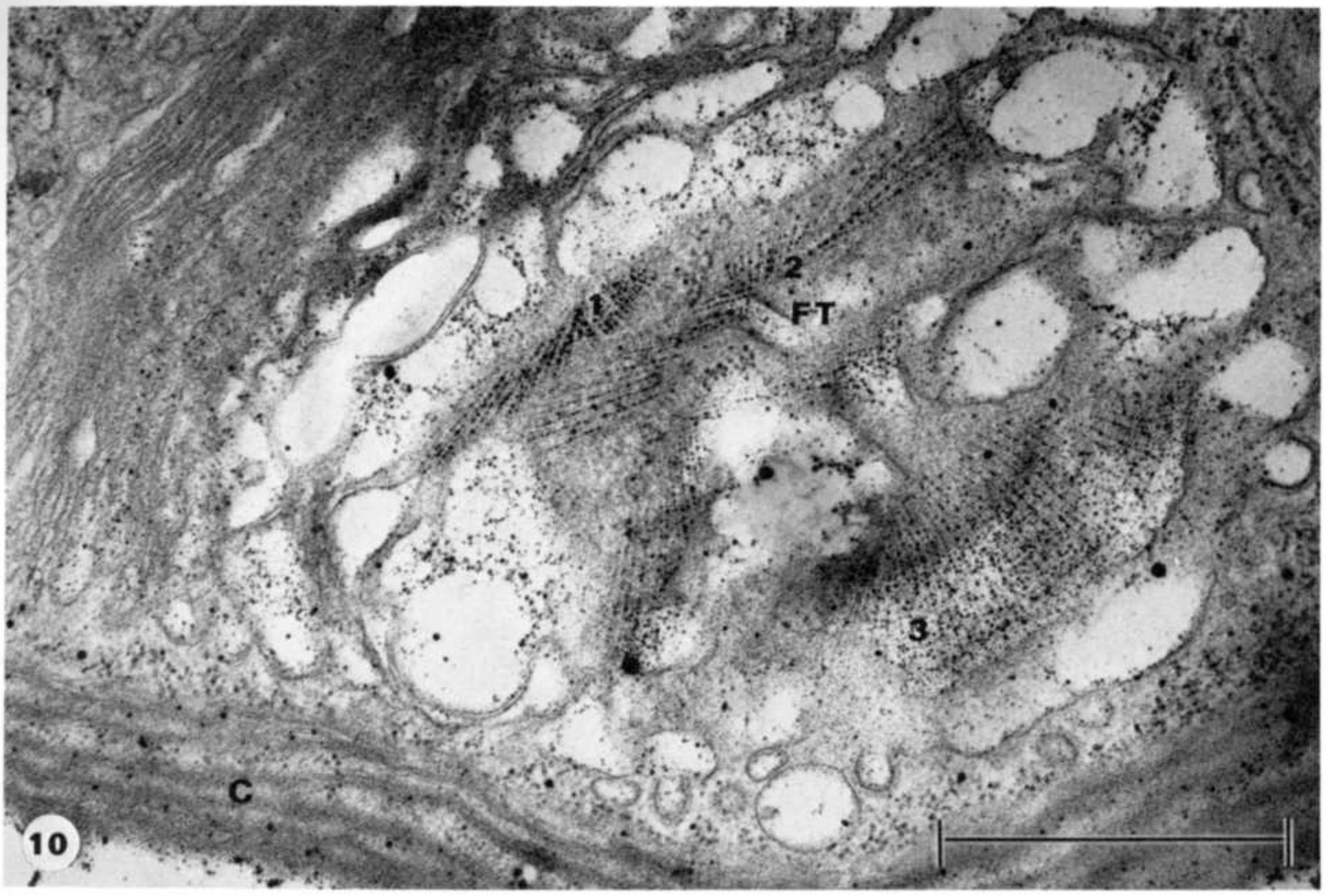

FIG. 10. Section of glutaraldehyde-osmium fixed vegetative cells of *Pleurochrysis*, stained for polysaccharide localization with periodic acid-silver methenamine and post stained with lead citrate. Magnification bar = 1.0 μm. Oblique section through the distal face of the Golgi apparatus. Visible is a folded radial configuration (1), and a recently unfolded radial network which is still elliptical (2) and which has a central feeding tubule (FT). In the completed scale (3), spiral microfibrils are visible from the lead citrate post-staining.

oblique views of the double row of microfibrils (Fig. 12). The mechanism of quadriradial synthesis and assembly has been clarified with the observation of double-row configurations almost perpendicular to their typical orientation, that is, at right angles to the normal long axis of the Golgi cisternae as seen in cross-section (Fig. 13). Considering the cross-sectional appearance of the entire cisterna, this configuration has been termed the Z-stage [10]. Taking into account this sequence of static configurations, it was concluded that the transformation of a double row of parallel microfibrils into the single-layered quadriradial arrangement could best be described as an unfolding of the radial microfibrils [10]. Once unfolded, the radial arrangement is still somewhat compressed along one axis as a result of the parallel arrangement of the microfibrils in the folded configuration. The transition from this slightly elliptical arrangement to the typical quadriradial arrangement is best seen in Figure 10.

From Figure 10 it can also be seen that the spiral microfibrils are not stained by the PA-silver methenamine reaction, but can be observed through standard lead post-staining. Despite the lack of staining, some insight into the synthesis of the spiral microfibril was gained from purely morphological evidence. Numerous micrographs revealed a tubule on the distal side of the cisterna containing unfolded radial microfibrils (Figs. 10, 14, and 15). In certain views, the opposite end of the tubule expanded into a dilated cisternal region. From this evidence, and the fact that spiral microfibrils are always on the distal side of the radial microfibrils [9],

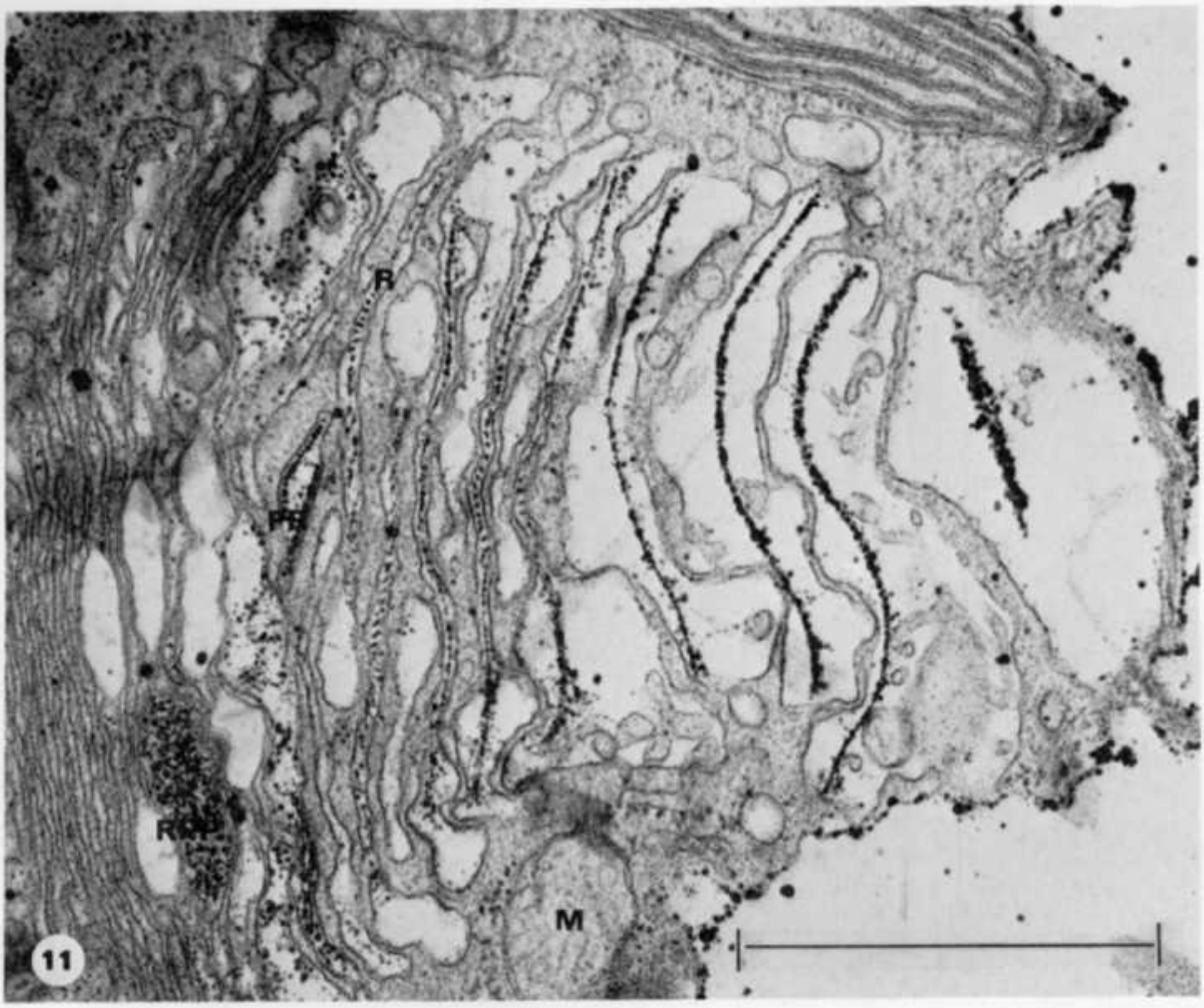

FIG. 11. Transverse section through a Golgi apparatus, with the distal face toward the right. Note the radial precursor pool (RPP) and folded radial configuration (FR) with an unfolded radial network (R) immediately distal to it. PA-silver methenamine staining followed by lead citrate. Magnification bar = 1.0 μm.

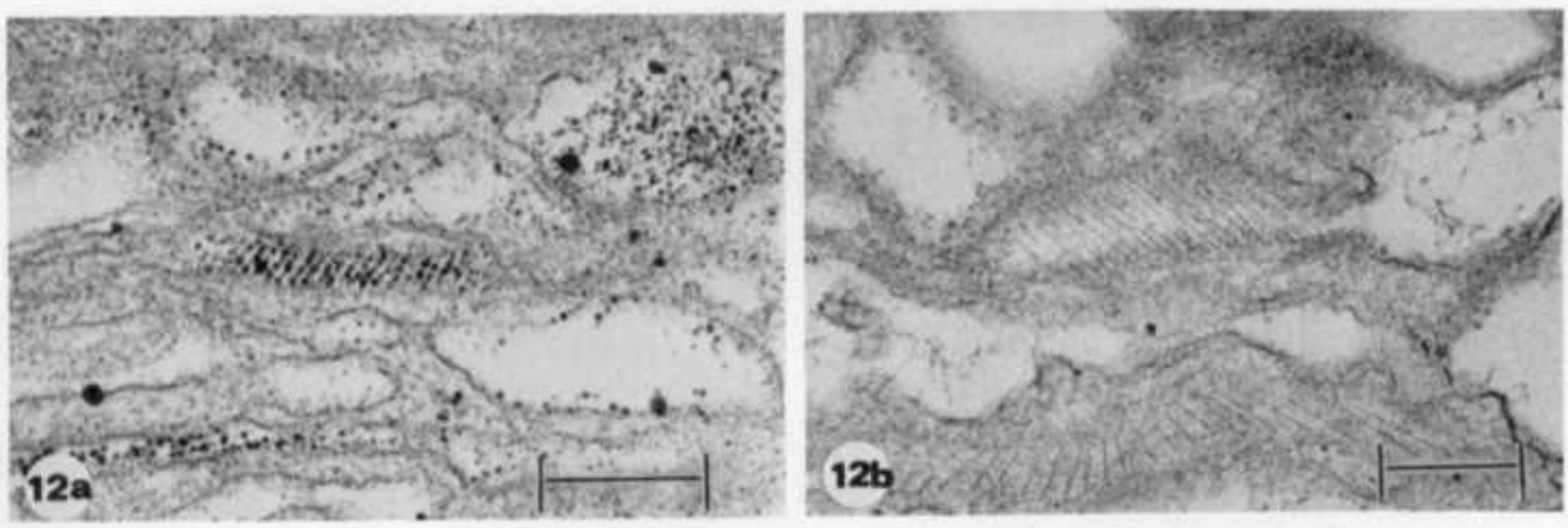

FIG 12. Longitudinal section of folded radial configuration, showing parallel radial microfibrils. Distal face of the Golgi apparatus is downward. (a) PA-silver methenamine localization on radial microfibrils. (b) Standard lead citrate post staining. Magnification bar = 0.1 μm.

the central feeding tubule has been tentatively advanced as the site of spiral microfibril synthesis (Figs. 16–21) [10].

The process of amorphous polysaccharide addition is best seen in Figure 15. In successive cisternae toward the distal face, the scale profile becomes thicker centripetally as the densely staining amorphous polysaccharide is deposited. Accom-

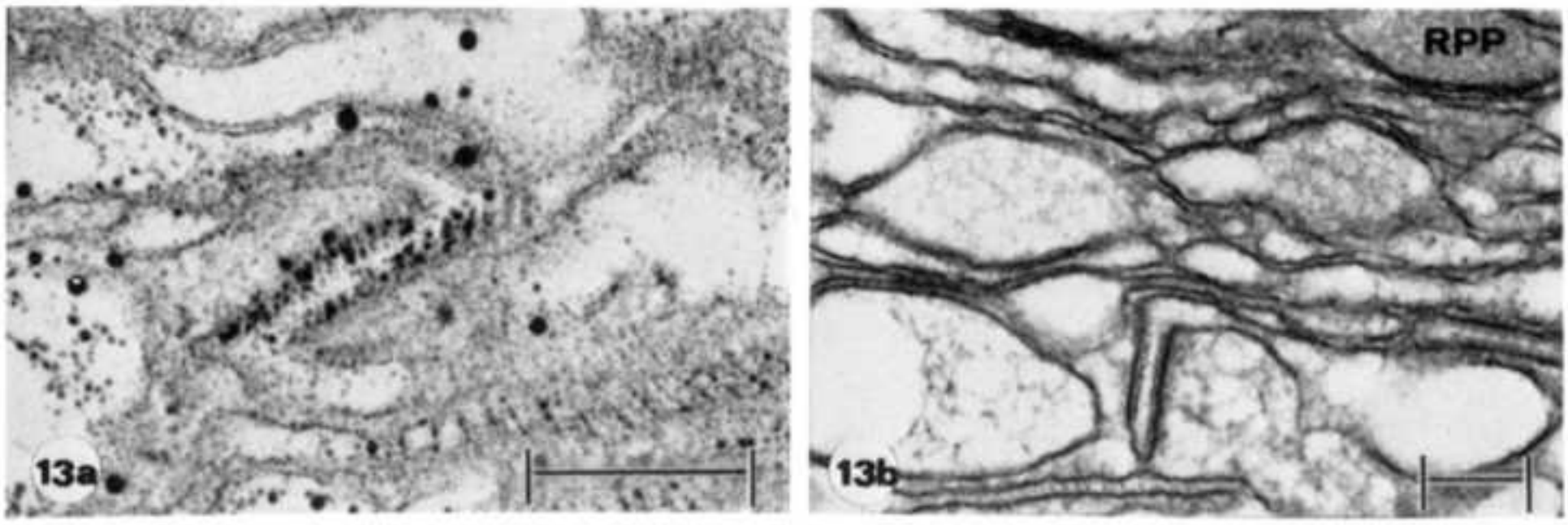

FIG. 13. Z stage of folded radial configuration, distal face downward. (a) PA-silver methenamine localization on the radial microfibrils. (b) Post-fixed with osmium-Ruthenium red. Note also the radial precursor pool (RPP). Magnification bar = 0.1 μm.

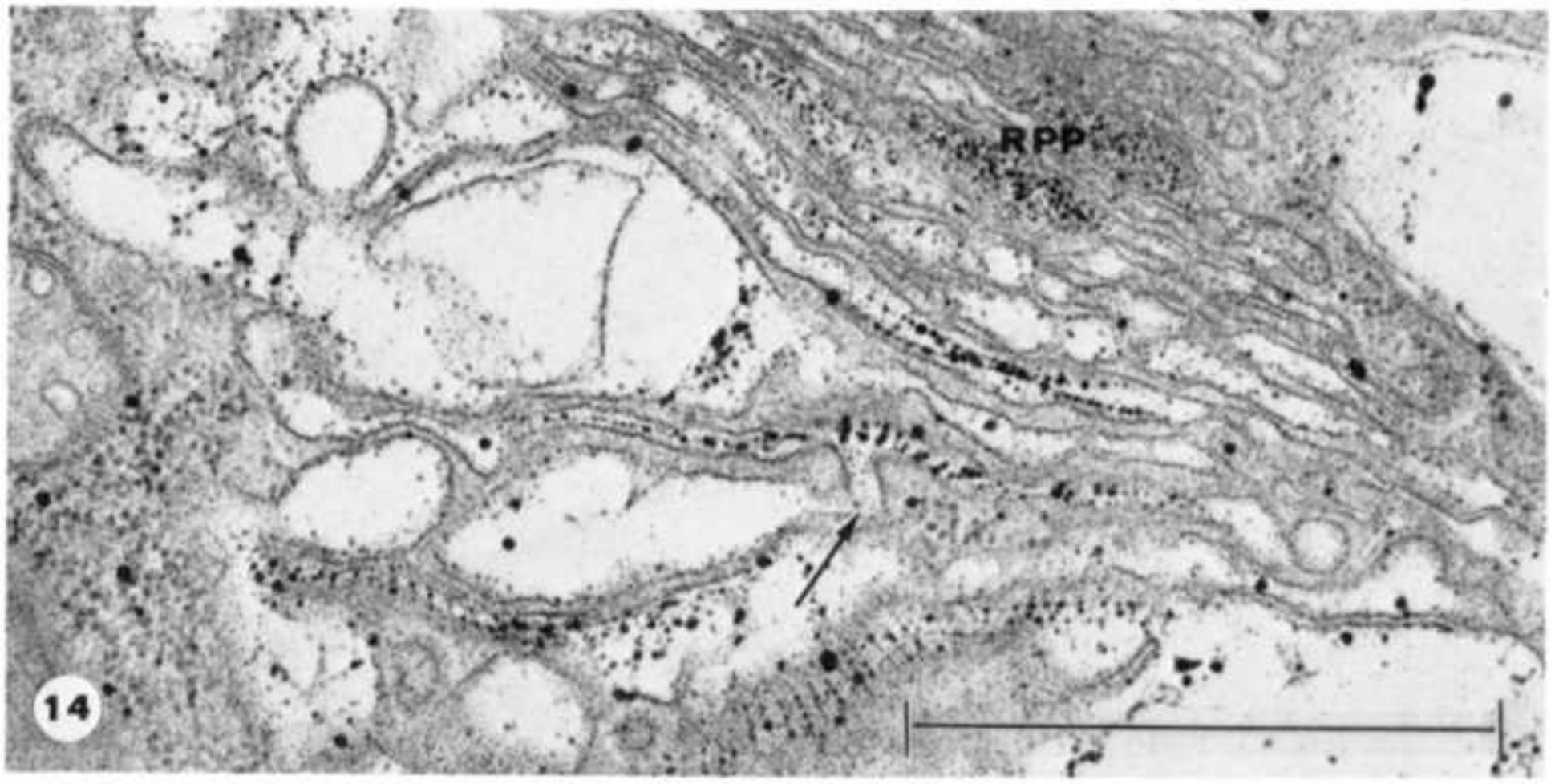

FIG. 14. Median section through the Golgi apparatus, distal face downward, showing a presumed central feeding tubule (arrow) opening onto a dilated cisternal region. PA-silver methenamine polysaccharide localization, post-stained with lead citrate. Magnification bar = 1.0 μm.

panying the increased staining is a dilation of the cisternal space, which, when completed, leaves the scale completely free of membrane contact. From the presence of small staining strands between the scale and the cisternal membrane, and the fact that the amorphous polysaccharide is quite hydrated, it is likely that the entire inflated cisterna is filled with the amorphous subcomponent which subsequently collapses from dehydration during processing.

Silver methenamine staining thus established a similarity between the radial and amorphous subcomponents, and indicated the presence of two moieties: one polysaccharide and the other possibly peptide. These results have been confirmed by the chemical analysis of isolated scales, as will be demonstrated in the second paper of this series. More importantly, the evidence from this staining procedure permitted subdivision of the Golgi apparatus into regions, which are distinct with respect to the biogenic events occurring in them, and also which can be identified on a strictly morphological basis. This morphological subdivision was invaluable in interpreting the results of enzyme localizations, considered in a later section.

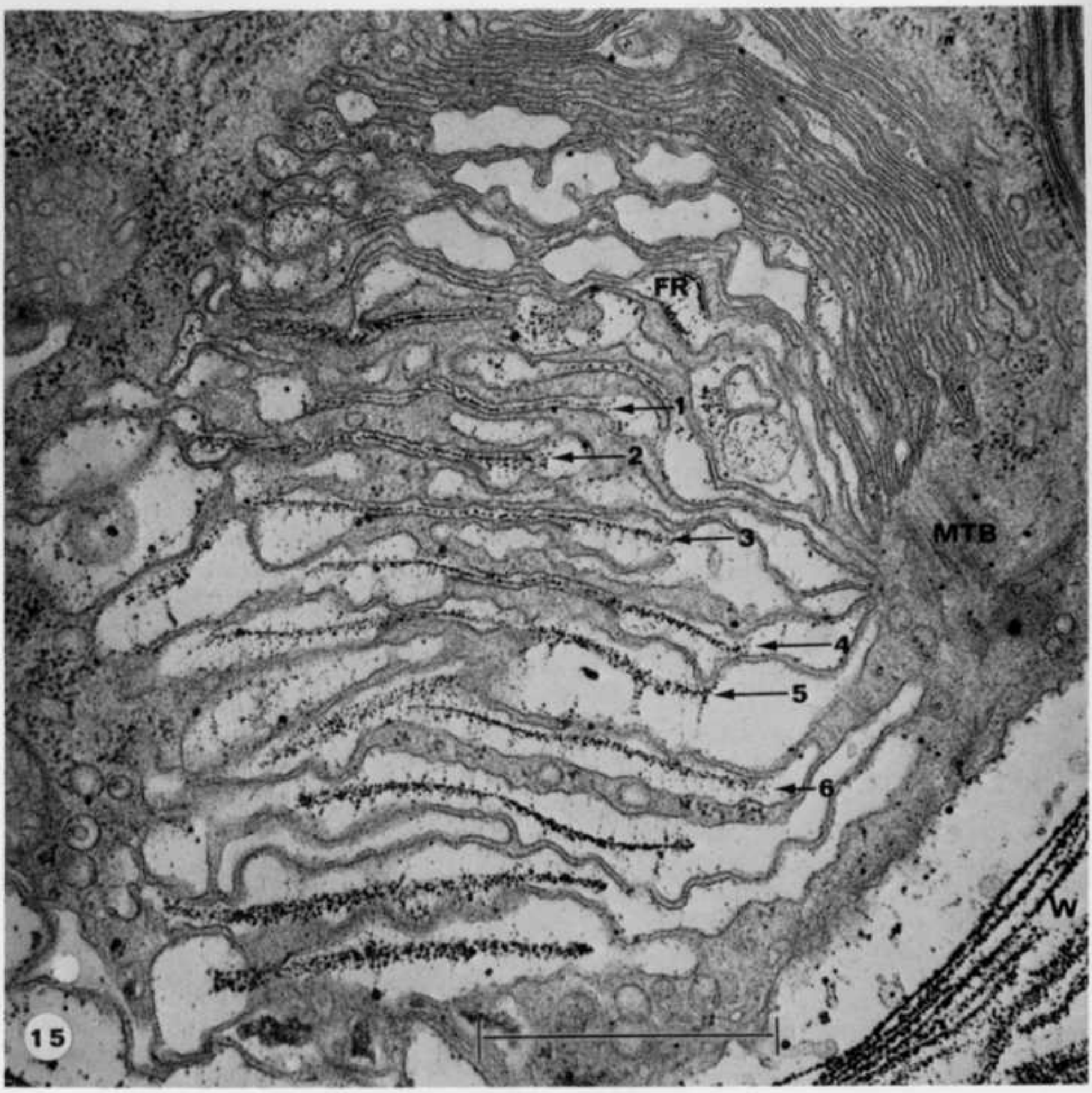

FIG. 15. Median transverse section through a Golgi apparatus, distal face downward. Note the folded radial configuration (FR), and the orientation of the cisternae toward the microtubular bundle (MTB). The increased staining profile (1 to 6) indicates the centripetal addition of the amorphous polysaccharide. Note the cell wall (W) in the lower right . PA-silver methenamine polysaccharide localization, with lead citrate post-staining. Magnification bar = 1.0 μm.

Scale Transport and Exocytosis

Attention will now be directed toward developments regarding the fate of the Golgi membranes and the regulatory mechanisms for controlling scale exocytosis. Two bundles of microtubules flank the secreting face of the Golgi apparatus (Fig. 23). These bundles consist of microtubules organized in a hexagonal array [8]. The microtubules terminate in a T-system where a single row of microtubules overlays the bundle. Microtubules have been observed in association with a sub-surface cisternal sac which lies adjacent to the plasma membrane, completely encompassing the cell except for the region immediately opposite the secreting face of the Golgi apparatus [8]. The microtubular bundle and sub-surface cisterna were first recognized from freeze-etch preparations in which no previous treatment with glycerol or glutaraldehyde was necessary. Earlier fixations failed to preserve

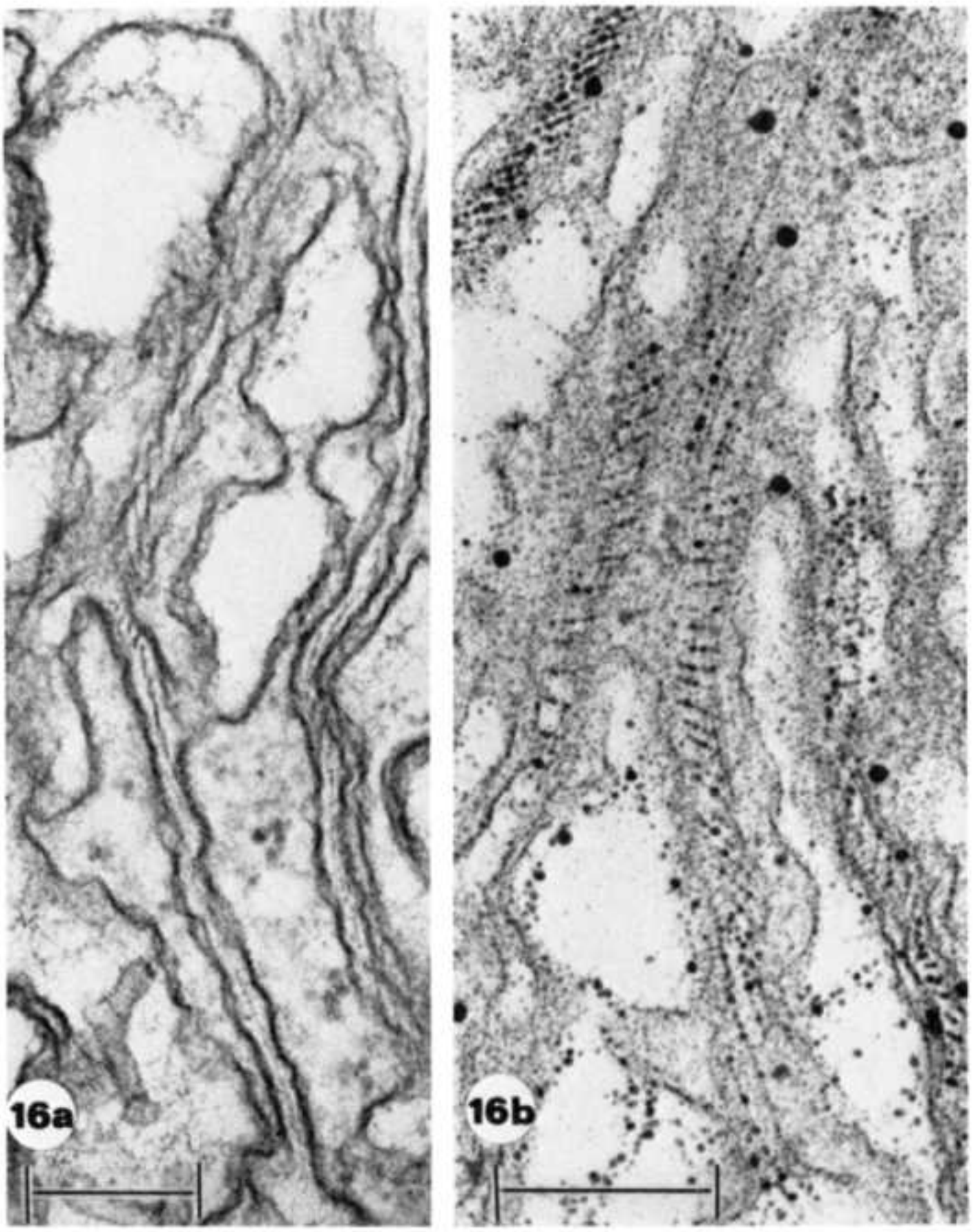

FIG. 16. Partially unfolded radial networks which exhibit a funnel or basket-shaped configuration, distal face downward or to the right. (a) Lead citrate post-staining. (b) PA-silver methenamine polysaccharide localization. Magnification bar = 0.1 μm.

the structure of the sub-surface cisterna. Subsequent improvements in the fixations, which included careful control of the osmolarity of the fixative as well as the use of tannic acid as a preservative with the glutaraldehyde [30, 31, 69], yielded new data on the structure and composition of the sub-surface cisternal sac. These refinements have revealed additional components, namely, plasmalemma invaginations extending into the sub-surface cisternal sac (Figs. 24–26). With the tannic acid fixation, myleinized membrane and "spherule" figures were preserved in the lumen of the sub-surface cisternal sac (Fig. 24). Furthermore, continuity of the sub-surface cisterna with the autophagic vacuolar system has been confirmed.

In order for exocytosis to occur, membranes of the Golgi apparatus must fuse with the plasma membrane. As described above, the plasmalemma invaginations may serve as specific loci for fusion with the Golgi cisternae. Are there specific regions of Golgi membrane which have the capacity to recognize plasmalemma invaginations? The periphery of the Golgi cisternae are characterized by distinct coatings (Fig. 23). These regions are not unlike the familiar "coated vesicles" which bud from the periphery of the Golgi cisternae [19]. An exception is that the coated regions have never been observed detached from the cisternae in *Pleur-*

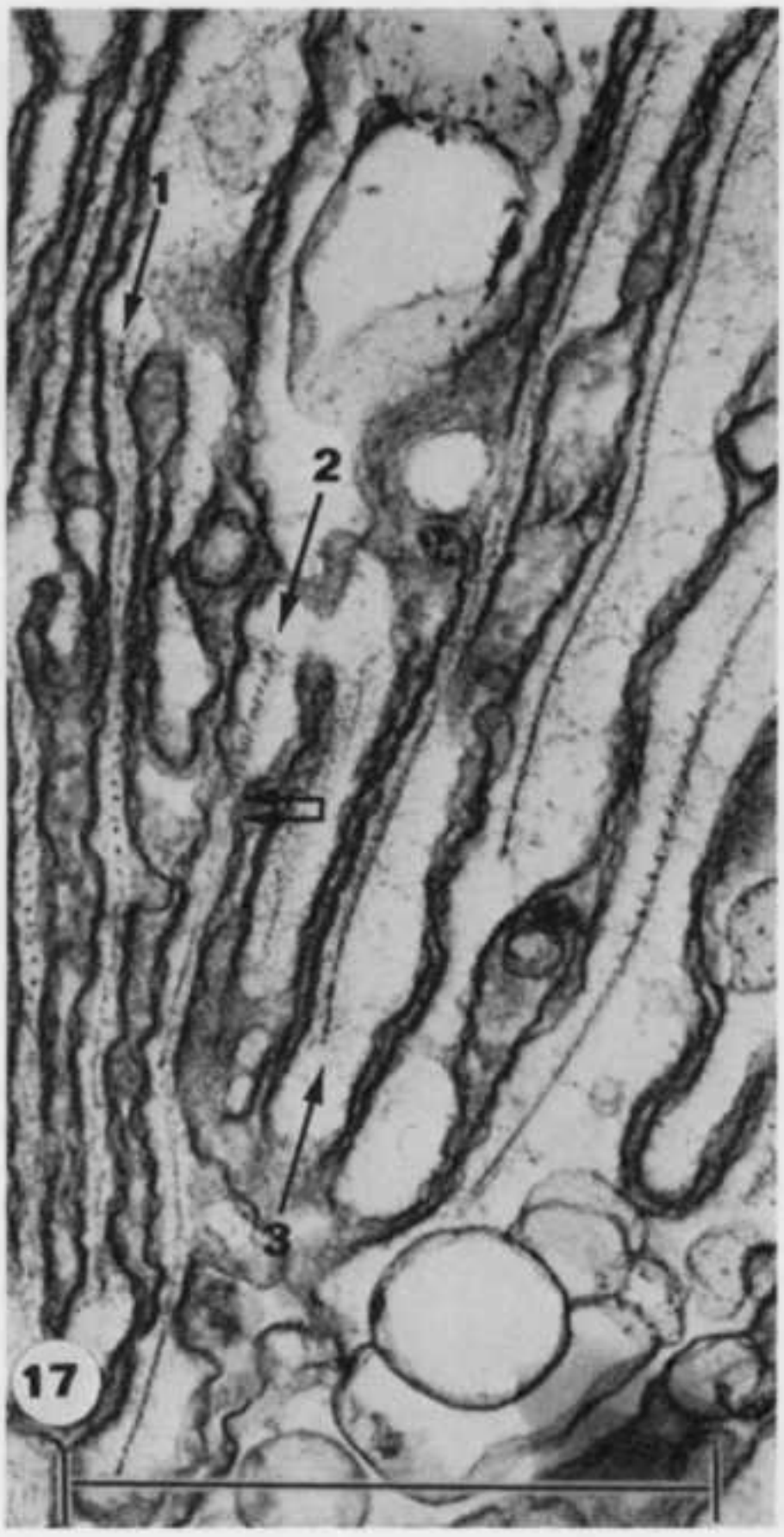

FIG. 17. Distal region of the Golgi apparatus showing the centripetal addition of the spiral microfibrils (1 to 3), distal face downward or to the right. At 2, note the proximity of the cisternal membranes to the radial microfibrils at the site where the spiral microfibrils are being added (double arrow). Post-stained with lead citrate. Magnification bar = 1.0 μm.

ochrysis. Since these coated regions of the Golgi cisternae are found in close proximity with the plasmalemma invaginations, they could represent recognition sites on the Golgi membrane which associate with and are involved in scale exocytosis.

Direct proof for the coated vesicle plasmalemma invagination association is lacking; however, treatments with colchicine have revealed interesting results, namely, the complete inhibition of scale exocytosis within 90 min after treatment [7]. The earliest effect of colchicine is observed after 15 min, at which time the plasmalemma invaginations cluster (Fig. 27). Within 30 min after treatment, the plasmalemma invaginations disappear. Scale production continues for several hours, but since exocytosis is blocked, intracellular digestion is initiated with the fusion of adjacent outermost cisternae. The cisternal vesicles contain several scales in each. In Figure 28, several stages of intracellular scale accumulation can be observed as well as autophagic vacuolar digestion of the scales.

During this investigation of scale exocytosis, we did not exclude the possibility of the plasmalemma invaginations having endocytotic functions. Cationized ferritin was selected as a tracer to test for the occurrence of endocytosis. Although the

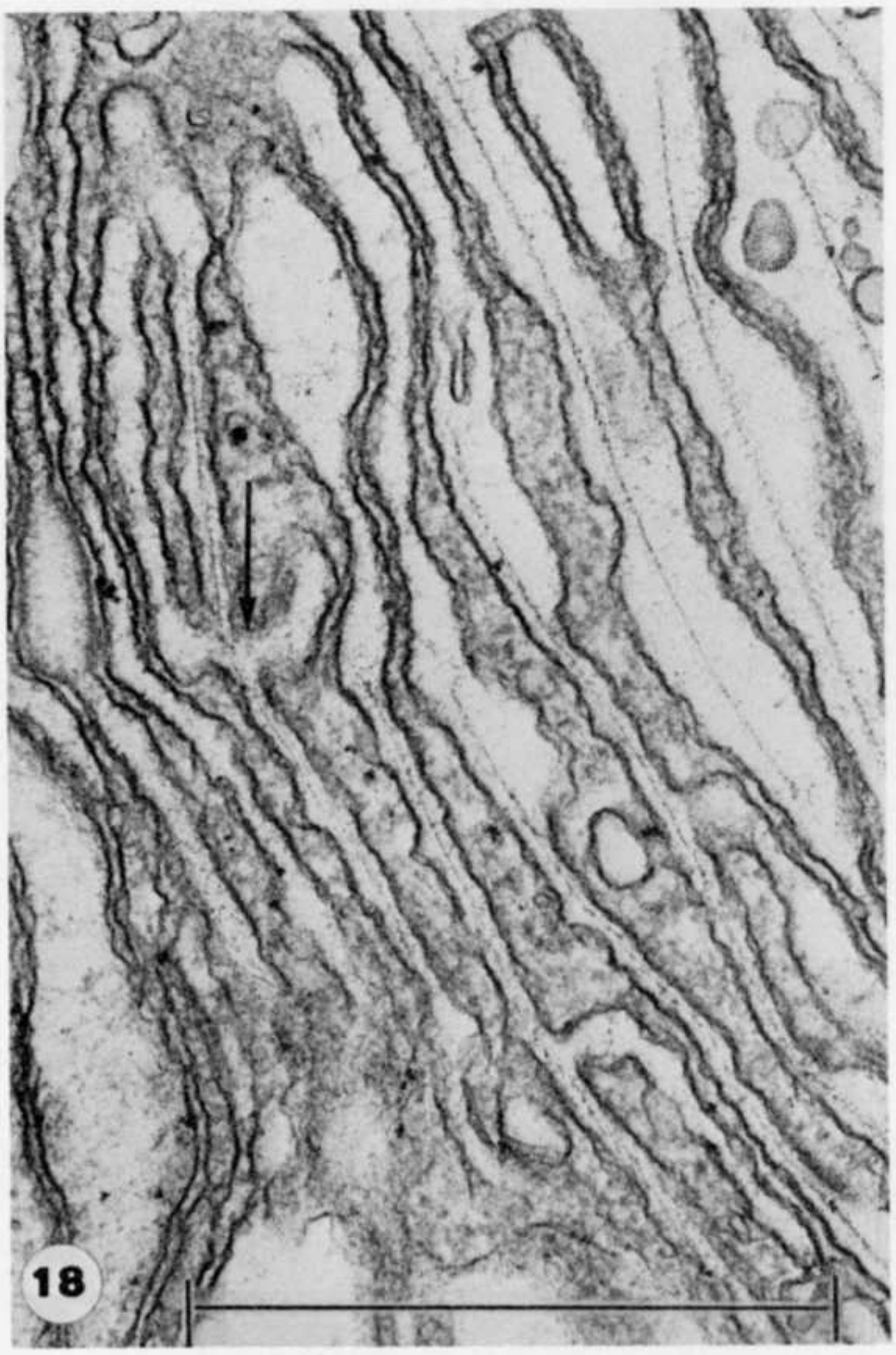

FIG. 18. Cisterna illustrating proximal and distal feeding tubule complex (arrow), distal face downward or to the right. Lead citrate post-stain. Magnification bar = 1.0 μm.

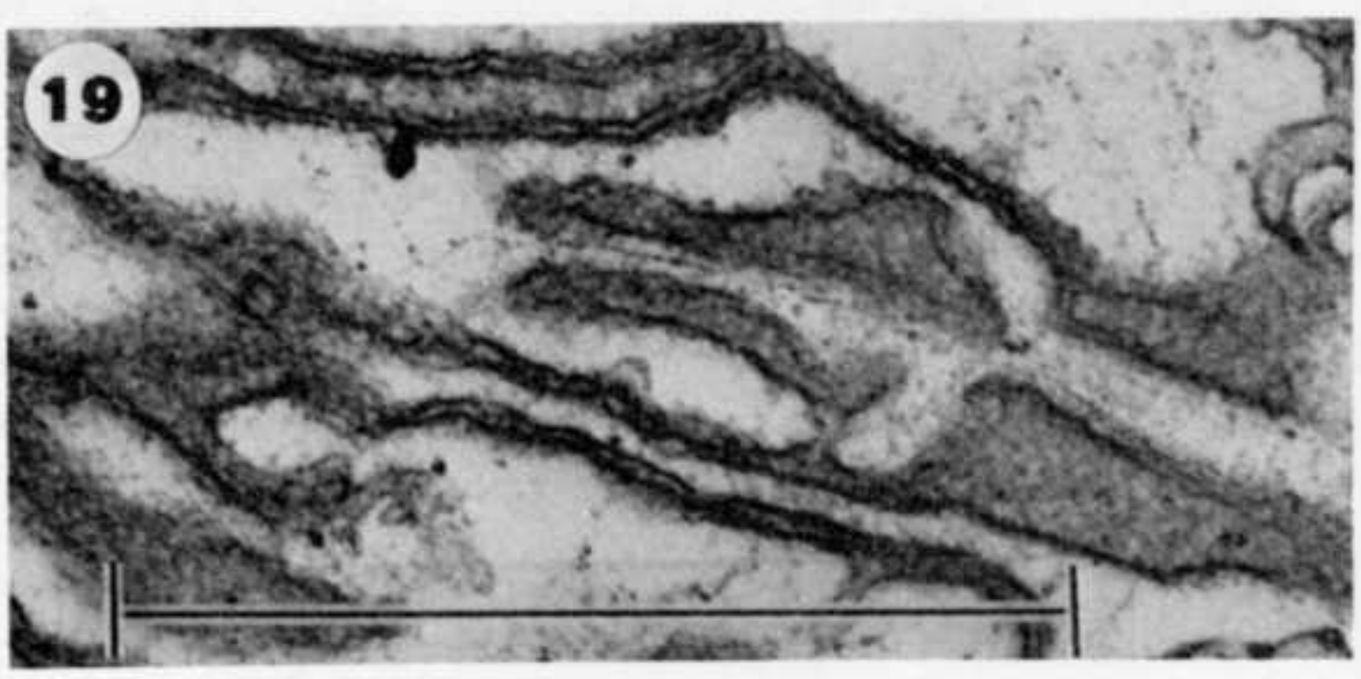

FIG. 19. Cisterna showing confluence between the proximal and distal central tubules, and the region of the lumen which contains the scale, distal face downward or to the right. Lead citrate post-stain. Magnification bar = 1.0 μm.

ferritin associated with the plasma membrane and the negatively charged sulfate groups on the radial microfibrils of the scales, it was never observed within the cell, suggesting that the plasmalemma invaginations do not function as endocytotic vesicles. Thus, an alternative choice for the role of the plasmalemma invaginations is that of exocytotic vesicles, although we have no direct experimental proof for this function.

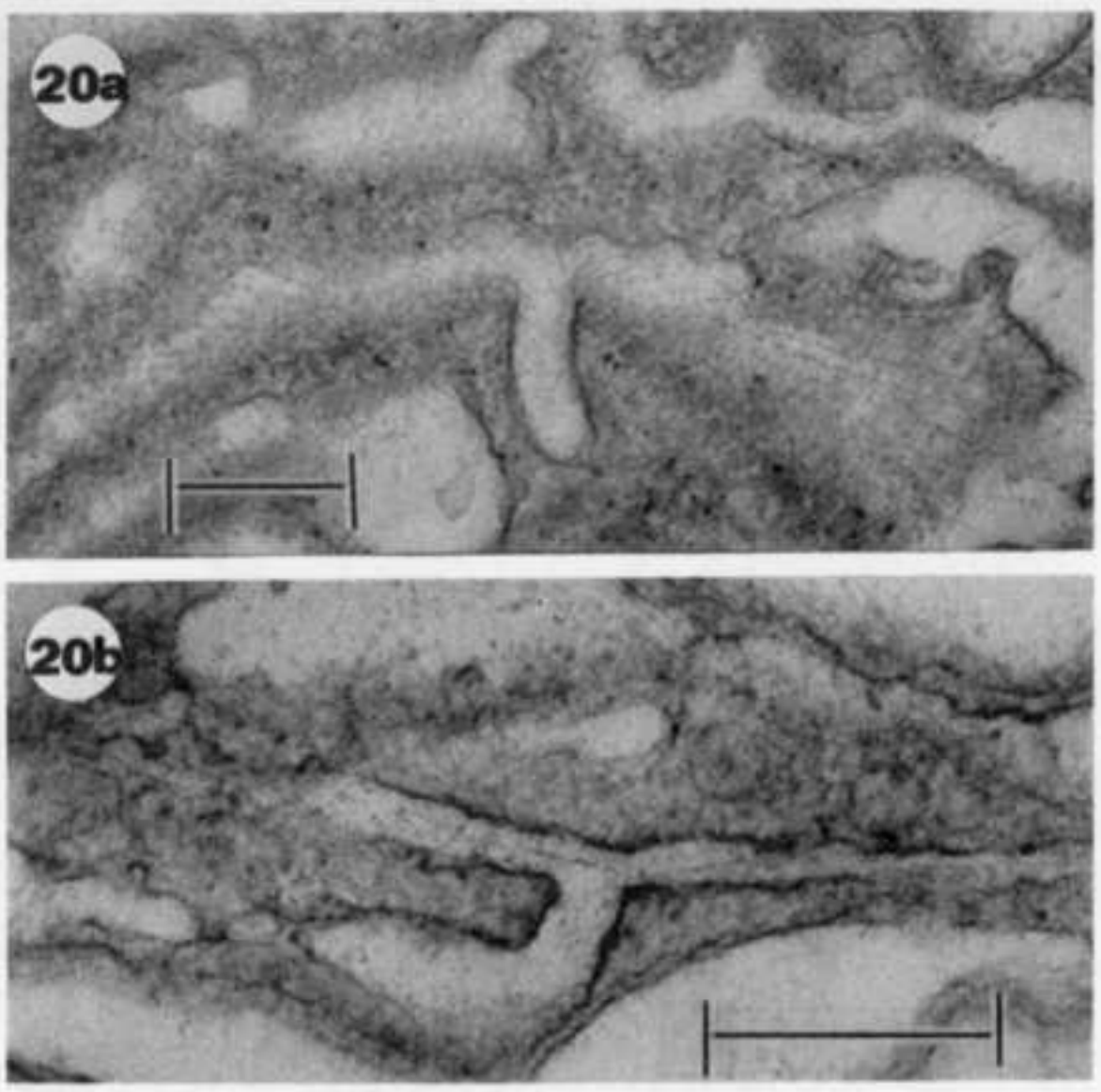

FIG. 20. Central feeding tubules, distal face downward or to the right. No spiral microfibrils are visible. Post-stained with lead citrate. Magnification bar = 0.1 μm.

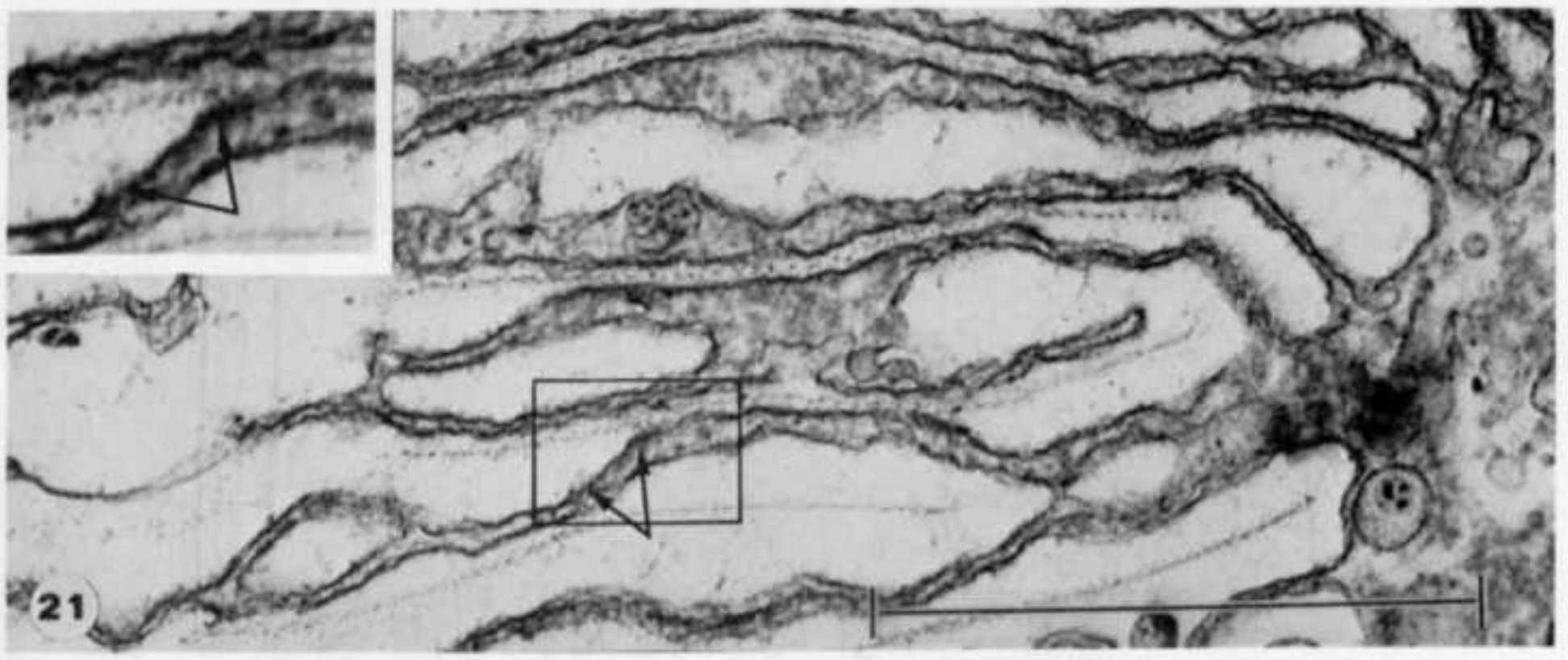

FIG. 21. Section through the Golgi apparatus at the region of spiral microfibril synthesis, distal face downward. Small granules (granule bands?) on the membrane are visible at the site of spiral microfibril addition (arrows; see inset). Lead citrate post-staining. Magnification bar = 1.0 μm.

Enzyme Localization

The localization of aryl sulfatase as the hydrolysis of p-NCS was identical with both barium and copper capture [109]. The barium sulfate reaction product can be seen in Figure 29, localized on radial microfibrils in the folded (double-row) configuration and immediately adjacent to a radial precursor pool. Compare this appearance with the folded radials in Figure 15, stained for polysaccharide localization. With copper as the capture reagent, the localization was similar, but at

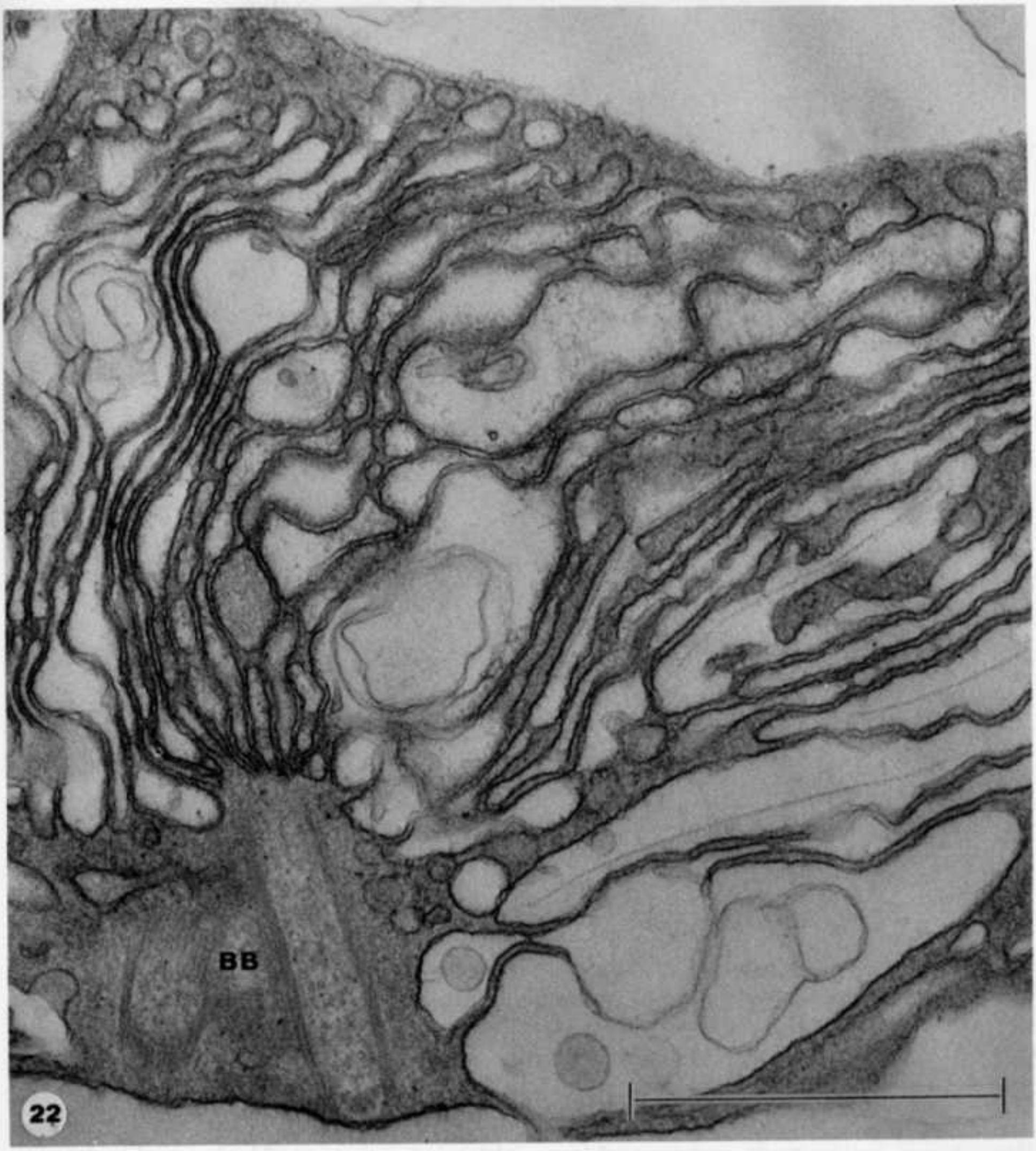

FIG. 22. Median section through the Golgi apparatus revealing the orientation of the cisternae in relation to the basal body complex (BB). Magnification bar - = 1.0 μm.

times the product filled the entire cisternal lumen (see Fig. 30), while at other times it was deposited only on the radial microfibrils themselves (see Fig. 31) as with barium capture. Within any batch of cells processed together, the deposition pattern was the same. Variation arose only between batches processed at different times. It is possible that localization only on the microfibrils is an artifact arising from fixation, with the fixative causing the enzyme to stick to the highly charged radial microfibrils. In any case, the reaction was specifically localized within only one to three cisternae in the region of radial microfibril synthesis. The enzyme is active for only a short period of time, as evidenced by Figures 32 and 33, which show inactive folded radial configurations immediately distal to active ones. The presence of precipitate on chloroplast membranes is a control reac-

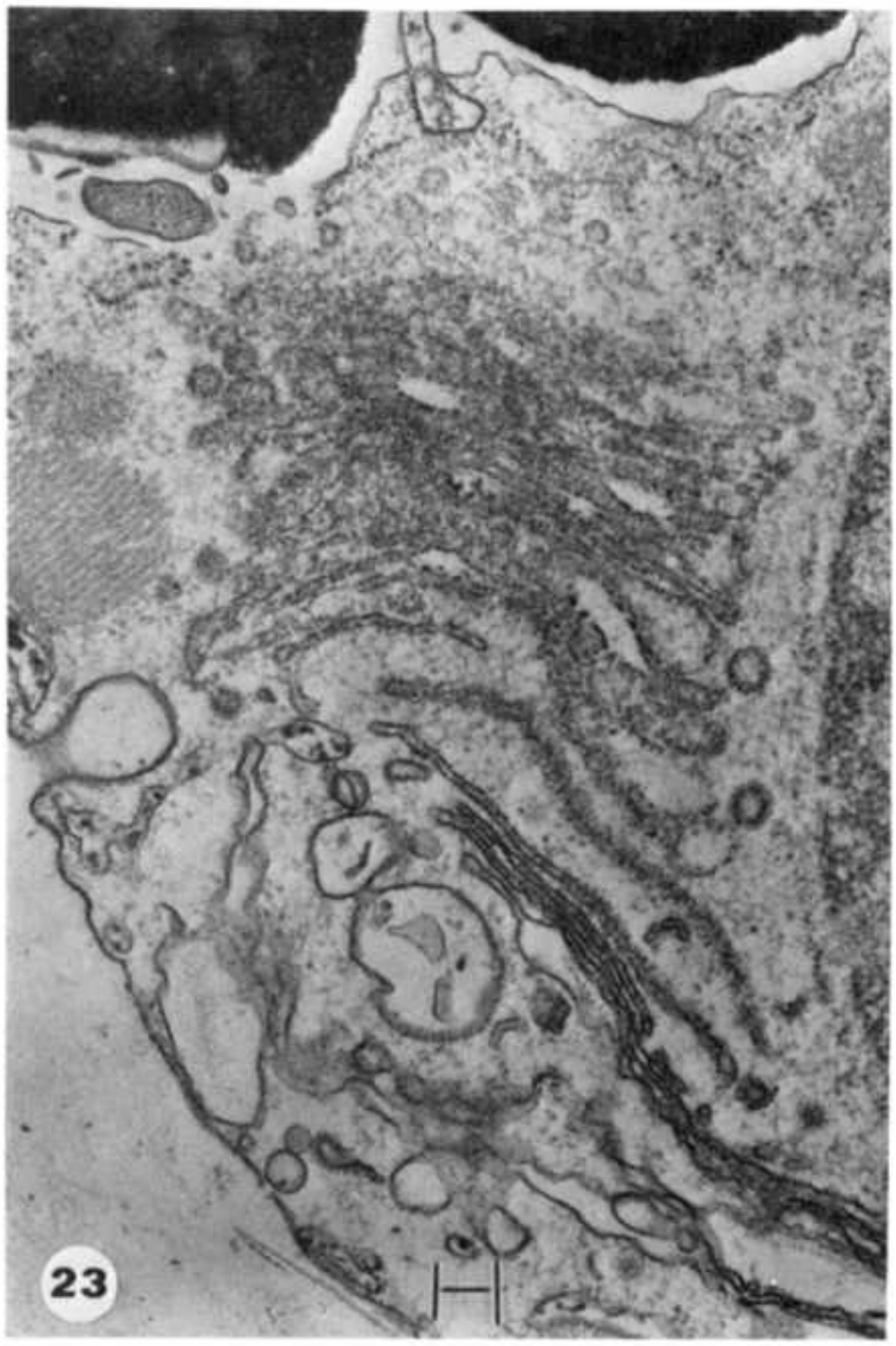

FIG. 23. Thin section demonstrating the plasmalemma invagination recently exposed on the cytoplasmic side by microtubular action on the subsurface cisterna. Note the proximity of the plasmalemma invagination to the coated vesicles associated with the periphery of the Golgi cisternae. Nucleus at far right. Magnification bar = 0.1 μm.

tion of the cupric ferricyanide medium resulting from the oxidative and reductive capabilities of gluteraldehyde-fixed chloroplasts [79].

Alkaline phosphatase (or nucleotide diphosphatase) activity, localized as the hydrolysis of the nucleotide diphosphates TPP and GDP, was present in the proximal and distal regions of the Golgi apparatus. Both substrates yielded a strong reaction in the distal region of spiral microfibril and amorphous polysaccharide synthesis, as seen in Figures 34–36. In a near-median cross-section of the distal region, the reaction product increases centripetally in successively distal cisternae, resulting in exactly the same profile as that observed with PA-silver methenamine staining (compare Fig. 15). Figure 37 is a section partially in the plane of the scale, substantiating the centripetal nature of the reaction. Considering the cellulosic nature of the spiral microfibrils, it was thought that the alkaline phosphatase reaction in the distal Golgi region might be involved in glycosyl transferase activity. However, when zoospores, which do not synthesize the amorphous polysaccharide, were incubated in the alkaline phosphatase medium, reaction product was not found in the distal Golgi region, indicating that the localization in vegetative

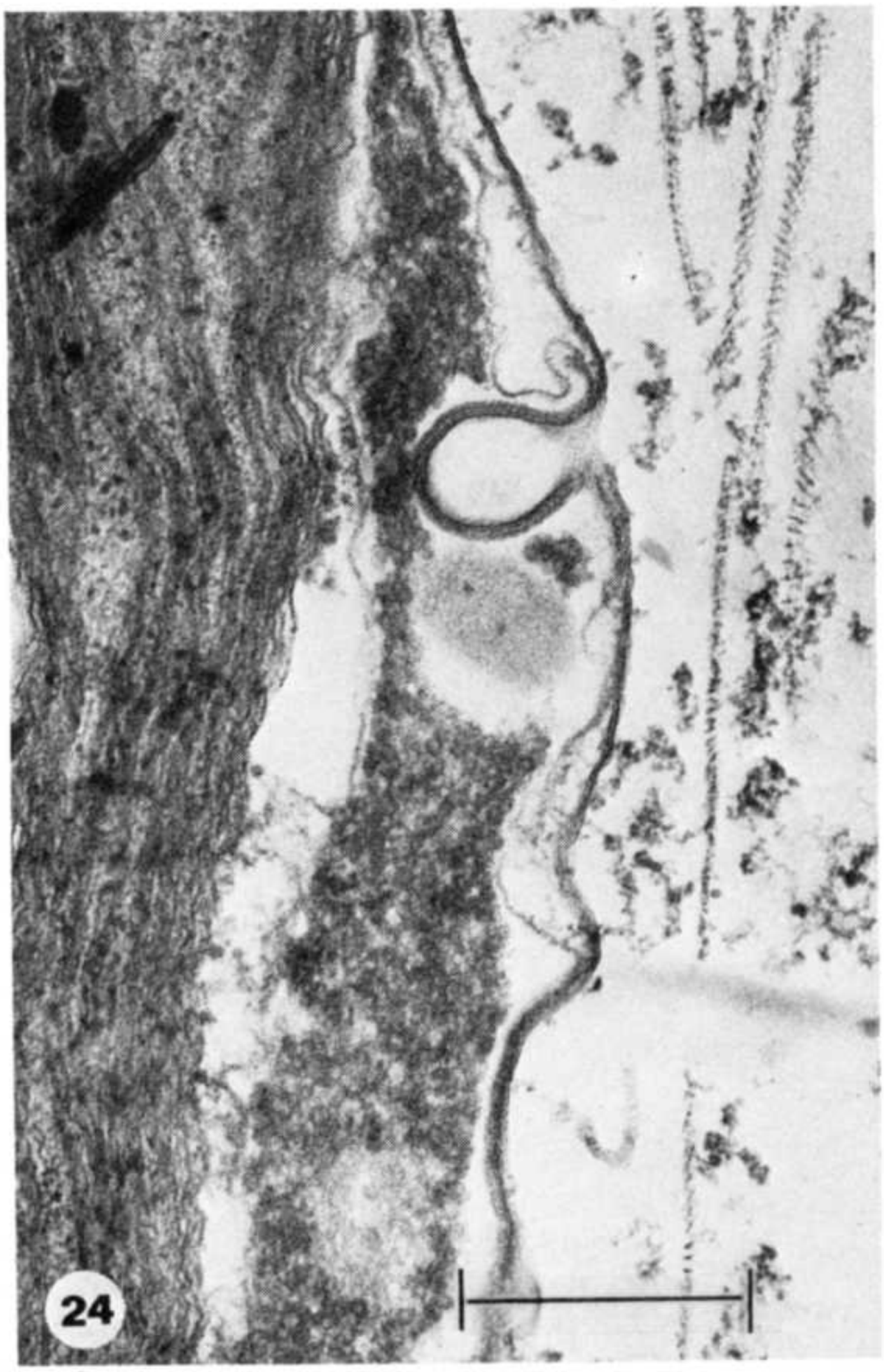

FIG. 24. Thin section (glutaraldehyde-tannic acid fixation procedure) illustrating the plasmalemma invagination and its relationship with the subsurface cisterna. Note the "spherule" electron-dense material within the lumen of the subsurface cisterna. Magnification bar = 0.1 μm.

is related to amorphous polysaccharide synthesis rather than spiral microfibril synthesis. Alkaline phosphatase activity at the proximal or forming face was sensitive to the substrate used. With GDP as substrate, localization in the proximal region was heavy (Fig. 35 and 36), while with TPP the reaction was quite sparse (Fig. 34). It is likely that GDP is the more natural substrate, in light of the role of GDP as a carrier of monosaccharides in polysaccharide synthesis [84, 40, 103].

The Golgi region in which acid phosphatase activity was localized depended upon the substrate present in the incubation medium. With DDNTP as the substrate, the reaction product was presented only in the region of radial microfibril synthesis (Figs. 38 and 39). Since the cupric ferricyanide incubation medium was the same as that used for aryl sulfatase localization, similar variation in reaction product was encountered. Figure 38 is an example of the reaction filling the entire cisternal lumen, while in Figure 39 the product is present only on the radial microfibrils of a folded configuration. With lead capture and β-GP as the substrate, the reaction product was localized at the distal Golgi region and in the subsurface cisterna which underlies the plasma membrane (Figs. 40 and 41). As seen

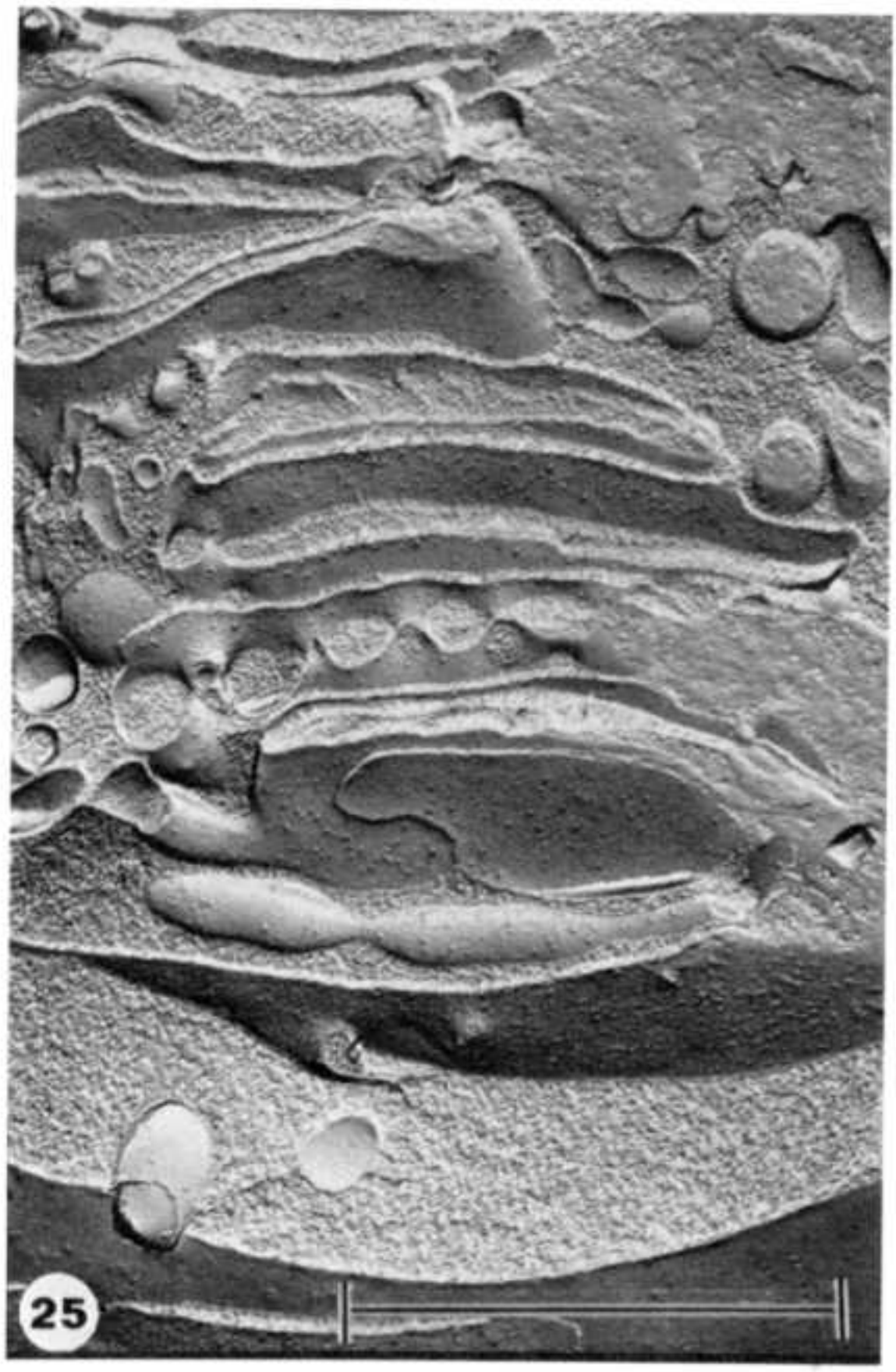

FIG. 25. Freeze-etch replica of the Golgi apparatus and the subsurface cisterna with a plasmalemma invagination. Magnification bar = 1.0 μm.

from Figure 40, this acid phosphatase activity did not coincide with the addition of the spiral and amorphous subcomponents, as was shown for alkaline phosphatase (compare with Figs. 34–36). Rather, the acid phosphatase activity appeared only in the distal-most cisternae after polysaccharide synthesis had been completed, while alkaline phosphatase activity was present in the region of spiral and amorphous synthesis and not at the distal-most cisternae or in the subsurface cisterna. Similar distal localization of acid phosphatase was observed in corn root tip by Dauwalder et al. [18]. Further evidence of the difference between the acid and alkaline phosphatase systems was gained from the use of GDP as the substrate in an acid phosphatase reaction. The result, seen in Figure 42, was virtually a complete absence of reaction product as compared with the same acid reaction using β-GP or the GDPase at alkaline pH.

The results of all enzyme localization reactions are summarized in Table II, in terms of the Golgi regions as established from PA-silver methenamine staining. Control incubations occasionally resulted in precipitate in the nucleus, some vacuoles, and at sites near the plasma membrane; but as this precipitate was also present in heat-treated cells, it was deemed non-enzymatic in origin.

TABLE II
Enzyme Localization in the Endomembrane System[a]

		Golgi Region						
			Radial Microfibril Synthesis					
Enzyme	Substrate	Forming Face	Precursor Pool	Folded Microfibrils	Region of Unfolding	Spiral Microfibril/ Amorphous Addition	Secreting Face	Subsurface Cisterna
Aryl sulfatase	p-NCS[b]	–	–	++	–	–	–	–
Alkaline	TPP[c]	+	–	+	–	++	+	–
phosphatase	GDP[d]	++	–	++	–	++	+	–
Acid	DDNTP[e]	–	–	++	–	–	–	–
phosphatase	β-GP[f]	–	–	–	–	–	++	++
	GDP	–	–	–	–	–	+	–

[a] + indicates occasional light deposition, ++ indicates consistant heavy deposition, – indicates lack of deposition.
[b] p-nitrocatechol sulfate.
[c] thiamine pyrophosphate.
[d] guanine diphosphate.
[e] di(dicyclohexylammonium)-2-napthylthiolphosphate.
[f] β-glycerolphosphate.

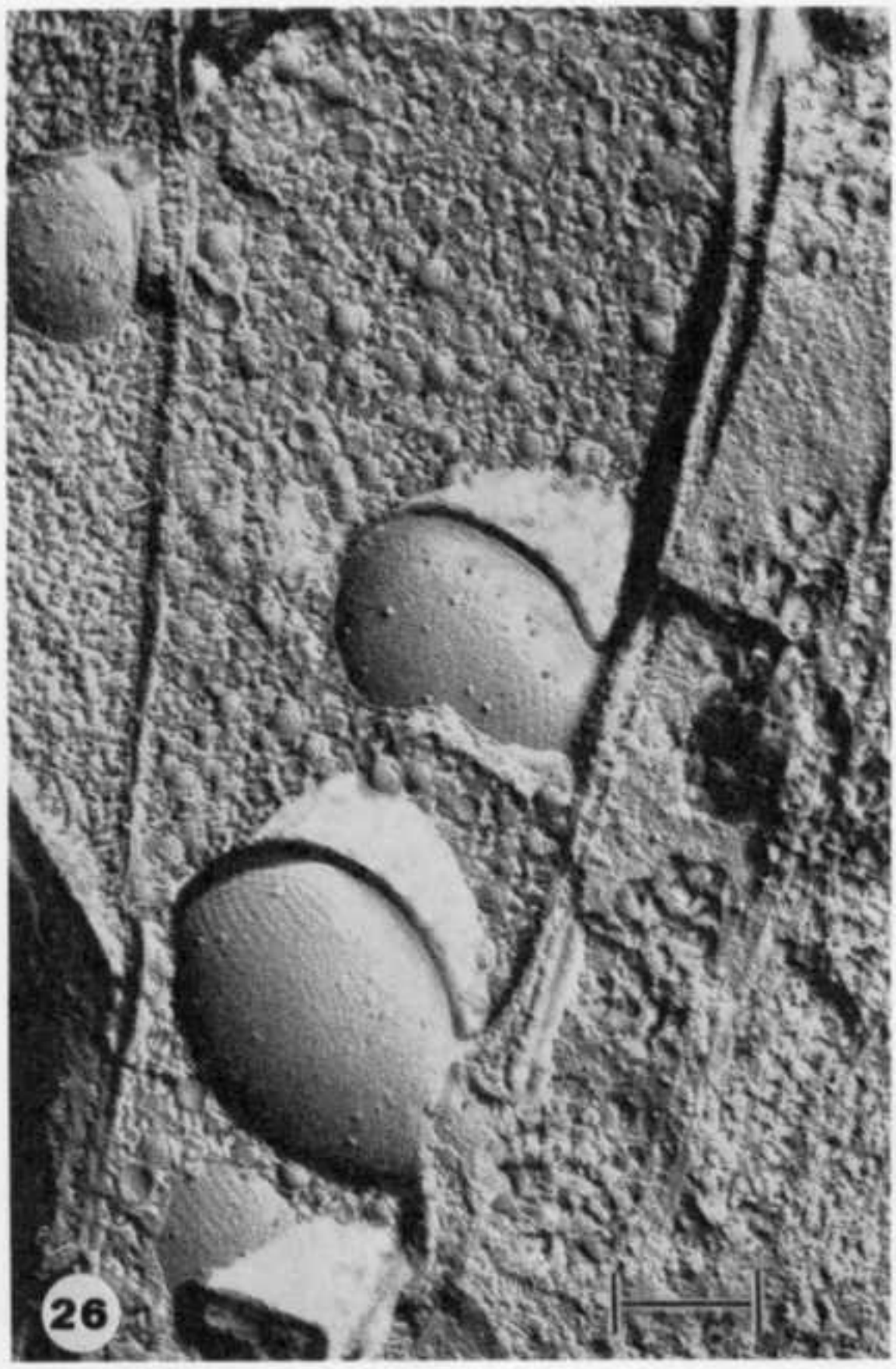

FIG. 26. Detailed view of the plasmalemma invagination and associated subsurface cisterna as revealed by freeze-etching. Note the ordered material between the plasma membrane and the subsurface cisternal membrane in the region of the invagination. Note also the spherule material in the lumen of the subsurface cisterna. Compare with the fixed material in Figure 24. Micrograph courtesy of Kay Cooper. Magnification bar = 0.1 μm.

DISCUSSION

It is obvious from the foregoing results that in *Pleurochrysis* the complex role of membranes in cell wall product assembly is under precise genetic control. The fact that two distinct phases exist within this complex life cycle opens the possibility for better understanding of regulatory mechanisms in scale biogenesis, particularly intracellular control mechanisms for determining which type of scale will be produced under a specific nutritional condition. We know essentially nothing about the life history of *Cricosphaera-Pleurochrysis,* although Rayns [104] has suggested an alternation of generations between a diploid coccolith-producing phase and a haploid benthic phase. Cytological evidence for this suggestion is still lacking. Our success in regulating the developmental phase with organic nitrogen sources tends to suggest that control mechanism may operate to induce a sexual state as shown in *Chlamyomonas* [86].

The cytological expression of these regulatory mechanisms is clearly demon-

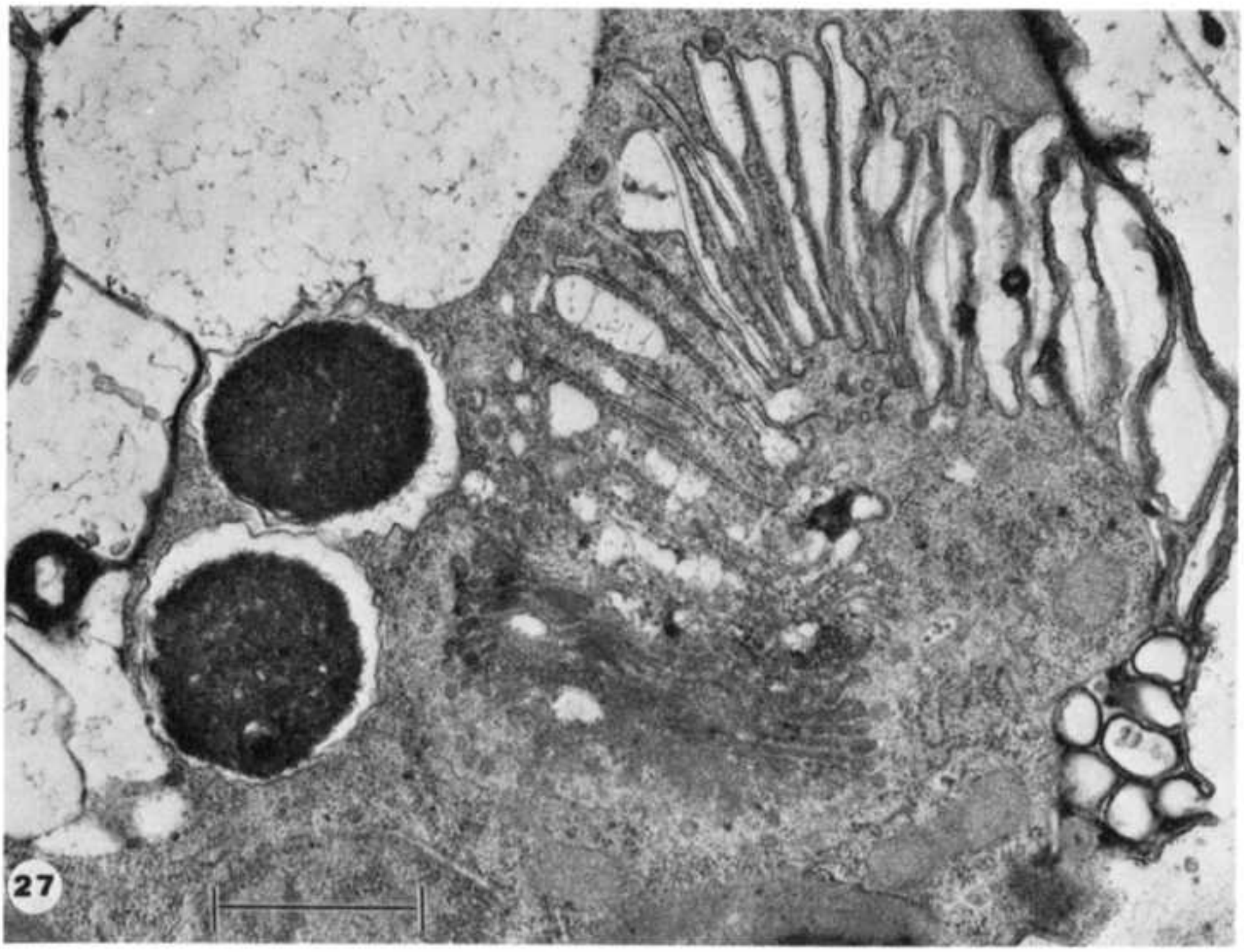

FIG. 27. After 15 min incubation with 1% Colchicine, demonstrating the early effects of the inhibition of exocytosis. Note the accumulation of the plasmalemma invaginations and the intracellular build-up of Golgi cisternae. The two electron-dense bodies to the left are autophagic vacuoles. Magnification bar = 1.0 μm.

strated in the ratio of spiral scale subcomponents. Recalling that there is abundant spiral microfibrillar material in scales of the *Pleurochrysis* phase would suggest a larger precursor pool for spiral subcomponents in this phase. With the suggestion that specific topographical regions of the ER budding from the nuclear membrane give rise to the precursor pools, it is tempting to postulate that the nuclear membrane and its elaborations play a fundamental role not only in regulating the temporal sequence of scale subcomponents, but also in controlling the quantity of subcomponent addition. The induction of mutant forms which show a defect for a particular scale subcomponent would constitute a most useful approach for exploring the regulatory mechanisms involved in scale assembly. With the fortuitous condition of being able to use morphology as an indicator of intracellular dynamic processes, we are one step closer to "observing" the genomic regulation of the synthesis of complex macromolecules and their subassemblies into cell wall subcomponents.

Secretion of products via the Golgi apparatus is explained in terms of membrane flow, a dynamic process in which membrane-bound regions associated with the nuclear envelope give rise to endoplasmic reticulum which buds off small vesicles that coalesce to produce the forming face of the Golgi apparatus. Cisternae of the Golgi apparatus eventually fuse with the plasma membrane at the secreting face and empty their contents into the surrounding extracellular space, a process

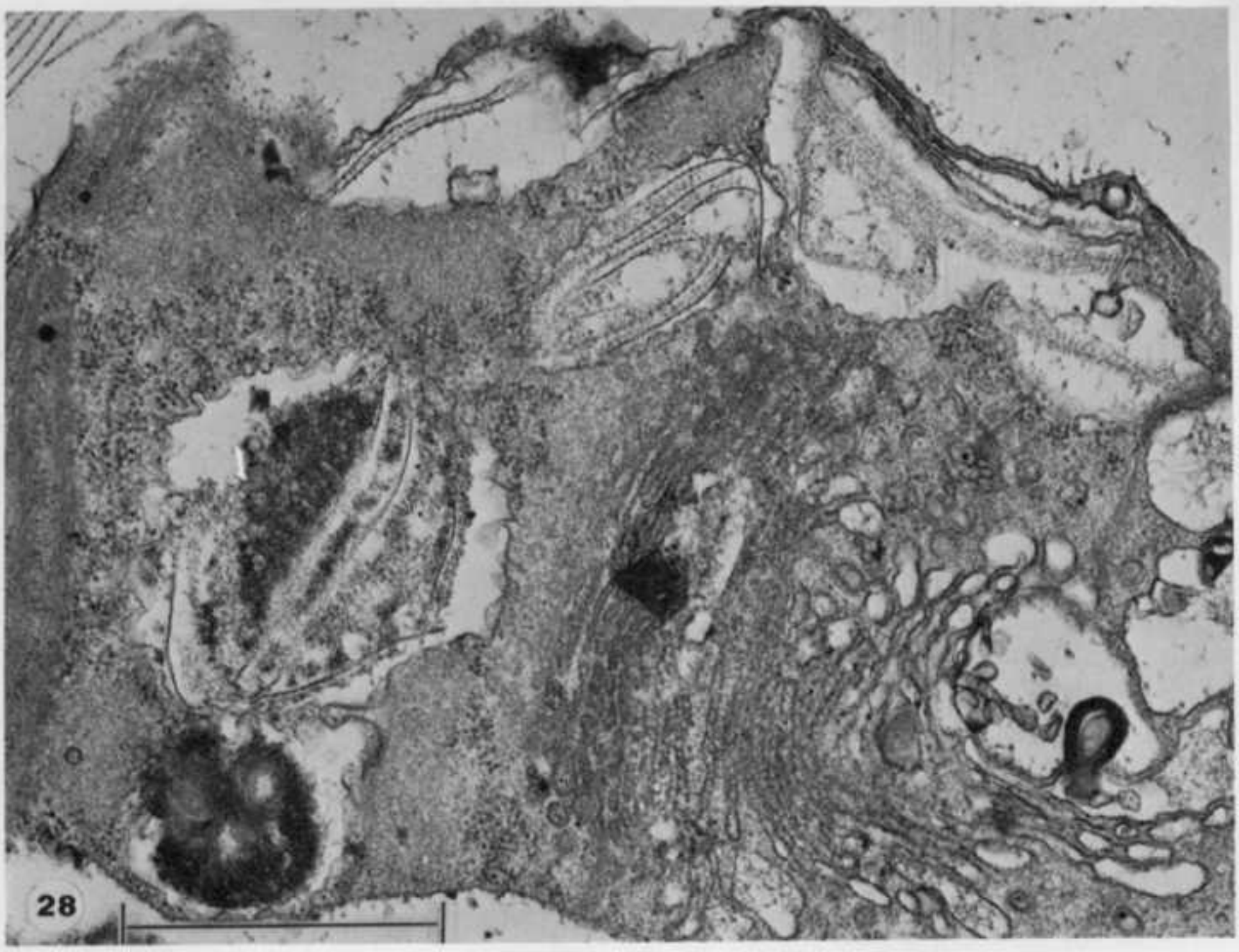

FIG. 28. After 90 min incubation with 1% Colchicine. Note the outermost cisternae with multiple numbers of scales within them. This appears to be caused by successive fusions of Golgi cisternae. Note the autophagic vacuole with several scales (left). Magnification bar = 1.0 μm.

called exocytosis [6]. The polarity of the Golgi apparatus is maintained by endomembrane differentiation, as evidenced by the change in membrane characteristics between the forming and secreting faces [36, 11]. At the forming face the cisternal membranes have dimensions and staining properties similar to those of nuclear envelope and encoplasmic reticulum. Passing through intermediate stages, the cisternal membranes at the secreting face exhibit properties identical to those of the plasma membrane. In *Pleurochrysis*, this membrane flow is accompanied by the synthesis and assembly of the three scale subcomponents. Considering that each cisterna sequentially synthesizes all three subcomponents, the membrane differentiation is then really temporal with respect to each cisterna. However, when this process is viewed in static electron micrographs, the result is a Golgi apparatus which appears to be spatially differentiated into several regions, each involved with a different portion of the total biogenic event. With this important distinction in mind, scale biogenesis can be discussed in terms of spatially differentiated regions of the Golgi apparatus. A cross-sectional model, incorporating all the morphological features of the scale biogenesis considered below, is presented in Figure 43.

At the forming face of the Golgi apparatus, before any recognizable product appears, there is intense alkaline nucleotide diphosphatase activity. This same activity has been associated with Golgi-mediated synthesis in vivo [34, 18, 103]. Novi-

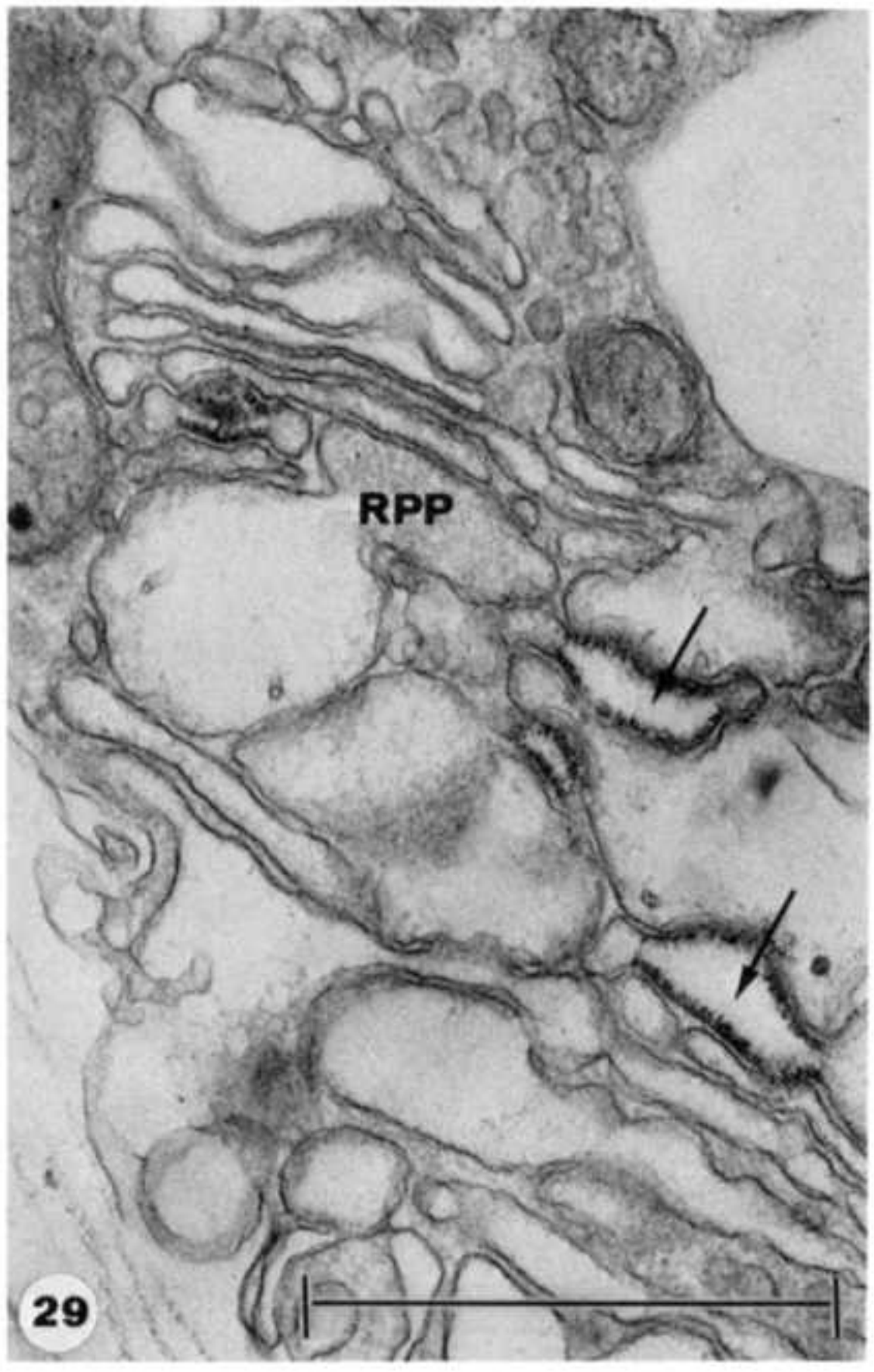

FIG. 29. Localization of aryl sulfatase activity as the hydrolysis of p-NCS—barium capture. Section through the Golgi apparatus with distal face downward. Note the precipitate on radial microfibrils in the folded configuration (arrows), adjacent to a radial precursor pool (RPP). Compare with the folded radial configuration in Figure. Magnification bar = 1.0 μm.

koff [83] has proposed that, since nucleotide diphosphates are a product of polysaccharide synthesis, their hydrolysis could help drive the transferase reaction:

$$\text{NDP-glucose} + (\text{glucose})_n \xrightarrow{\text{transferase}} (\text{glucose})_{n+1} + \text{NDP}$$

$$\text{NDP} \xrightarrow{\text{phosphatase}} \text{NMP} + P_i$$

Working with polysaccharide-synthesizing fractions isolated from pea seedlings, Ray and co-workers [103] concluded that nucleotide diphosphatase activity "probably represents inactivated polysaccharide synthetase." In scale biogenesis, the following events at the forming face are dependent upon polysaccharide synthesis: (1) the continued elaboration of enzymes involved in scale subcomponent synthesis, and (2) the formation of the radial precursor product. The first event, the

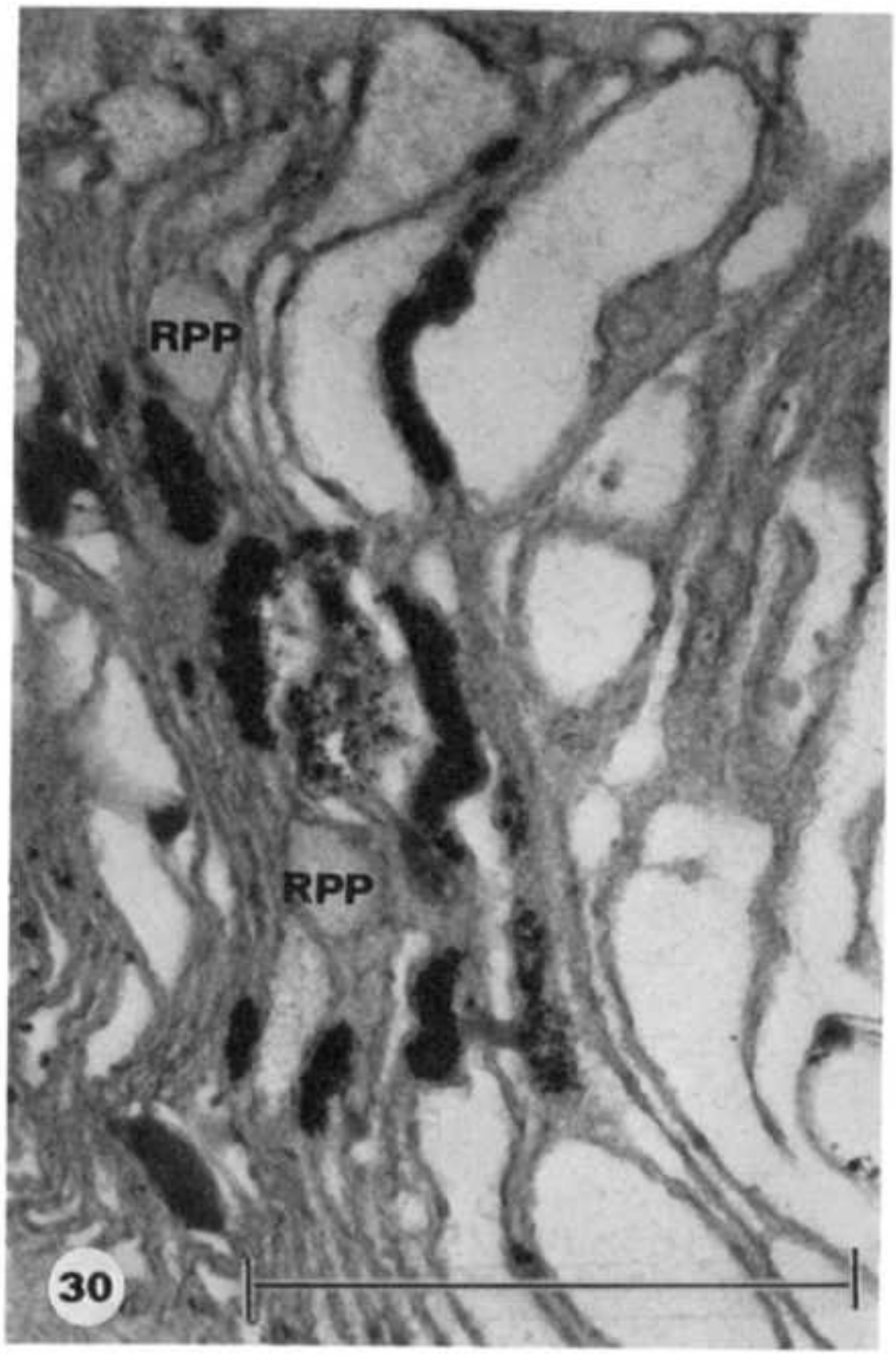

FIG. 30. Localization of aryl sulfatase activity as the hydrolysis of p-NCS—copper capture. Section through Golgi apparatus with distal face to the right, with the precipitate filling the cisternal lumen in the region of the radial precursor pool (RPP). Magnification bar = 1.0 μm.

synthesis and attachment of carbohydrate groups to complex macromolecules, has been proposed as the primary role of the Golgi apparatus in secreting cells [130]. The latter process is the synthesis of the first identifiable polysaccharide product in scale biogenesis.

The synthesis of the radial microfibrils in the folded configuration occurs as three separate events: polymerization, crystallization, and sulfation. In the precursor pool, the polysaccharide product is sufficiently polymerized to be retained through preparation for electron microscopy, but not yet fibrillar. Crystallization of the precursor into microfibrils occurs immediately adjacent to the cisternal membranes, suggesting a template mechanism similar to that proposed for higher plant polysaccharide synthesis by Marx-Figini [64, 65]. The last event, sulfation, is indicated by the localization of aryl sulfatase and acid DDNTPase, which Hanker [38] has shown to be involved in the elaboration of a sulfated product by secretory amyloblasts. The possible role of these enzymes in sulfate metabolism is presented in Figure 44. By hydrolyzing 3′phosphoadenosine—5′phosphosulfate (PAPS, the sulfate donor in sulfotransferase reactions), the acid hydrolases provide a mechanism for controlling the amount of PAPS available [3] and, in some systems, account for most of the PAPS hydrolyzed [2]. In addition to this regula-

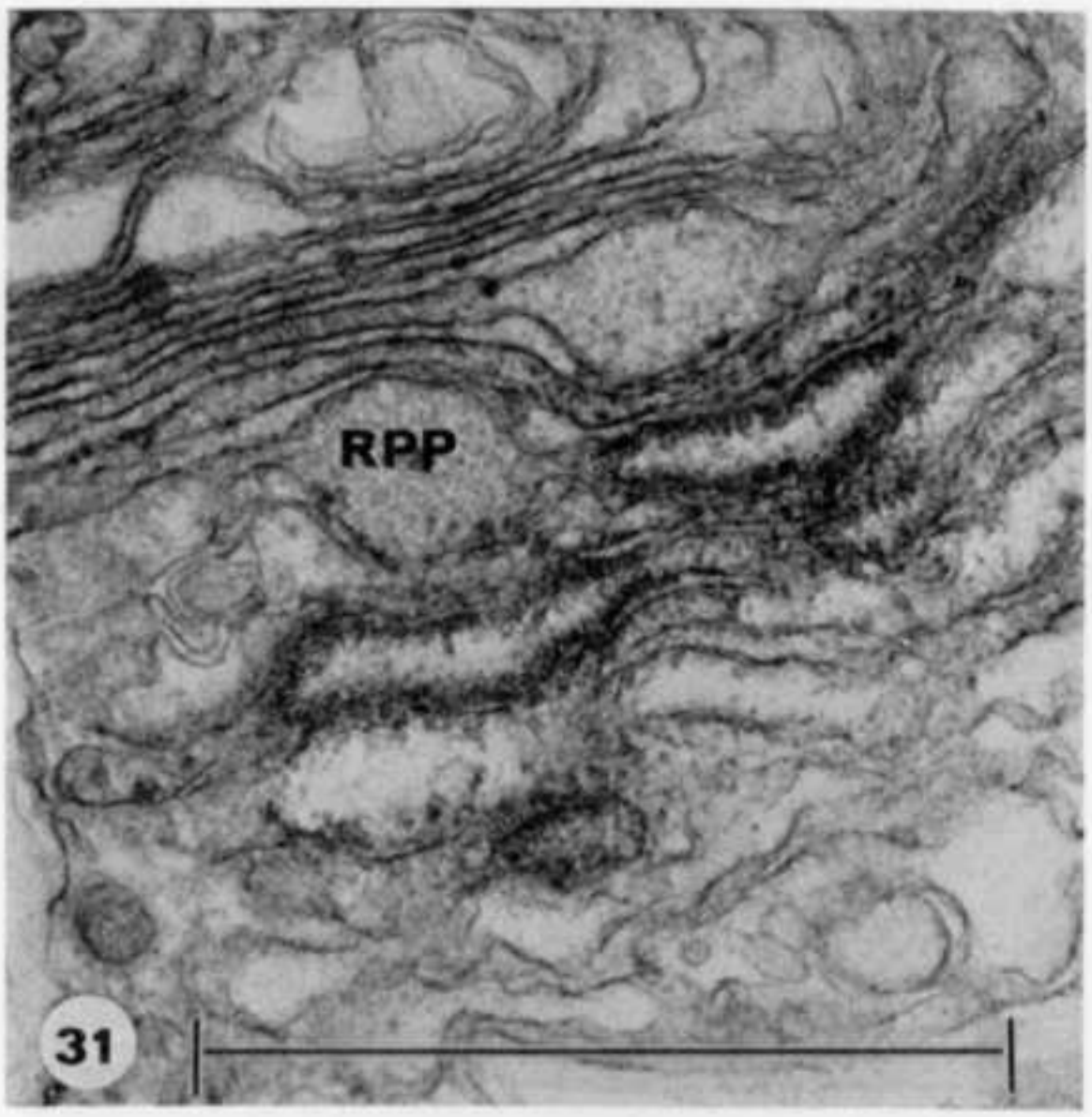

FIG. 31. Localization of aryl sulfatase activity as the hydrolysis of p-NCS—copper capture. Section through Golgi apparatus with distal face downward, with the precipitate confined to the folded radial microfibrils. Note adjacent radial precursor pool (RPP). Post-stained with lead citrate. Magnification bar = 1.0 μm.

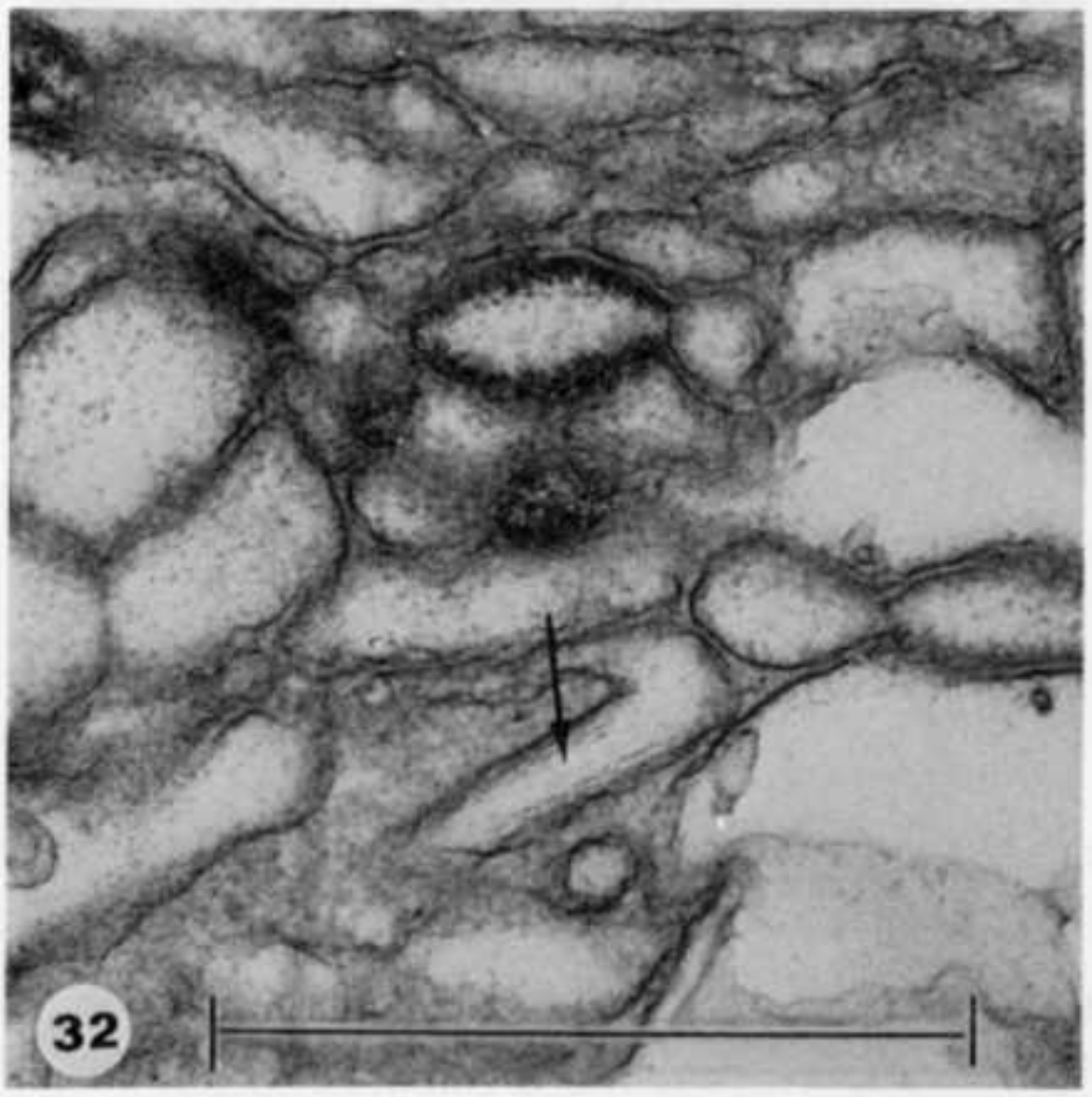

FIG 32. Aryl sulfatase localization on folded radial microfibrils with nonreactive radial microfibrils immediately distal (arrows)—barrium capture. Post-stained with lead citrate. Magnification bar = 0.1 μm.

tory function, the hydrolysis of p-NCS may represent sulfotransferase activity itself, since phenolic sulfates have sufficiently high energy to act as sulfate donors in some in vitro reactions [121, 132]. That sulfation occurs in the Golgi apparatus has also been demonstrated by the incorporation of $^{35}SO_4^=$, in which the Golgi ap-

FIG 33. Aryl sulfatase localization on folded radial microfibrils with nonreactive radial microfibrils immediately distal (arrows)—copper capture. Post-stained with lead citrate. Magnification bar = 0.1 μm.

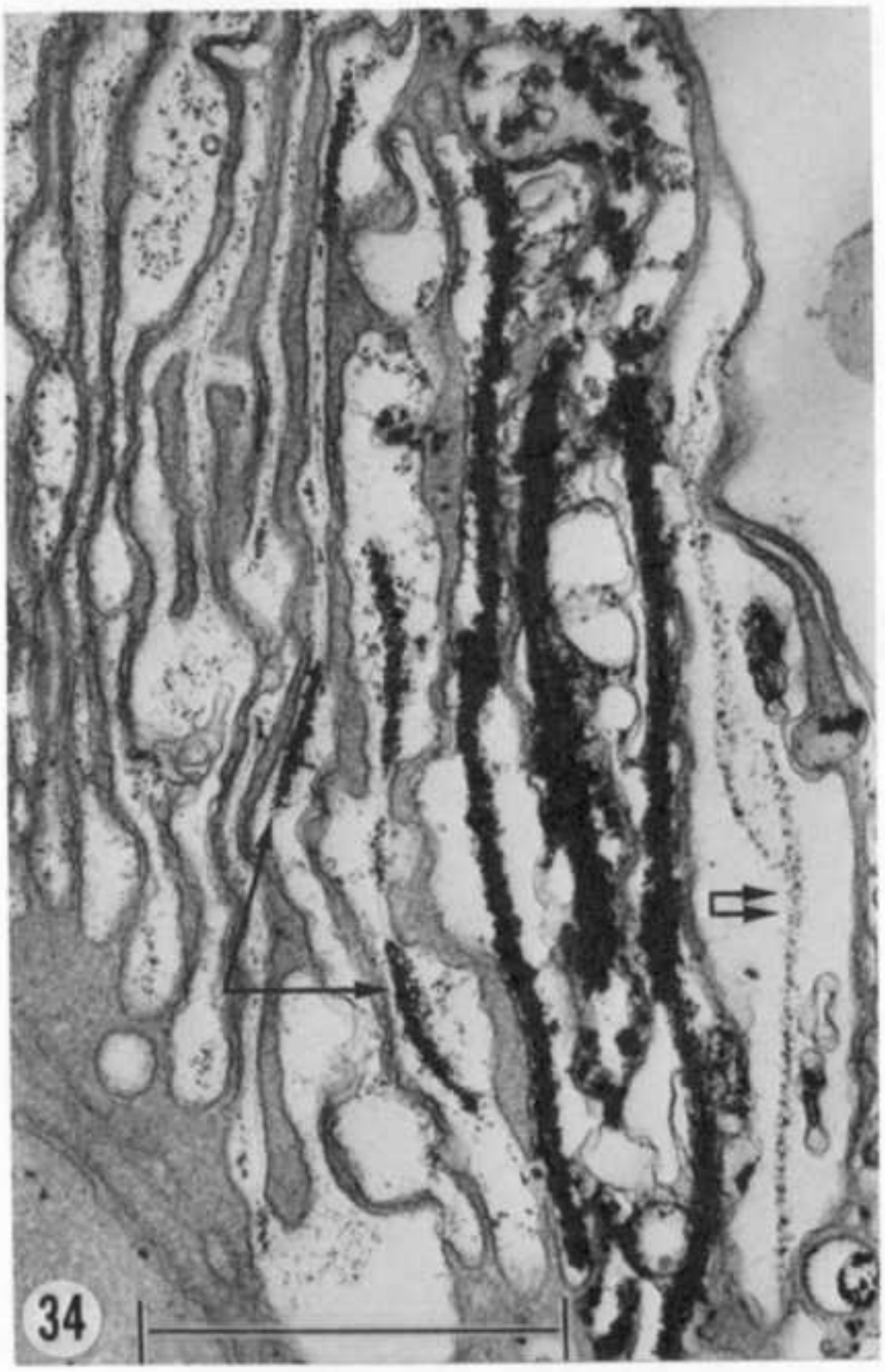

FIG. 34. Alkaline phosphatase localization in the Golgi apparatus; distal face is downward or to the right. TPP as the substrate. Note the centripetal progression of the precipitate (arrows) and loss of staining at the distal-most cisterna (double arrow). Post-stained with lead citrate. Magnification bar = 1.0 μm.

paratus was the first site of radioactivity [4, 133]. Less well understood is the timing of sulfation, whether prior to, concomitant with, or following polymerization. Using in vitro sulfotransferase systems, the sulfation of mono-, di-, and oligosaccharides has been demonstrated, as well as the sulfation of completed polymers with no possibility of chain elongation [119, 120, 32]. In *Pleurochrysis*, it is

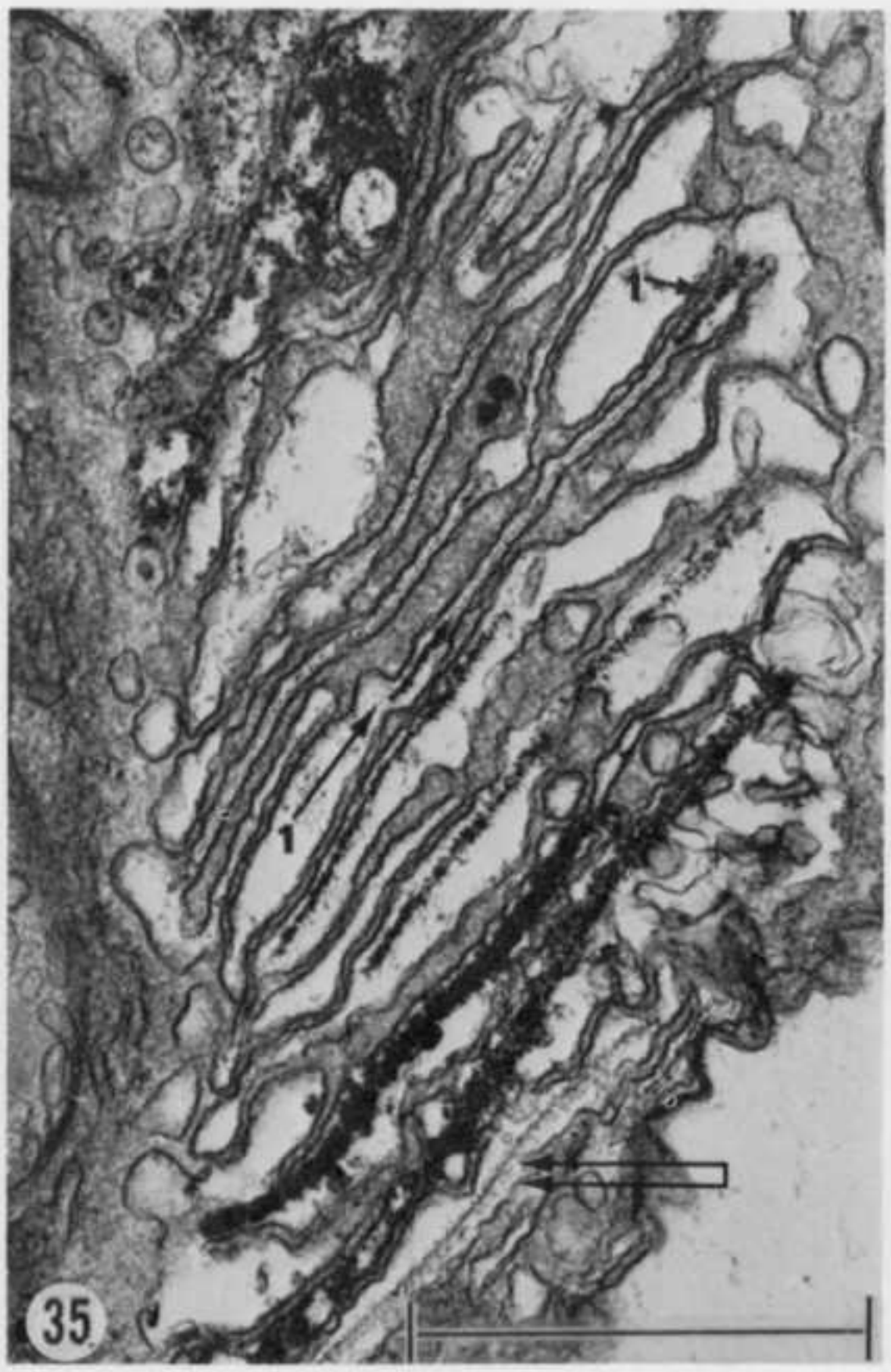

FIG. 35. Alkaline phosphatase localization in the Golgi apparatus; distal face is downward or to the right. GDP as the substrate, showing precipitate localization in proximal and distal Golgi regions. Note the centripetal staining pattern (1) and the loss of stain in the distal-most cisterna (double arrow). Post-stained with lead citrate. Magnification bar = 1.0 μm.

clear that sulfation occurs after some polymerization has already taken place, but since it is uncertain whether or not crystallization of the microfibrils involves further chain elongation, no conclusions can be drawn concerning the timing of sulfation in terms of the parameters discussed above.

Once the radial microfibrils have been formed in the folded configuration, a highly specific membrane flow accounts for the transition into the quadriradial arrangement, with the microfibrils still remaining closely attached to the cisternal membrane. The process apparently occurs quite rapidly because, while Z-stages are found frequently, partially unfolded scales have been observed only a few times during the entire course of this study (Fig. 16). In the region of unfolding, there is no activity of the enzymes studied, as is most evident for GDPase in Figure 37. The motive force responsible for unfolding, and the means by which it may be transmitted, is completely unknown. Unlike other Golgi apparatus studied [71, 72], that of *Pleurochrysis* does not exhibit intercisternal rods, fibrils, or other elements which might be invoked in explaining unfolding. While there exists a prominent microtubular bundle in relation to the Golgi apparatus [8], depolymerization of the microtubules with colchicine does not prevent scale synthesis [10].

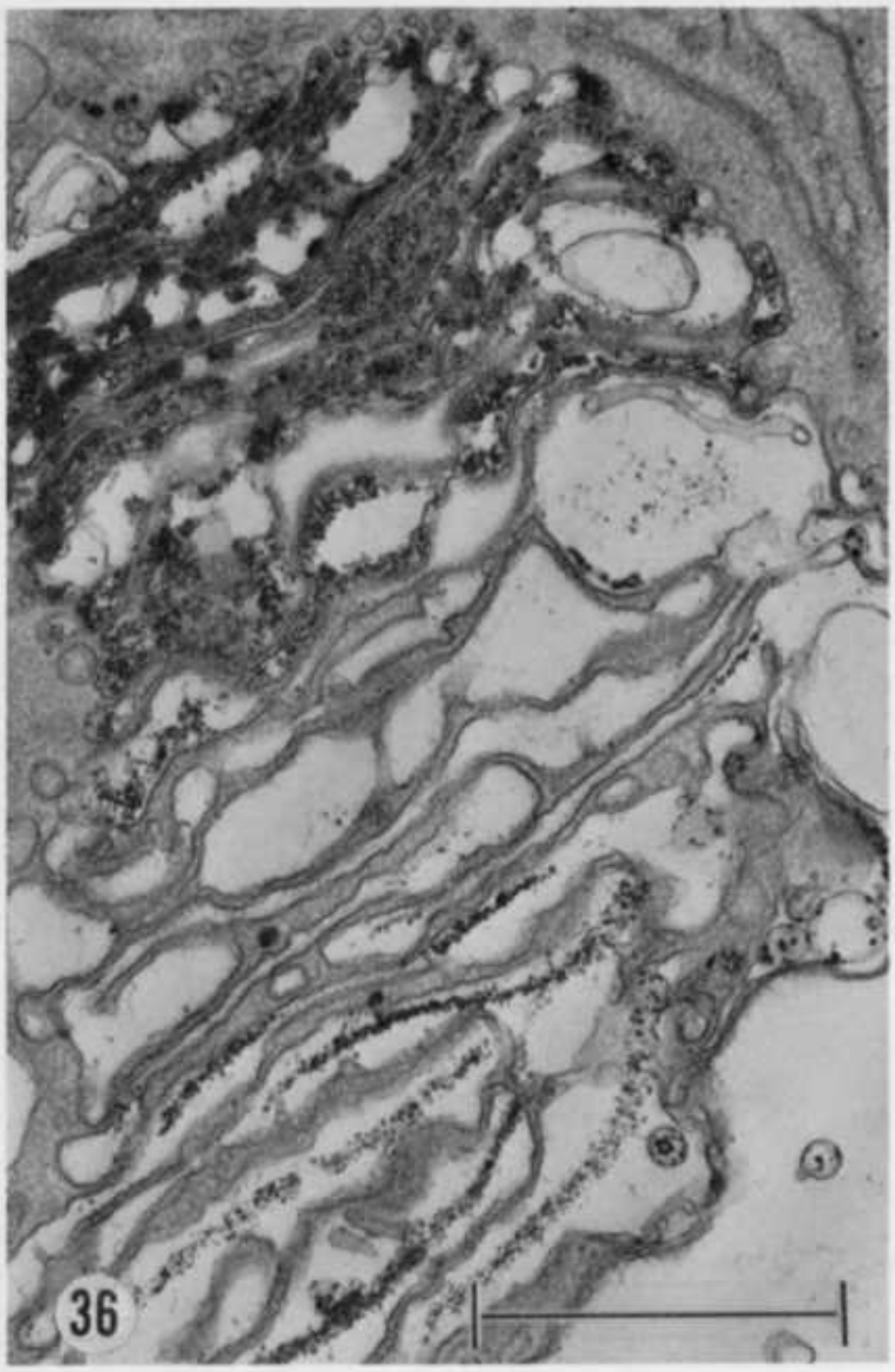

FIG. 36. Alkaline phosphatase localization in the Golgi apparatus; distal face is downward or to the right. GDP as the substrate, showing strong localization in the proximal and distal Golgi regions, with no localization in the region of unfolding. Post-stained with lead citrate. Magnification bar = 1.0 μm.

Since the unfolding process may involve a contractile mechanism, a promising avenue of research is the use of heavy meromyosin which could indicate the presence of actin-like contractile proteins [87]. However, based on present evidence, all that can be said of unfolding is that it occurs.

After the radial network has unfolded, synthetic activity is resumed with the addition of the cellulosic spiral microfibrils. This addition begins at the periphery of the radial network and continues centripetally, requiring approximately five successive cisternal differentiations for completion (Fig. 17). Concerning the actual process of cellulose synthesis, two alternate mechanisms must be considered:

(1) The central feeding tubule concept, in which the spiraling band of microfibrils is synthesized at a single locus and fed into the restricted lumen of the cisterna to be deposited onto the radial microfibrils (restricted terminal synthesis).
(2) In situ synthesis by membrane-bound enzyme systems which are activated sequentially, perhaps by the availability of constituent monosaccharides as the cisterna enlarges centripetally (sequential templating).

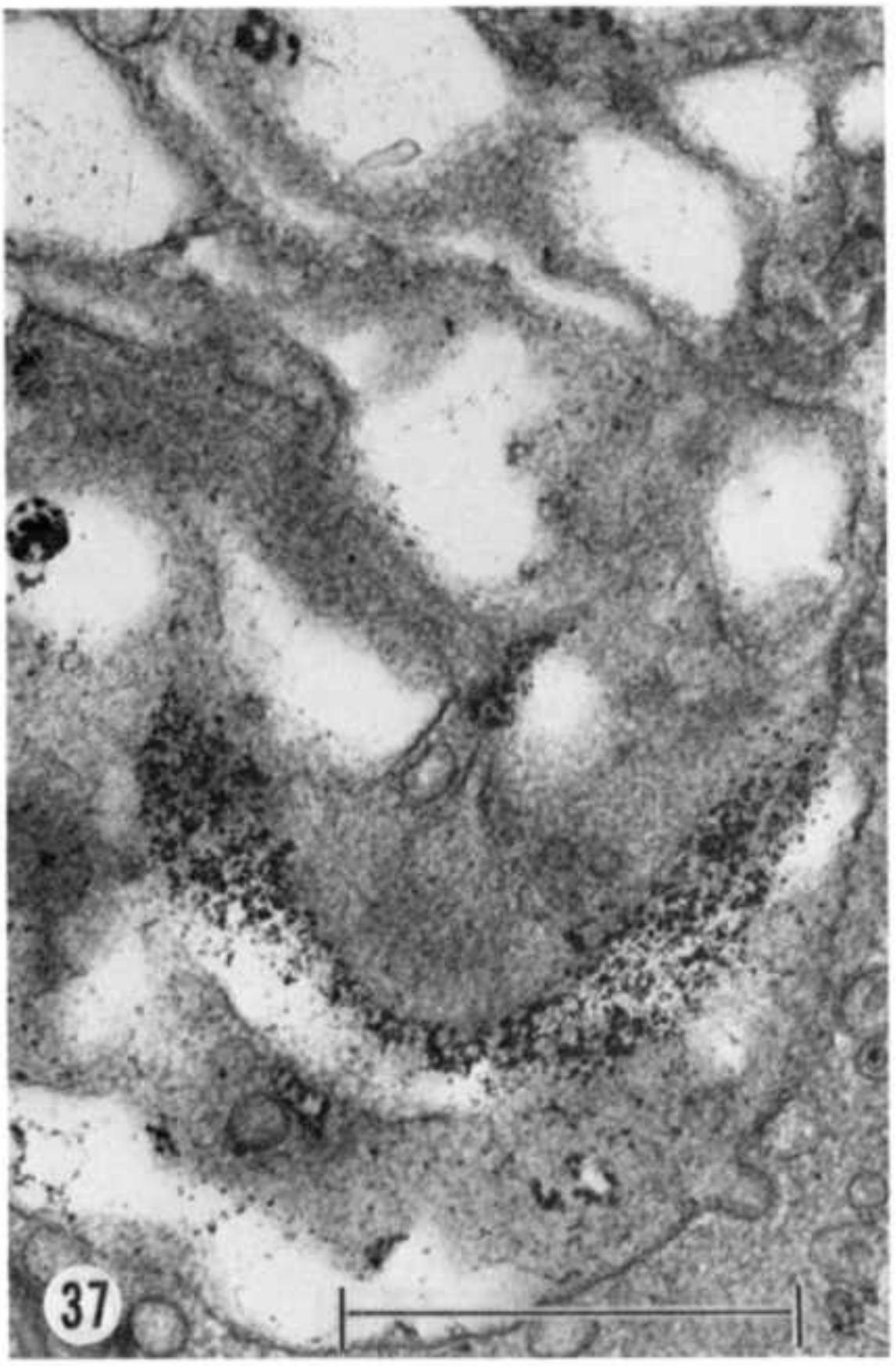

FIG. 37. Alkaline phosphatase localization in the Golgi apparatus; distal face is downward or to the right. TPP as the substrate. Section partially in the plane of a scale showing a stage of centripetal staining. Post-stained with lead citrate. Magnification bar = 1.0 μm.

Principle support for the feeding tubule mechanism is derived from the morphological features of scale ultrastructure. Spiral microfibrils at the center of the scale exhibit breakage loci [9] (Fig. 1) which result from bending a cellulose microfibril beyond the limit of its flexibility. It is difficult to imagine how such breaks would arise if the microfibrils are synthesized in situ rather than being constrained into the spiral configuration after synthesis. Furthermore, the smallest unit of the spiral arrangement is not a single microfibril but a band of eight to ten parallel microfibrils (Fig. 2), suggesting that the microfibrils of the band are synthesized simultaneously and then the band is arranged into the spiral configuration. No microfibrils have ever been observed in the central feeding tubule (Fig. 20), but this absence is rather inconclusive in light of the observation in the next paper that 2N TFA-extracted scale cellulose cannot be visualized with electron-dense stains. Thus, the microfibrils could be synthesized in the feeding tubule while the coating material, responsible for maintaining the spiral configuration and conferring positive stainability, is added at the time of attachment to the radials.

In lieu of absolute substantiation of the feeding tubule mechanism, the template proposal may be supported by two morphological observations. The first is the

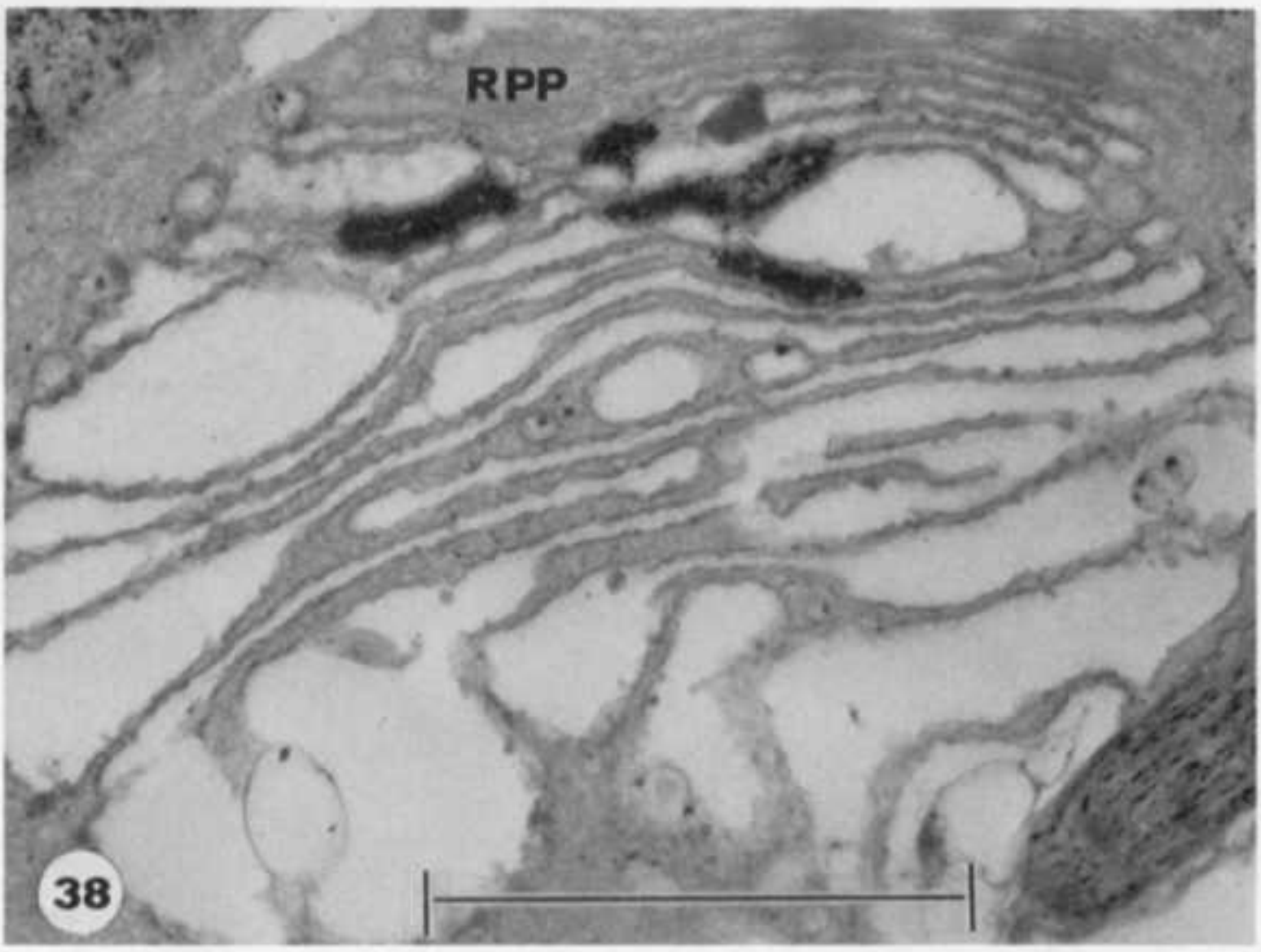

FIG. 38. Acid phosphatase localization in section through the Golgi apparatus, with the distal face downward or to the right—DDNTP as the substrate. Deposition filling the cisternal lumen immediately distal to a radial precursor pool (RPP). Magnification bar = 1.0 μm.

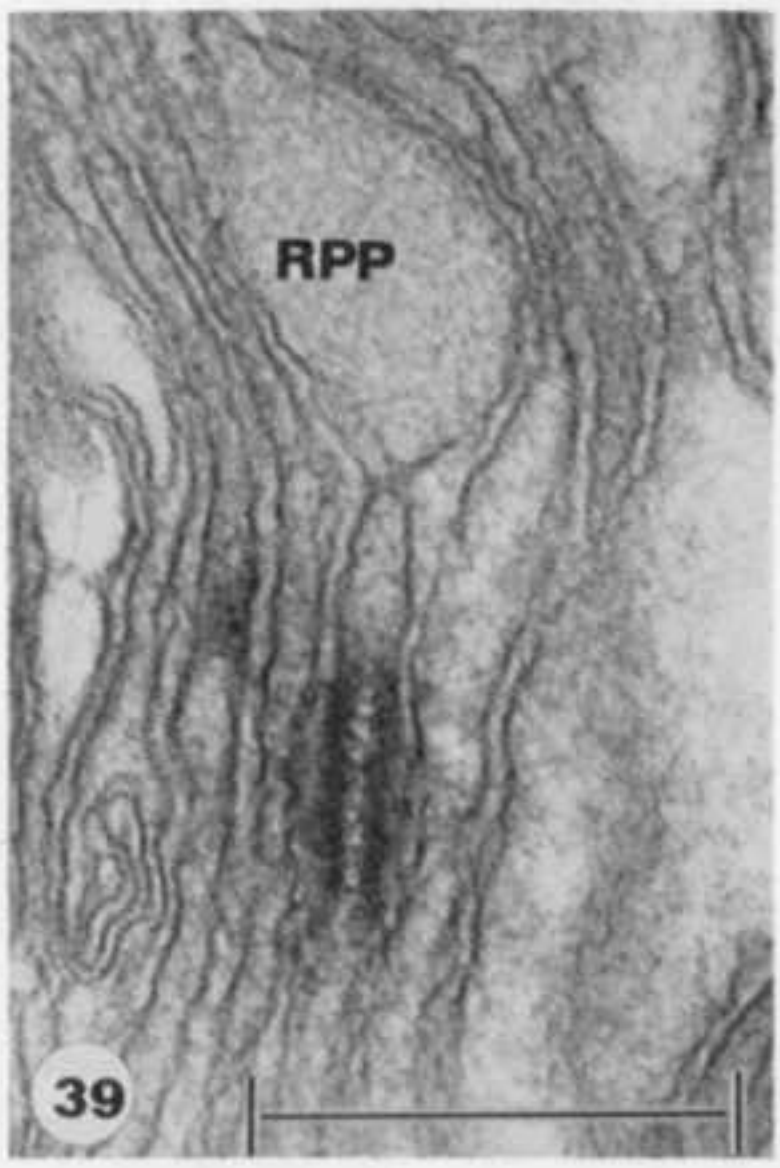

FIG. 39. Acid phosphatase localization in section through the Golgi apparatus, with the distal face downward or to the right—DDNTP as the substrate. Localization on the folded radial configuration in the same cisterna as the radial precursor pool (RPP). Magnification bar = 0.1 μm.

obvious fact that the spiral microfibrils appear only in place on the radial network, as mentioned above. Second, the particular configuration of the cisternal membranes at the site where the spiral microfibrils first appear suggests membrane involvement. As seen from Figure 17, the cisternal membranes at this site are positioned more closely to the radial microfibrils than in any other area. The mem-

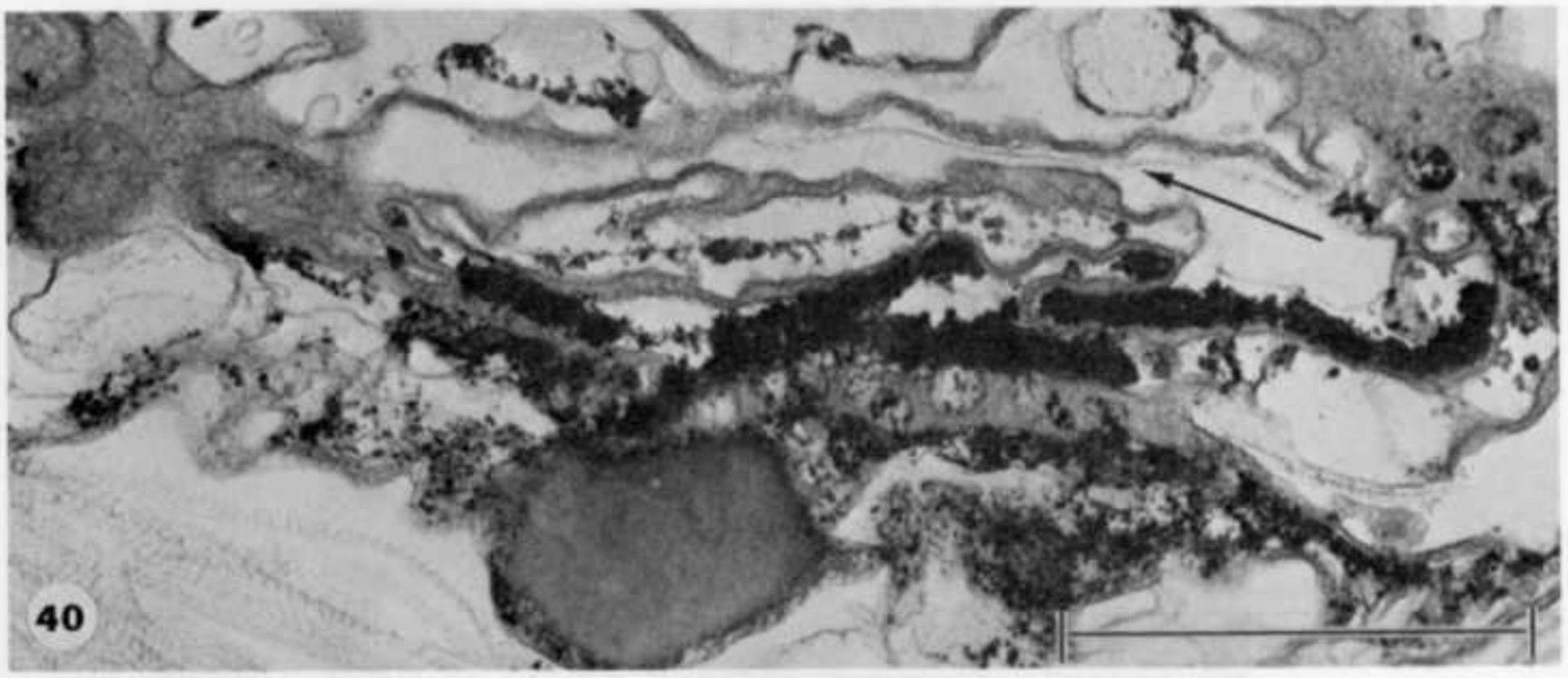

FIG. 40. Acid phosphatase localization in section through the Golgi apparatus, with the distal face downward or to the right—β-GP as the substrate. Localization in the distal-most cisternae, but conspiciously absent from a cisternal profile characteristic of spiral and amorphous additions (arrow). Post-stained with lead citrate. Magnification bar = 1.0 μm.

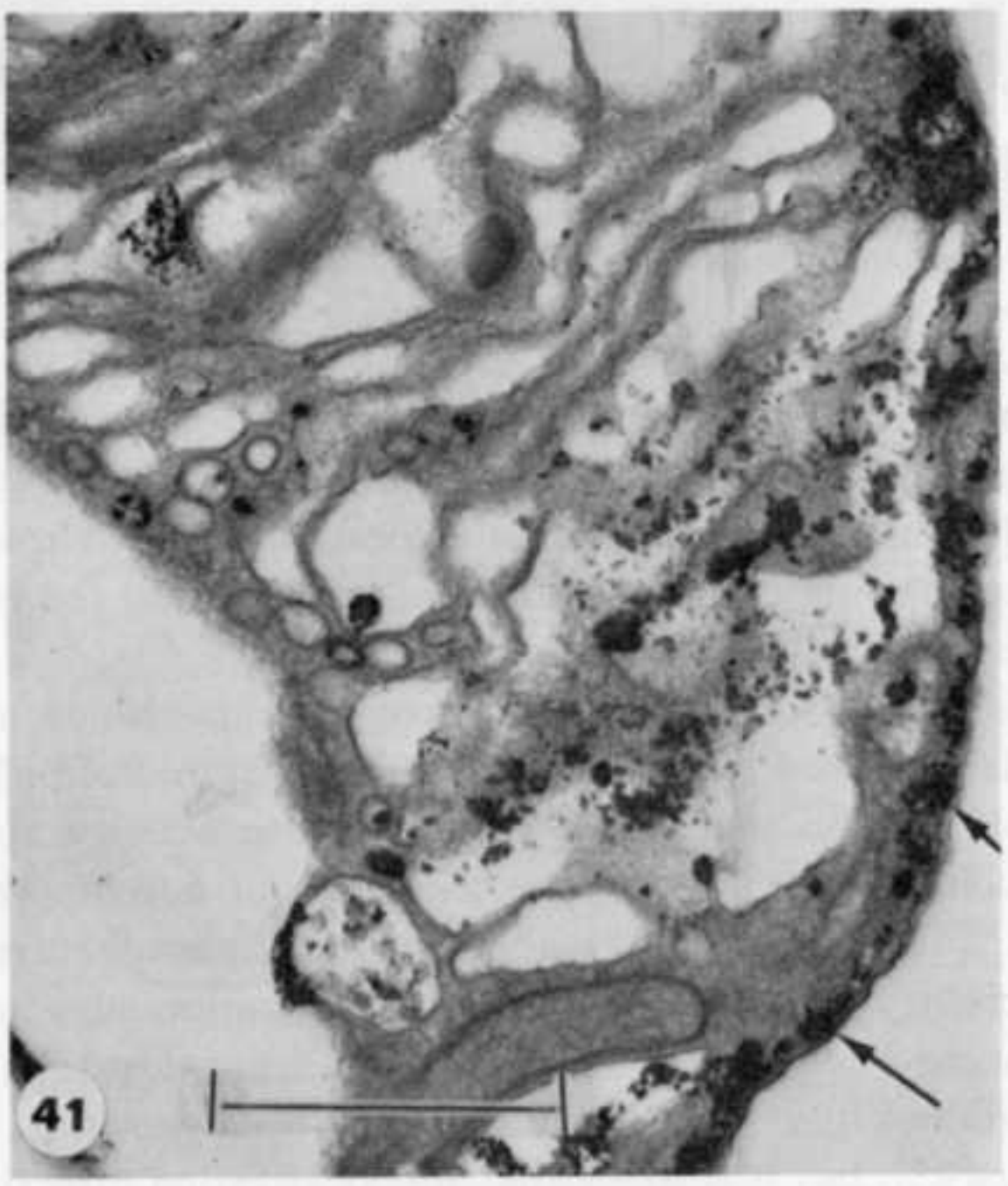

FIG. 41. Acid phosphatase localization in section through the Golgi apparatus, with the distal face downward or to the right—β-GP as the substrate, showing localization in the subsurface cisterna (arrows) as well as the distal-most cisternae of the Golgi apparatus. Post-stained with lead citrate. Magnification bar = 1.0 μm.

branes at this site often appear thicker or more darkly stained, and in one instance, small granular structures are attached to the membrane (Fig. 21). The synthesis of cellulose by membrane-bound granules is a mechanism currently favored by some investigators [94, 95, 80, 14, 107, 108]. However, only in the case of yeast cells have the fibrils been observed in direct continuity with ordered arrays of

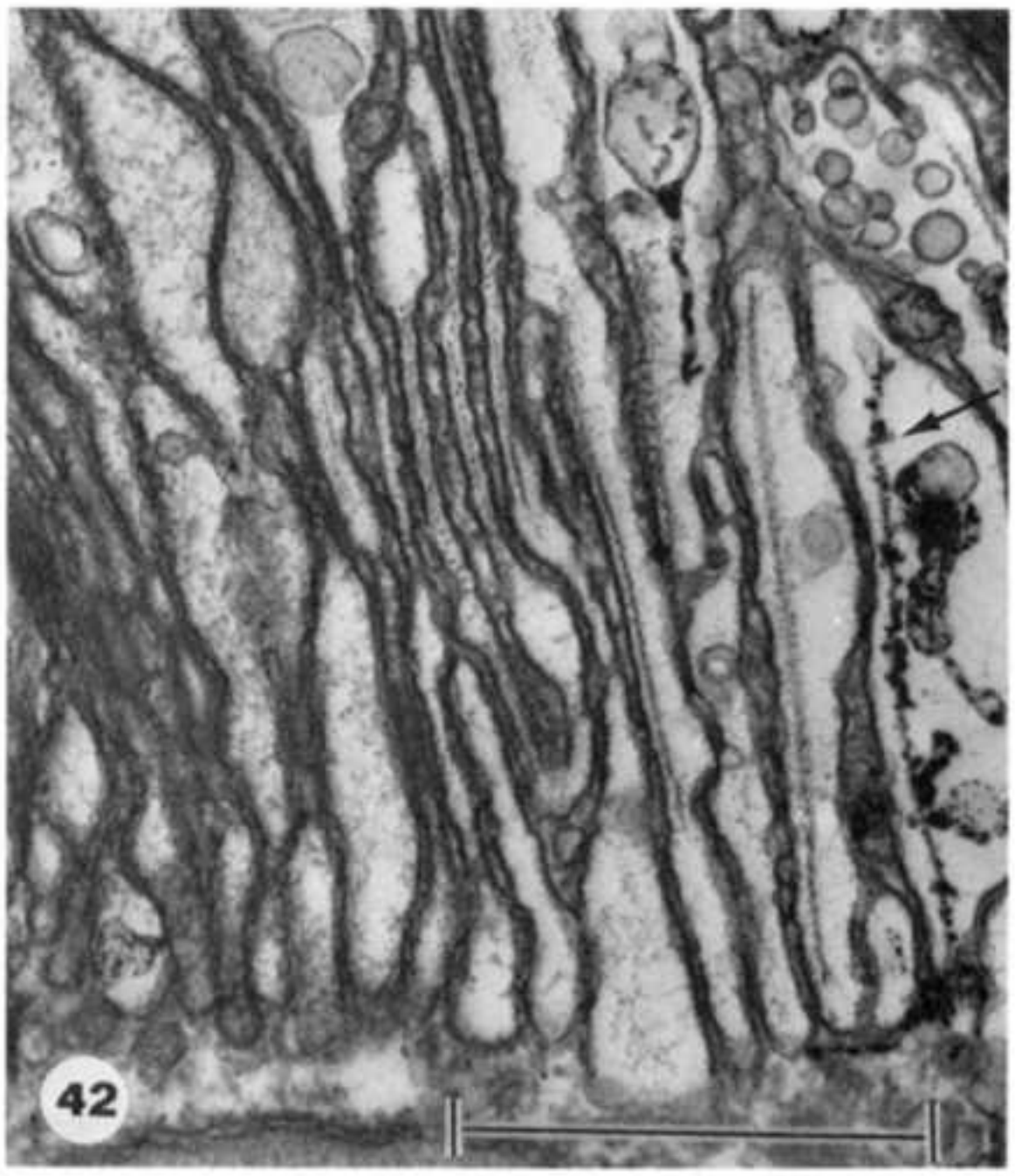

FIG. 42. Acid phosphatase localization in section through the Golgi apparatus, with the distal face downward or to the right—GDP as the substrate, illustrating absence of localization except in one distal cisterna (arrow). Post-stained with lead citrate. Magnification bar = 1.0 μm.

granules [75], and it has since been demonstrated that these fibrils are not cellulosic [107].* Thus, the relationship between membrane-bound granules and cellulose microfibrils remains an implication at best, and, in *Pleurochrysis* at least, the role of the granules may be that of ordering and coating the cellulose microfibrils which were synthesized at another site.

Addition of the pectin-like amorphous subcomponents also occurs centripetally, following immediately after the deposition of the spiral microfibrils. Again, as in the proximal Golgi region, nucleotide diphosphatase activity appears to be involved in polysaccharide synthesis. In their study of developing corn root tips, Dauwalder et al. [18] also found that nucleotide diphosphatase activity corresponded with secretory activity. While their localization suggested that the enzyme was membrane-bound, the localization in *Pleurochrysis* is directly on the polysaccharide product itself. Phosphatases have been shown to be a constituent of some cell walls [95], but it is likely that the localization directly on intracisternal scales in *Pleurochrysis* is an artifact since the wall itself shows no reactivity. When amorphous synthesis is completed, the entire cisterna is enlarged and the scale is now freed from contact with the cisternal membranes.

With the entire scale synthesized and assembled, the distal-most cisterna fuses with the plasma membrane to release the scale by exocytosis. During active secretion, one scale is released approximately every two minutes [5], implying the fusion of Golgi cisternae with the plasma membrane at the same rate. If the cell

* With freeze-etching, Brown and Montezinos (*Proc. Nat. Acad. Sci., 73,* 143 (1976)) recently observed a semi-cylindrical complex in association with the plasma membrane which synthesizes and assembles cellulosic microfibrils by the tip growth mode. These observations greatly favor the feeding tubule mechanism in *Pleurochrysis.*

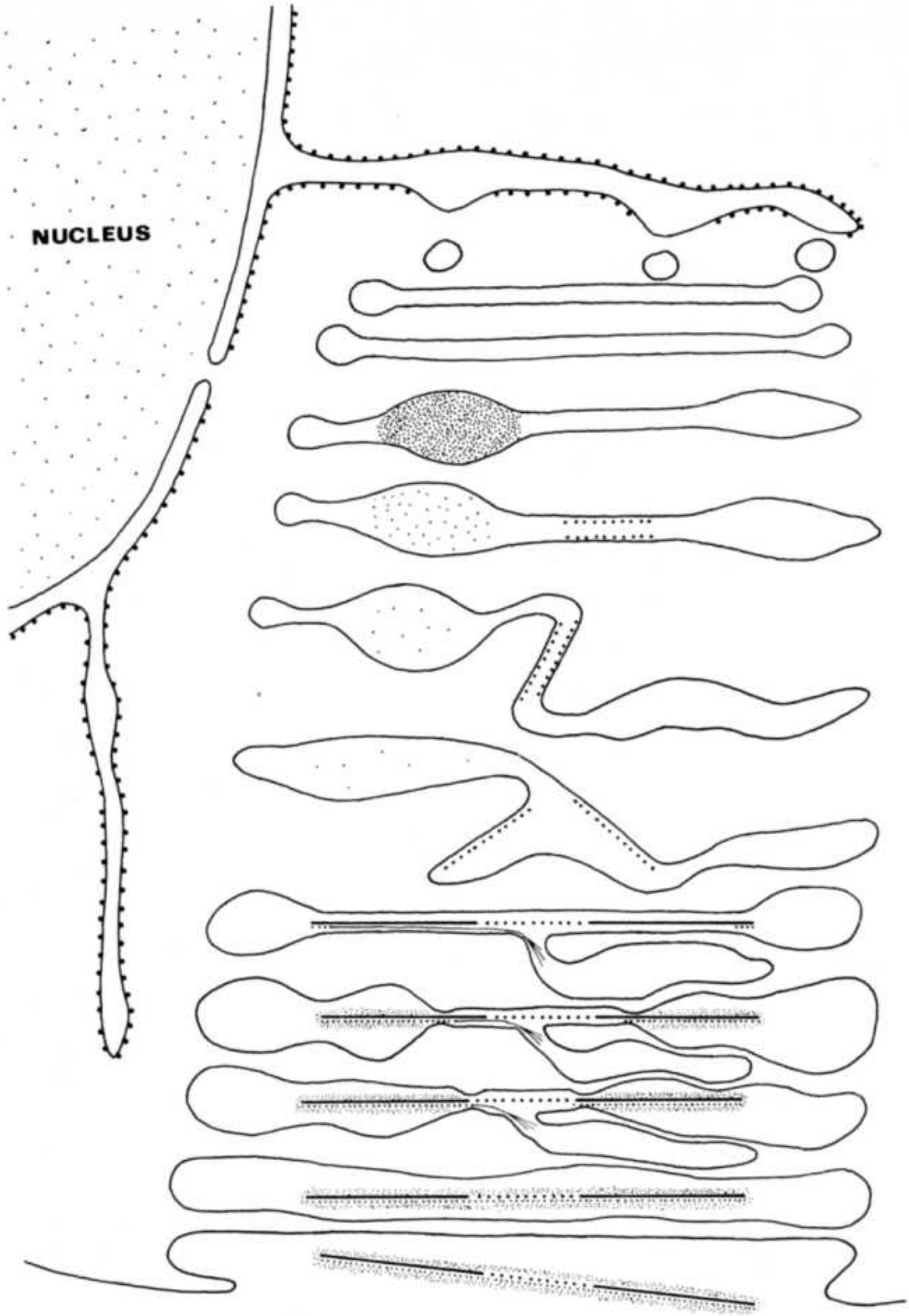

FIG. 43. A cross-sectional model of scale assembly in *Pleurochrysis*. See text for details relating to specific stages of assembly.

is to avoid a rapid increase in volume, some of this membrane must be recycled. There are two alternative hypotheses for the role of the subsurface cisterna and the plasma membrane invaginations in recycling (Fig. 45).

Hypothesis A favoring endocytosis suggests that membrane flow might occur from the Golgi cisternal membranes, as they fuse with and become incorporated into the plasma membrane via the plasmalemma invaginations, to the lumen of the subsurface cisterna where the myelinized and spherule figures are found. *Hypothesis B* presumes a temporal fusion of Golgi cisternal membranes with the

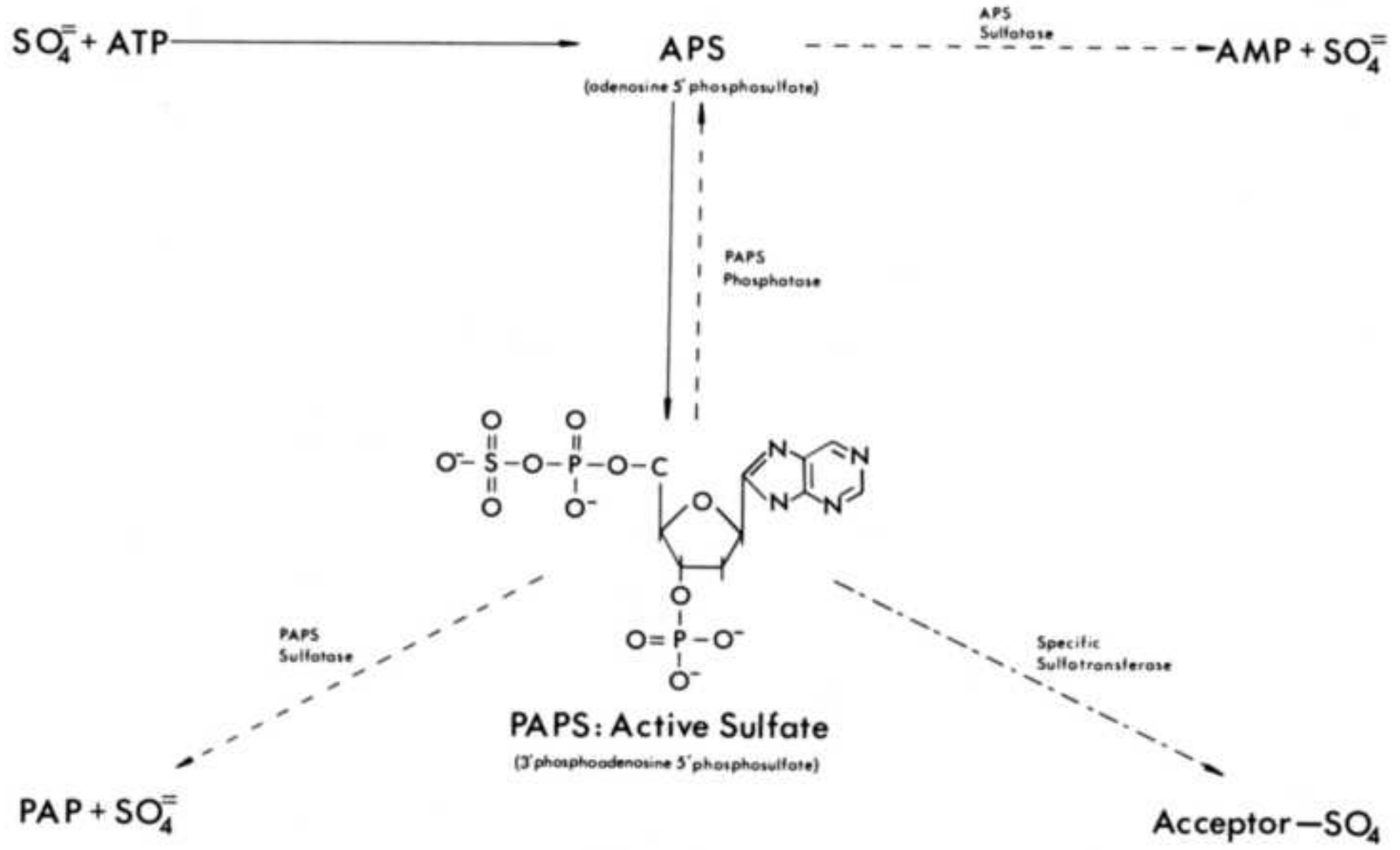

FIG. 44. Postulated role of acid hydrolases in sulfate metabolism. Sulfate activation (—); regulatory hydrolases (– –); sulfotransferase (– - –).

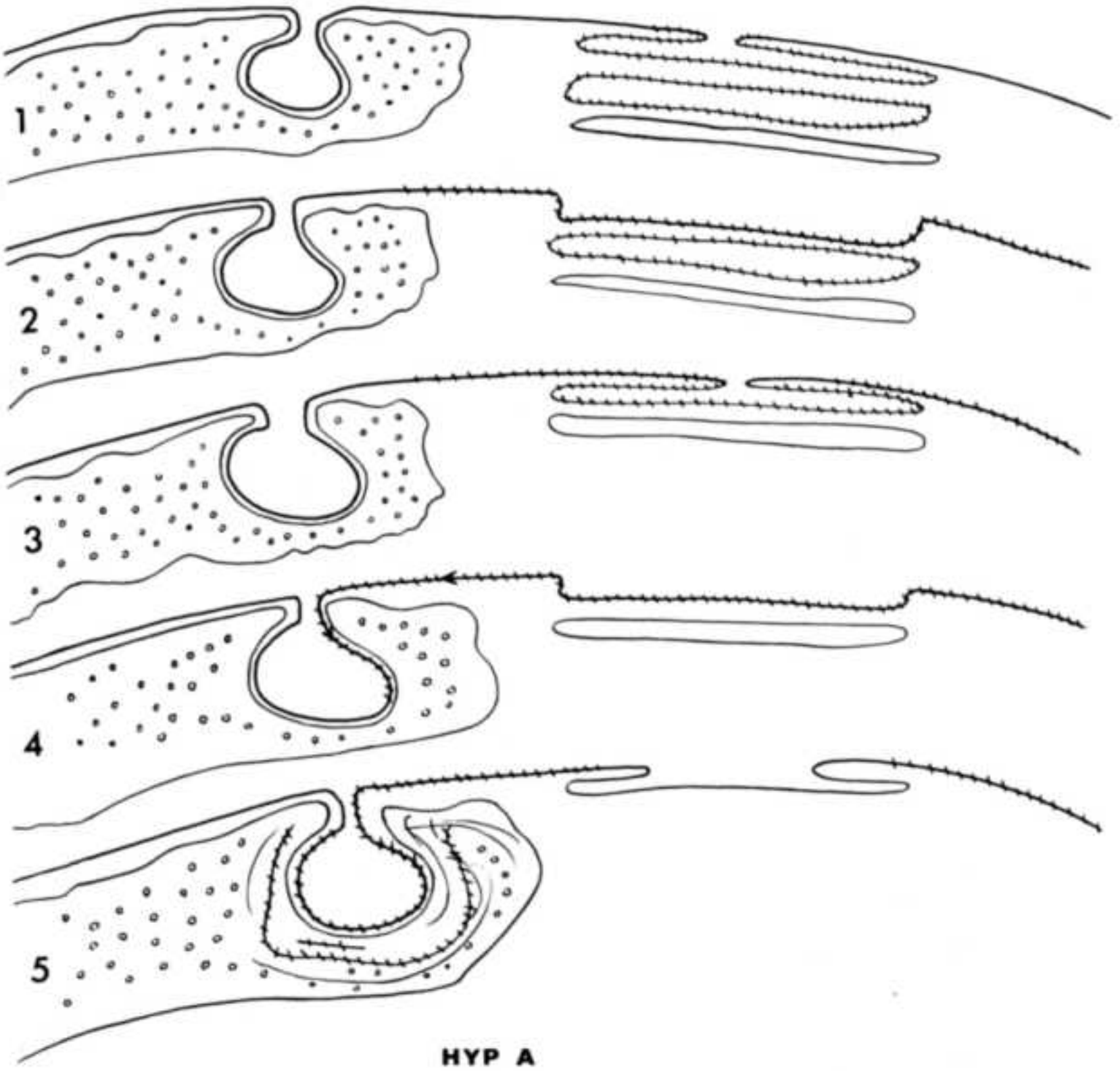

FIG. 45 (*continued*)

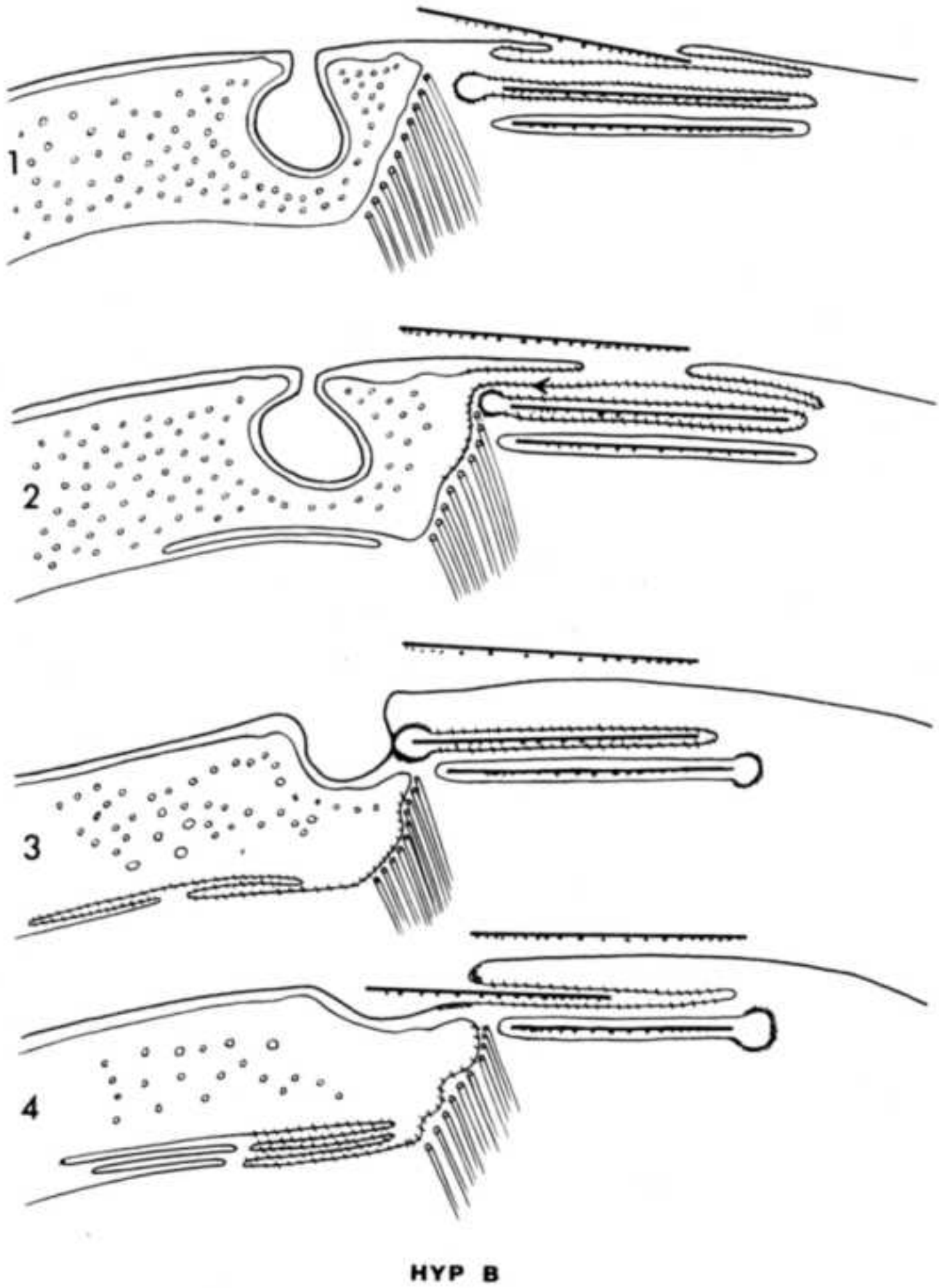

FIG. 45. Two alternative hypotheses for membrane recycling during scale exocytosis. *Hypothesis A:* Dotted area denotes lumen of the subsurface cisterna. Hatched lines refer to a hypothetical tracer introduced into the membranes to follow membrane flow. Arrows depict the proposed direction of membrane flow. This hypothesis favors endocytotic uptake of excess plasma membrane. *Hypothesis B:* The same indicators are used as in Hypothesis A. This hypothesis favors a subsurface cisternal capture of excess Golgi membrane followed by repeated infolding and ultimate release of excess membrane into the lumen. A microtubular bundle is shown, and its role in the uncovering of compatible sites for scale exocytosis is explained in the text.

plasma membrane only during the moment of scale exocytosis. Then Golgi membranes would be captured directly by the subsurface cisternal membranes. In *Hypothesis B,* the microtubular bundle plays an important role in the movements of the subsurface cisterna. It is known that the protoplast movement is inhibited under the influence of colchicine [6]. If the presumed microtubule-mediated movement were inhibited under the influence of colchicine, the plasmalemma invaginations and their intracellular receptor sites would not be uncovered. Perhaps the coalescence of the plasmalemma invaginations immediately prior to their disappearance would suggest the delay of cisternal sac movement as well as scale exocytosis. In stages 1–4 of *Hypothesis B,* note that the protoplasmic movements are a result of cisternal membrane uptake. Note also that the "coated" vesicles of the

Golgi membranes are depicted as a Golgi donor region for the compatible plasmalemma receptor site. If the plasmalemma receptor site is blocked by colchicine treatment, the Golgi donor site could fuse directly with the cisternal membrane, thus transporting both membrane *and* product to the autophagic vacuole via the lumen of the subsurface cisternal sac. Under normal conditions, only membrane is transported by this route. Membrane uptake via infolding of the subsurface cisternal sac would seem more reasonable than plasma membrane transfer to the sac since pinching of plasmalemma invaginations has never been observed. The only noted configurations of the plasmalemma invaginations include scalloped invaginations, deep cylindrical invaginations, and cylindrical invaginations with the typical "neck" region (Figs. 24, 25).

It is clear from the foregoing discussion that recycling of membrane and product occurs in the distal region of the Golgi apparatus and the subsurface cisterna. This interpretation is supported by the localization of acid phosphatase in these regions. That this enzyme activity is not involved in polysaccharide synthesis has been demonstrated morphologically and by substrate specificity. More likely, this acid hydrolase activity is involved in the lysis of the Golgi membrane and/or product during recycling.

In this presentation, we have focused upon the life history, cytological aspects of scale assembly and transport, and cytochemical enzyme localization within the Golgi apparatus and the subsurface cisternal sac. These investigations hopefully have set the stage for the next paper in this series which will cover, in detail, aspects of scale composition, with special reference to the cellulosic subcomponent.

The authors would like to express their appreciation to Mr. Richard Santos for the excellent technical assistance in the research and preparation of this paper. They are also indebted to Kay Cooper for several electron micrographs and to the following individuals for helpful discussions: H. Stanley Bennett, David Montezinos, Anahid Kavookjian, Kiyoshe Hama, Yukio Tanaka, and Werner Herth. The authors appreciate the cytochemical expertise of Jacob S. Hanker and his generous gifts of specialized chemicals. Dereck Lamport is owed a debt of gratitude for his assistance in the identification of scale subcomponents. Ron Chandross and Richard Bear made available their x-ray diffraction facilities, and to them the authors are most appreciative. They also thank Aristotle Domnas for the use of his biochemical laboratory and many helpful discussions.

REFERENCES

[1] P. Albersheim, W. D. Bauer, K. Keestra, and K. W. Talmadge, in *Biogenesis of Plant Cell Wall Polysaccharides*, F. Loewus, Ed., Academic Press, New York, 1973, p. 117.
[2] J. Austin, D. Armstrong, D. Stumpf, T. Luttenegger, and M. Dragoo, *Biochim. Biophys. Acta, 192*, 29 (1969).
[3] A. S. Balasubramanian and B. K. Bachhawat, *Brain Res., 20*, 341 (1970).
[4] N. B. Berg and R. W. Young, *J. Cell Biol., 50*, 469 (1971).
[5] R. M. Brown Jr., *J. Cell Biol., 41*, 109 (1969).
[6] R. M. Brown Jr., *Publ. z. Wissen. Filmen. Sektion Biologie, 7*, 361 (1974).
[7] R. M. Brown Jr., International Symposium on Plant Cell Differentiation, Lisbon, Portugal, 1974, *Portugale Acta Biologica Ser. A, 14*, 369.
[8] R. M. Brown Jr. and W. W. Franke, *Planta, 96*, 354 (1971).
[9] R. M. Brown Jr., W. W. Franke, H. Kleinig, H. Falk, and P. Sitte, *J. Cell Biol., 45*, 246 (1970).
[10] R. M. Brown Jr., W. Herth, W. W. Franke, and D. Romanovicz in *Biogenesis of Plant Cell Wall Polysaccharides*, F. Loewus, Ed., Academic Press, New York, 1973, p. 207.
[11] R. M. Brown Jr. and R. C. Santos, personal communication.

[12] I. Christensen, in *Botanik, 2,* No. 2, T. W. Bocher, M. Lange, and T. Sorenson, Eds., Munksgaard, Copenhagen 1962.
[13] J. R. Colvin, *Can. J. Biochem. Physiol., 39,* 1921 (1961).
[14] J. R. Colvin, *CRC Critical Reviews of Macromolecular Sciences* Vol. 1, 1972, p. 47.
[15] J. R. Colvin and M. Beer, *Can. J. Microbiol., 6,* 631 (1960).
[16] D. Danon, L. Goldstein, Y. Marikovsky, and E. Skutelsky, *J. Ultrastruct. Res., 38,* 500 (1972).
[17] W. M. Darley, D. Porter, and M. S. Fuller, *Arch. Mikrobiol., 90,* 89 (1973).
[18] M. Dauwalder, W. G. Whaley, and J. E. Kephart, *J. Cell Sci., 4,* 455 (1969).
[19] W. W. Douglas, J. Nagasawa, and R. Schulz, *Mem. Soc. Endocrinol., 19,* 353 (1971).
[20] K. C. Ellis and J. O. Warwicker, *J. Polym. Sci., 56,* 339 (1962).
[21] D. G. Fisher and J. Mann, *J. Polym. Sci., 42,* 189 (1960).
[22] L. C. Fowkes and J. D. Pickett-Heaps, *Protoplasma, 74,* 19 (1972).
[23] W. W. Franke, *Planta, 90,* 370 (1970).
[24] A. Frey-Wyssling, *Science, 119,* 80 (1954).
[25] A. Frey-Wyssling, K. Muhlethaler, and R. W. G. Wyckoff, *Experientia, 4,* 475 (1948).
[26] E. Frei and R. D. Preston, *Proc. Roy. Soc., B160,* 293 (1964).
[27] E. Frei and R. D. Preston, *Proc. Roy. Soc., B160,* 314 (1964).
[28] E. Frei and R. D. Preston, *Proc. Roy. Soc., B169,* 127 (1968).
[29] J. S. Furtado and L. S. Olive, *Nova Hedwigia, 21,* 537 (1971).
[30] Y. Futaesaku, V. Mizuhira, H. Nakamura, *Histochem. and Cytochem.* (abs), 155 (1972).
[31] Y. Futaesaku and V. Mizuhira, *8th Int. Cong. Electron Microscopy Canberra,* (abs) 2 (1974).
[32] E. George, M. Singh, and B. K. Bachhawat, *J. Neurochem., 17,* 189 (1970).
[33] L. Glaser, *J. Biol. Chem., 232,* 627 (1958).
[34] S. Goldfischer, E. Essner, and A. B. Novikoff, *J. Histochem. Cytochem., 12,* 72 (1964).
[35] J. C. Green and D. H. Jennings, *J. Expl. Botn., 18,* 359 (1967).
[36] S. N. Grove, C. E. Bracker, and D. J. Morré, *Science, 161,* 171 (1968).
[37] H. G. Gundlach, W. H. Stein, and S. Moore, *J. Biol. Chem., 234,* 1754 (1959).
[38] J. S. Hanker, L. P. Thornburg, P. E. Yates, and D. K. Romanovicz, *Histochem., 41,* 207 (1975).
[39] J. S. Hanker, P. E. Yates, D. H. Clapp, and W. A. Anderson, *Histochemie, 30,* 201 (1975).
[40] W. Z. Hassid *Science, 165,* 137 (1969).
[41] W. Z. Hassid, E. F. Neufeld, and D. S. Feingold, *Proc. Nat. Acad. Sci., 45,* 905 (1959).
[42] W. Herth, W. W. Franke, J. Stadler, H. Bittiger, G. Keilich, and R. M. Brown, Jr., *Planta, 105,* 79 (1972).
[43] G. Honjo and M. Watanabe, *Nature, 181,* 326 (1958).
[44] V. K. Hopsu-Havu, A. U. Arstila, H. J. Helminen, H. O. Kalimo, G. G. Glenner, *Histochemie, 8,* 54 (1967).
[45] G. G. Jewell and C. A. Saxton, *Histochem. J., 2,* 17 (1970).
[46] A. W. Kahn and J. R. Colvin, *Science, 133,* 2014 (1961).
[47] D. T. A. Lamport, in *Advances in Botanical Research,* Vol. 2., R. D. Preston, Ed., Academic Press, New York, 1965, p. 151.
[48] D. T. A. Lamport, *Ann. Rev. Plant Physiol., 21,* 235 (1970).
[49] D. T. A. Lamport, in *Biogenesis of Plant Cell Wall Polysaccharides,* F. Loewus, Ed. Academic Press, New York, 1973, p. 149.
[50] B. S. C. Leadbeater, *Brit. Phycol. J., 5,* 57 (1970).
[51] B. S. C. Leadbeater, *Sarsia, 49,* 65 (1972).
[52] B. S. C. Leadbeater, *Sarsia, 49,* 107 (1972).
[53] G. G. Leppard, J. R. Colvin, D. Rose, and S. M. Martin, *J. Cell Biol., 50,* 63 (1971).
[54] R. St. John Manley, J. W. Jonker, D. Cooper, and T. C. Pound, *Nature New Biol., 229,* 88 (1971).
[55] I. Manton, *J. Cell Sci., 1,* 375 (1966).
[56] I. Manton, *J. Cell Sci., 2,* 265 (1967).
[57] I. Manton and H. Ettl, *J. Linn. Soc. (Bot.), 59,* 175 (1965).
[58] I. Manton and K. Harris, *J. Linn. Soc. (Bot.), 59,* 397 (1966).
[59] I. Manton and G. F. Leedale, *Phycologia, 1,* 37 (1961).
[60] I. Manton and G. F. Leedale, *Arch. Mikro., 47,* 115 (1963).
[61] I. Manton and G. F. Leedale, *J. Mar. Biol. Ass. U. K., 49,* 1 (1969).
[62] V. Marinozzi, *J. Biophys. Biochem. Cytol., 9,* 121 (1961).
[63] H. Mark and K. H. Meyer, *Z. physik. Chem., B2,* 115 (1929).

[64] M. Marx-Figini, *Nature, 210,* 755 (1966).
[65] M. Marx-Figini and G. V. Schulz, *Biochim. Biophys. Acta., 112,* 81 (1966).
[66] E. R. McCall, N. M. Morris, V. W. Tripp, and R. T. O'Connor, *Appl. Spectrosc., 25,* 196 (1971).
[67] K. H. Meyer and L. Misch, *Helv. Chim. Acta., 20,* 232 (1937).
[68] B. Millman and J. R. Colvin, *Can. J. Microbiol., 7,* 383 (1961).
[69] V. Mizuhira and Y. Futaesaku, *8th Int. Cong. Electron Microscopy, Canberra, 2,* (abs) 340 (1974).
[70] O. Moestrup, *Biol. J. Linn. Soc., 6,* 111 (1974).
[71] H. H. Mollenhaur and D. J. Morré, *Ann. Rev. Plant Physiol., 17,* 27 (1966).
[72] H. H. Mollenhaur, D. J. Morré, and C. Totten, *Protoplasma, 78,* 443 (1973).
[73] H. Moor and K. Muhlethaler, *J. Cell Biol., 17,* 609 (1963).
[74] D. J. Morré, H. H. Mollenhauer, and C. E. Bracker, in *Origin and Continuity of Cell Organelles,* J. Reinert and H. Ursprung, Eds., Springer-Verlag, New York, 1971, p. 82.
[75] K. Muhlethaler, *J. Polym. Sci. Part C, 28,* 305 (1969).
[76] S. M. Mukherjee and H. J. Woods, *Biochim. Biophys. Acta., 10,* 499 (1953).
[77] I. A. Nieduszynski and E. D. T. Atkins, *Biochim. Biophys. Acta., 222,* 109 (1970).
[78] I. Nieduszynski and R. D. Preston, *Nature, 225,* 273 (1970).
[79] I. Nir and D. C. Pease, *J. Ultrastruc. Res., 42,* 534 (1973).
[80] D. H. Northcote, *Proc. Roy. Soc., B173,* 21 (1969).
[81] D. H. Northcote, *Endeavour, 30,* 26 (1971).
[82] D. H. Northcote and J. D. Pickett-Heaps, *Biochem. J., 98,* 159 (1966).
[83] P. M. Novikoff, A. B. Novikoff, N. Quintana, and J. J. Hauw, *J. Cell Biol., 50,* 859 (1971).
[84] L. Ordin and M. A. Hall, *Plant Physiol., 42,* 205 (1967).
[85] D. E. Outka and D. C. Williams, *J. Protozool., 18,* 285 (1971).
[86] D. J. Owen, Ph.D. dissertation, University of North Carolina, 1973.
[87] B. A. Palevitz, J. F. Ash, and P. K. Hepler, *Proc. Nat. Acad. Sci., 71,* 363 (1974).
[88] M. Parke, I. Manton, and B. Clarke, *J. Mar. Biol. Ass. U. K., 34,* 579 (1955).
[89] M. Parke, I. Manton, and B. Clarke, *J. Mar. Biol. Ass. U. K., 35,* 387 (1956).
[90] M. Parke, I. Manton, and B. Clarke, *J. Mar. Biol. Ass. U. K., 37,* 209 (1958).
[91] M. Parke, I. Manton, and B. Clarke, *J. Mar. Biol. Ass. U. K., 38,* 169 (1959).
[92] R. N. Pienaar, *J. Phycol., 5,* 321 (1969).
[93] J. D. Pickett-Heaps, *J. Histochem. Cytochem., 15,* 442 (1967).
[94] R. D. Preston, in *Formation of Wood in Forest Trees,* M. H. Zimmerman, Ed., Academic Press, New York, 1964, p. 169.
[95] R. D. Preston, *The Physical Biology of Plant Cell Walls,* Chapman and Hall, London, 1974.
[96] R. D. Preston and W. T. Astbury, *Proc. Roy. Soc., B122,* 76 (1937).
[97] R. D. Preston and J. Cronshaw, *Nature, 181,* 248 (1958).
[98] R. D. Preston, E. Nicolai, R. Reed, and A. Millard, *Nature, 162,* 665 (1948).
[99] R. D. Preston and G. W. Ripley, *Nature, 174,* 76 (1954).
[100] E. G. Pringsheim, *Arch. Mikrobiol., 21,* 401 (1955).
[101] A. Rambourg, *Histochem. Cytochem., 15,* 409 (1967).
[102] A. Rambourg and C. P. Leblond, *J. Cell Biol., 32,* 27 (1967).
[103] P. M. Ray, T. Shininger, and M. Ray, *Proc. Nat. Acad. Sci., 64,* 605 (1969).
[104] D. G. Rayns, *J. Mar. Biol. Ass. U. K., 42,* 481 (1962).
[105] A. J. J. Rees, G. F. Leedale, and H. A. Cmiech, *Br. Phycol. J., 9,* 273 (1974).
[106] E. S. Reynolds, *J. Cell Biol., 17,* 208 (1963).
[107] D. G. Robinson and R. D. Preston, *Planta, 104,* 234 (1972).
[108] D. G. Robinson, R. K. White, and R. D. Preston, *Planta, 107,* 131 (1972).
[109] D. Romanovicz and R. M. Brown, Jr., in *Proceedings Thirty-Second Annual Meeting Electron Microscopy Society of America,* Claitor's, Lousiana, C. J. Arceneaux, Ed., 1974, p. 92.
[110] H. Ruska, *Kolloid Z., 92,* 276 (1940).
[111] H. Ruska and M. Kretschmer, *Kollid Z., 93,* 163 (1940).
[112] D. Sadava and M. J. Chrispeels, *Science, 165,* 299 (1969).
[113] D. Sadava and M. J. Chrispeels, in *Biogenesis of Plant Cell Wall Polysaccharides,* F. Loewus, Ed., Academic Press, New York, 1973, p. 165.
[114] B. D. Saksena, K. C. Agarwal, and G. S. Jauhri, *J. Polym. Sci., 62,* 347 (1962).
[115] E. Schnepf and G. Deichgraber, *Protoplasma, 68,* 85 (1969).

[116] O. L. Sponsler, *Nature, 125,* 633 (1930).
[117] H. A. von Stosch, *Naturwissenschaften, 45,* 140 (1955).
[118] H. A. von Stosch, in *Proceedings of the Fourth International Seaweed Symposium,* A. de Virville and J. Feldmann, Eds., McMillan, New York, 1964.
[119] S. Suzuki and J. L. Strominger, *J. Biol. Chem., 235,* 267 (1960).
[120] S. Suzuki and J. L. Strominger, *J. Biol. Chem., 235,* 274 (1960).
[121] S. Suzuki, N. Takahashi, and F. Egami, *Biochim. Biophys. Acta., 24,* 444 (1957).
[122] J. A. Swift, *J. Roy. Microsc. Soc., 88,* 449 (1968).
[123] J. A. Swift and C. A. Saxton, *J. Ultrastruct. Res., 17,* 23 (1967).
[124] E. W. Thompson and R. D. Preston, *J. Exp. Bot., 19,* 690 (1968).
[125] W. J. Van Der Woude, C. A. Lembi, D. J. Morre, J. I. Kindinger, and L. Ordin, *Plant Physiol., 54,* 333 (1974).
[126] B. Vian and J. C. Roland, International Symposium on Plant Cell Differentiation, Lisbon, Portugal, 1974, *Portugale Acta Biologica Ser. A, 14.*
[127] C. L. Villemez, Jr., G. Franz, and W. Z. Hasid, *Plant Physiol., 42,* 1219 (1967).
[128] C. L. Villemez, Jr., J. M. McNab, and P. Albersheim, *Nature, 218,* 878 (1968).
[129] J. M. Westafer, Thesis, B. S. in Biology with Honors, University of North Carolina, Chapel Hill, 1974.
[130] W. G. Whaley, *International Symposium on Plant Cell Differentiation,* M. S. Pais, Ed., Lisbon, Portugal, 1975, in press.
[131] W. G. Whaley, M. Dauwalder, and J. Kephart, in *Origin and Continuity of Cell Organelles,* J. Reinert and H. Ursprung, Eds., Springer-Verlag, New York, 1971, p. 7.
[132] B. Wortman, *J. Biol. Chem., 236,* 974 (1961).
[133] R. W. Young, *J. Cell Biol., 57,* 175 (1973).